Variation in Human Herpesvirus 6B telomeric integration, excision and transmission between tissues and individuals

Wood, M.L.[1], Veal, C.[1], Neumann, R.[1], Suárez, N.M.[2], Nichols, J.[2], Parker, A.J.[1], Martin, D.[1], Romaine, S.P.R[3,4], Codd, V.[3], Samani, N.J.[3], Voors, A.A.[5], Tomaszewski, M.[6], Flamand, L.[7], Davison, A.J.[2], and Royle, N.J.[1]

[1] Department of Genetics and Genome Biology, University of Leicester, Leicester, United Kingdom.
[2] MRC-University of Glasgow Centre for Virus Research, Glasgow, United Kingdom.
[3] Department of Cardiovascular Sciences, University of Leicester, Leicester, United Kingdom.
[4] NIHR Leicester Biomedical Research Centre, Glenfield Hospital, Leicester, United Kingdom.
[5] University of Groningen, Department of Cardiology, University Medical Center Groningen, Groningen, The Netherlands.
[6] Division of Cardiovascular Sciences, School of Medical Sciences, Faculty of Biology, Medicine and Health, University of Manchester, Manchester, United Kingdom.
[7] Department of Microbiology, Infectious Diseases and Immunology, Faculty of Medicine, Université Laval, Quebec City, Québec, Canada

Running Title:
HHV-6B transmission in populations

Abstract

Human herpesviruses 6A and 6B (HHV-6A/6B) are ubiquitous pathogens that persist lifelong in latent form and can cause severe conditions upon reactivation. They are spread by community-acquired infection of free virus (acqHHV6A/6B) and by germline transmission of inherited chromosomally-integrated HHV-6A/6B (iciHHV-6A/6B) in telomeres. We exploited a hypervariable region of the HHV-6B genome to investigate the relationship between acquired and inherited virus and revealed predominantly maternal transmission of acqHHV-6B in families. Remarkably, we demonstrate that some copies of acqHHV-6B in saliva from healthy adults gained a telomere, indicative of integration and latency, and that the frequency of viral genome excision from telomeres in iciHHV-6B carriers is surprisingly high and varies between tissues. In addition, newly formed short telomeres generated by partial viral genome release are frequently lengthened, particularly in telomerase-expressing pluripotent cells. Consequently, iciHHV-6B carriers are mosaic for different iciHHV-6B structures, including circular extra-chromosomal forms that have the potential to reactivate. Finally, we show transmission of an HHV-6B strain from an iciHHV-6B mother to her non-iciHHV-6B son. Altogether we demonstrate that iciHHV-6B can readily transition between telomere-integrated and free virus forms.

Max 5 keywords : excision/integration/human herpesvirus 6/latency/telomere/

Introduction

Human herpesviruses 6A and 6B (HHV-6A/6B; species *Human betaherpesvirus 6A* and *Human betaherpesvirus 6B*) are closely related viruses, sharing approximately 90% sequence identity (Ablashi *et al*, 2014). Their genomes comprise a unique region (U) of approximately 140 kb flanked on each side by a direct repeat (DR) of approximately 8 kb (DR_L on the left and DR_R on the right). A tandem repeat reiteration is located near each end of DR. T1 at the left end consists of 1-8 kb of telomere (TTAGGG) and degenerate telomere-like repeats (Huang *et al*, 2014; Lindquester & Pellett, 1991; Zhang *et al*, 2017). T2 at the right end is much shorter and contains only (TTAGGG) repeats (Achour *et al*, 2009; Zhang *et al.*, 2017). HHV-6A/6B have the capacity to integrate into human telomeres, most likely through a homology-dependent recombination mechanism facilitated by the perfect telomere repeats in T2 (Arbuckle *et al*, 2010; Wallaschek *et al*, 2016b). The precise integration mechanism has not been defined, and searches for regulatory viral or host factors are underway (Gilbert-Girard *et al*, 2017; Gilbert-Girard *et al*, 2020; Wallaschek *et al*, 2016a; Wight *et al*, 2018).

HHV-6A/6B infect over 90% of the global population in early childhood, this usually manifests with mild symptoms but nevertheless often requires medical attention (Asano *et al*, 1994; Hall *et al*, 1994; Kondo *et al*, 1993; Ward & Gray, 1994; Zerr *et al*, 2005). As with most herpesviruses, HHV-6A/6B enter lifelong latency following primary infection, and the most serious impacts on health appear to occur when the virus reactivates. Reactivation of free virus acquired in the community (acqHHV-6A/6B) has been shown to cause viral encephalitis, drug-induced hypersensitivity syndrome/drug reaction with eosinophilia and systemic symptoms (DIHS/DRESS) and acute graft-versus-host disease (aGVHD) (Aihara *et al*, 2003; Eshki *et al*, 2009; Pritchett *et al*, 2012; Prusty *et al*, 2018; Yao *et al*, 2010; Yoshikawa *et al*, 2006). In addition, HHV-6A infection has been associated with multiple sclerosis and other chronic neurological conditions (Yao *et al.*, 2010). Herpesviruses typically achieve latency by forming circular DNA episomes within specific cell types, but HHV-6A/6B episomes have not been detected and it has been proposed that latency of these viruses is achieved through telomeric integration (Arbuckle *et al.*, 2010).

As a result of historical germline integrations into telomeres, approximately 1% of the population carries inherited chromosomally integrated HHV-6A/6B (iciHHV-6A/6B), usually with a full-length copy of the viral genome in every cell (Arbuckle *et al.*, 2010; Daibata *et al*, 1999; Huang *et al.*, 2014; Leong *et al*, 2007; Morris *et al*, 1999; Tanaka-Taya *et al*, 2004). HHV-6A/6B appear to have the potential to integrate into any telomere however, most contemporary instances of iciHHV-6A/6B are derived from a relatively small number of ancient integrations in a limited number of

chromosome ends (Aswad *et al*, 2021; Greninger *et al*, 2018; Kawamura *et al*, 2017; Liu *et al*, 2018; Liu *et al*, 2020; Miura *et al*, 2018; Tweedy *et al*, 2016; Zhang *et al.*, 2017). For example, iciHHV-6B is commonly found integrated into the telomere on the short arm of chromosome 17 (17p) in populations of European descent and iciHHV-6A is commonly found in the long arm of chromosome 22 (22q) in Japan. Integration sites have been determined in a variety of studies by one or a combination of the following methods: Fluorescent *in situ* hybridisation (FISH); PCR amplification from subterminal sequences adjacent to human telomeres (subtelomere) into the viral genome; inverse PCR and comparison with known subtelomere sequences; long-read sequencing; optical genome mapping (Daibata *et al.*, 1999; Huang *et al.*, 2014; Luppi *et al*, 1998; Nacheva *et al*, 2008) (Aswad *et al.*, 2021; Greninger *et al.*, 2018; Kawamura *et al.*, 2017; Liu *et al.*, 2020; Miura *et al.*, 2018; Tweedy *et al.*, 2016; Wight *et al*, 2020; Zhang *et al.*, 2017).

Detection of viral gene expression in some iciHHV-6A/6B carriers has raised the possibility of a deleterious impact on the individual's health over their lifetime (Huang *et al.*, 2014; Peddu *et al*, 2019; Strenger *et al*, 2014). Similarly, the presence of a large viral genome within in a telomere has been shown to cause localised instability that may influence telomere DNA damage signalling and function (Huang *et al.*, 2014; Wood & Royle, 2017; Zhang *et al*, 2016). Recent studies have also indicated an association between iciHHV-6A/6B and angina pectoris (Gravel *et al*, 2015); unexplained infertility (Miura *et al*, 2020); an increased risk of aGVHD following haematopoietic stem cell transplantation when either the donor or recipient has iciHHV-6A/6B (Hill *et al*, 2017; Weschke *et al*, 2020); complications following solid organ transplantation when there was iciHHV-6A/6B donor/recipient mismatch (Bonnafous *et al*, 2018; Bonnafous *et al*, 2020; Petit *et al*, 2020); and possibly an increased risk of pre-eclampsia (Gaccioli *et al*, 2020).

There is increasing evidence that iciHHV-6A/6B genomes can reactivate fully (Endo *et al*, 2014) and then be transmitted as acqHHV-6A/6B (Gravel *et al*, 2013; Hall *et al*, 2010), but the chain of events leading to reactivation is unknown. Telomeres are terminated by a single-stranded 3' overhang that can strand-invade into the upstream double-stranded telomeric DNA to form a telomere loop (t-loop) (Doksani *et al*, 2013; Griffith *et al*, 1999; Wang *et al*, 2004). This secondary structure is stabilised by TRF2, a component of the Shlerterin complex that binds to double-stranded telomere repeats, and plays a protective role by preventing the ends of linear chromosomes being detected as double-strand breaks and inappropriately repaired (de Lange, 2018; Schmutz *et al*, 2017; Stansel *et al*, 2001; Van Ly *et al*, 2018). However, t-loops can be excised as telomere repeat-containing t-circles (Pickett *et al*, 2009; Pickett *et al*, 2011; Sarek *et al*, 2015; Tomaska *et al*, 2019) by the SLX1-4 complex, which is a structure-specific endonuclease (Fekairi *et al*, 2009; Vannier *et al*, 2012; Wan *et al*, 2013), and unregulated excision of t-loops results in critically short telomeres (Deng

et al, 2013; Pickett *et al.*, 2011; Rivera *et al*, 2017). We and others have proposed that release of the viral genome is a prerequisite for reactivation of iciHHV-6A/6B and that this release is driven by normal t-loop processing (Huang *et al.*, 2014; Prusty *et al*, 2013; Wood & Royle, 2017).

Here, we have investigated iciHHV-6A/6B genomes (with a particular focus on iciHHV-6B), their associated telomeres and their relationships to acqHHV-6B genomes in families and communities. We exploited the proximal hypervariable region of T1 (pvT1) in the HHV-6B genome to distinguish between acqHHV-6B strains and to predict relationships between iciHHV-6B and acqHHV-6B in families. For the first time, we have detected acqHHV-6B telomeric integration in saliva DNA from healthy adults. The frequency of partial or complete iciHHV-6B excision varied between germline and somatic cells, with notably high frequencies in two pluripotent cell lines, and we present evidence of HHV-6B transmission from an iciHHV-6B carrier mother to her non-iciHHV-6B son. In summary, our study demonstrates that HHV-6B can readily transition between iciHHV-6B and acqHHV-6B forms, and vice versa.

Results

DR_R-pvT1 tracking of HHV-6B transmission

To explore the relationship between iciHHV-6A/6B and acqHHV-6A/6B, we identified a genomic marker (pvT1) capable of distinguishing viral strains by nested PCR and sequencing. To investigate DR_R-pvT1 specifically, the first round of amplification was achieved using a primer anchored at the right end of U near DR_R and a primer in DR on the other side of T1 (Figure 1A). The second round of amplification and subsequent sequencing involved a primer (TJ1F) anchored in a short, conserved sequence approximately 400 bases into the T1 telomere-like repeat array and a second primer in DR. A total of 102 DNA samples were analysed: iciHHV-6B from 39 individuals (38.2%) and acqHHV-6B from 63 (61.8%) individuals (Supplementary Table 1). The analysis showed that DR_R-pvT1 can be divided into three regions (left, middle and right), with most of the variation being due to differences in the number and distribution of telomere (TTAGGG) and degenerate telomere-like repeats (predominantly CTAGGG and CTATGG) in the left and middle regions. Maps of the repeat pattern are shown for a subset of samples in Figure 1B, and the complete dataset is provided in Figure 1 – figure supplement 1.

Among the 102 repeat patterns, 93 were different from each other, and 90 of these were detected in only a single donor or family. Amongst the 12 repeat patterns shared between individuals, eight were identical to each other, and seven of these were from closely related viral

genome sequences in iciHHV-6B carriers with a shared 9q integration. The eighth was found in saliva DNA from an individual (SAL030) with acqHHV-6B (Figure 1 – figure supplement 1). Among the remaining four repeat patterns, two were in iciHHV-6B samples (NWA008 and DER512) that share the same 17p integration site, and two were in acqHHV-6B samples (SAL023 and TEL-FA G1P1). Remarkably, the pvT1 repeat pattern was different in almost every unrelated individual with acqHHV-6B (61/63, 96.8%) and also in the majority of iciHHV-6B individuals (30/39, 77.0%; 29/31, 93.5%, when the entire 9q iciHHV-6B group was excluded).

Although DR_R-pvT1 is highly variable among acqHHV-6B genomes in unrelated individuals, this is not the case within families (Figure 1C, Figure 1 – figure supplement 2). Saliva DNA was analysed from 36 individuals in eight families (without iciHHV-6A/6B) and DR_R-pvT1 was successfully amplified and sequenced from 34 of them (94%). Eighteen of the 20 children (90%) in these families had the same repeat pattern as one of their parents, presumably as a result of acqHHV-6B transmission directly from a parent (maternal transmission in six of the eight families and paternal transmission in one) or indirectly via a sibling (Figure 1 – figure supplement 2). In contrast, the analysis revealed that one child in each of two families must have contracted acqHHV-6B from outside their immediate family (TEL-FC G2P2 and TEL-FM G2P1, Figure 1 – figure supplement 2). As a control, analysis of DR_R-pvT1 repeat patterns in iciHHV-6B carriers in the CEPH1375 family demonstrated the stability of the repeat patterns across three generations (Figure 1C). All six individuals, shown previously to be iciHHV-6B carriers (Huang *et al.*, 2014), shared an identical pattern indicating that DR_R-pvT1 does not necessarily acquire mutations from one generation to the next. In summary, DR_R-pvT1 analysis was used successfully to distinguish HHV-6B strains and to monitor transmission of iciHHV-6B and acqHHV-6B between family members.

Phylogeny of iciHHV-6A/6B in relation to integration events

Progress has been made recently in sequencing iciHHV-6A/6B and acqHHV-6A/6B genomes by generating overlapping PCR amplicons (Zhang *et al.*, 2017) or an oligonucleotide hybridisation enrichment process (Aswad *et al.*, 2021; Greninger *et al.*, 2018; Telford *et al*, 2018). However, the evolutionary histories of iciHHV-6A/6B genomes and their relationships with acqHHV-6A/6B genomes remain unclear. Moreover, it is not known how many founder germline integration events have occurred. To expand the data required to answer such questions, we screened various cohorts and families to identify additional iciHHV-6A/6B-positive samples (Supplementary Table 1), and then selected several key samples for viral genome sequencing using the overlapping PCR amplicon approach (Huang *et al.*, 2014; Zhang *et al.*, 2017). These samples included five iciHHV-6A and four

189 iciHHV-6B samples from the BIOSTAT-CHF cohort, four other iciHHV-6A samples, one iciHHV-6A cell
190 line (HGDP00628 (Huang *et al.*, 2014)), and a pluripotent cell line (d37) from an iciHHV-6B carrier. In
191 total, ten iciHHV-6A and five iciHHV-6B genomes were sequenced.

192 Distance-based phylogenetic networks of iciHHV-6A/6B and acqHHV-6A/6B genomes were
193 generated, including the 15 newly sequenced iciHHV-6A/6B genomes and iciHHV-6A/6B genomes
194 representing previously identified clades and integration sites (Figure 2, Supplementary Table 1).
195 These networks reinforce previous findings (Aswad *et al.*, 2021; Greninger *et al.*, 2018; Tweedy *et al.*,
196 2016; Zhang *et al.*, 2017) showing that the majority of iciHHV-6A genomes in European and North
197 American carriers (including the ten newly sequenced) originate from three integration events at
198 17p, 18q and 19q, with the time to the most recent common ancestor estimated at 23 to 105
199 thousand years ago (Figure 2, Supplementary Table 2). The networks also confirm that iciHHV-6B
200 carriers with European and North America ancestry originate from a larger number of integration
201 events that occurred more recently (21 to 25 thousand years ago; Supplementary Table 2) (Aswad *et*
202 *al.*, 2021; Greninger *et al.*, 2018; Zhang *et al.*, 2017). Inclusion of the newly sequenced iciHHV-6B
203 genomes added two new iciHHV-6B clades to the phylogenetic network, each defined by a distinct
204 integration site (Figure 2). As a consequence of the complex evolution of subterminal sequences in
205 the human genome (Riethman, 2008), the chromosomal locations in these iciHHV-6B clades will
206 require further verification by an independent method, but they represent two more independent
207 germline telomeric integration events.

208 As an aid to analysing the increasing number of HHV-6A/6B genome sequences, we
209 developed HHV-6 Explorer (https://www.hhv6explorer.org/), which is an online interface for
210 monitoring clade-specific variation in DNA and predicted protein sequences. An analysis of sequence
211 variation in relation to integration site using this tool produced new insights, for example by
212 demonstrating that two potentially inactivating mutations, U14 in an iciHHV-6B clade and in U79 in
213 an iciHHV-6A clade, must have arisen after integration (Figure 2 – figure supplement 1).

214

215 **Predicting chromosomal iciHHV-6B integration sites from DR_R-pvT1 repeat patterns**

216 To explore whether DR_R-pvT1 repeat patterns reflect the phylogenetic relationships between
217 iciHHV-6B genomes, 19 for which DNA was available, were subjected to DR_R-pvT1 analysis. The
218 results show that iciHHV-6B genomes with a high degree of overall sequence similarity also shared
219 similar DR_R-pvT1 repeat patterns. For example, individuals with 9q iciHHV-6B have a characteristic
220 CTATGG- TTAGTG-CTATGG motif in the middle region of DR_R-pvT1, as well as a TTAGAG repeat that

is found infrequently outside this group. Also, viral sequences assigned to the 17p major iciHHV-6B group by genome sequence identity and shared 17p subtelomere-iciHHV-6B junction sequences (HGDP01065, HGDP01077, DER512, 801018 and ORCA1622) (Zhang *et al.*, 2017) had similar DR_R-pvT1 repeat patterns with two characteristic GTAGTG repeats at the left end (Figure 3A).

From these observations, we hypothesised that DR_R-pvT1 repeat patterns may be used to predict both the integration site for newly identified iciHHV-6B carriers and the identity of closely related viral strains, without the need to sequence viral genomes. Based on similarity between DR_R-pvT1 repeat patterns, the integration site was predicted for nine iciHHV-6B genomes for which genome sequences were not available (Figure 3A). For example, the repeat patterns in YOR546, CRL-1730 and 6-iciHHV-6B were identical or almost identical to those in a large group of iciHHV-6B genomes with a 9q integration site (Nacheva *et al.*, 2008; Shioda *et al*, 2018). PCR amplification of the subtelomere-iciHHV-6B junction was used to validate several of the predictions arising from these results. For example, DR_R-pvT1 analysis placed 410005 and 308006 in the same phylogenetic clade as the 401027 iciHHV-6B genome (Figure 3, Figure 2), and common ancestry was confirmed by sequence similarity across the subtelomere-iciHHV-6B junction fragment (amplified by primer 2p2, Figure 3B-C, Figure 2) in all three samples. Similarly, the iciHHV-6B genomes in d44, LAT018, NWA008 and KEN071 share DR_R-pvT1 repeat patterns and subtelomere-iciHHV-6B junction fragments similar to the large group of iciHHV-6B genomes integrated at 17p (17p major) (Figure 3B-C, (Zhang *et al.*, 2017)). In summary, the integration sites of iciHHV-6B genomes that had not been sequenced were predicted based on a high degree of similarity between DR_R-pvT1 repeat patterns, and six of these predictions were subsequently tested and validated by an independent method.

Chromosomal integration of acqHHV-6B

Telomeric integration provides a means by which acqHHV-6A/6B may achieve latency. Although *de novo* integration has been shown to occur in cell culture (Arbuckle *et al.*, 2010; Arbuckle *et al*, 2013; Collin *et al*, 2020; Gilbert-Girard *et al.*, 2020; Gravel *et al*, 2017; Wallaschek *et al.*, 2016b), there is little evidence that it occurs contemporaneously *in vivo* (Moustafa *et al*, 2017). To investigate this, we collected saliva DNA samples from 52 healthy donors and used triplicate digital droplet PCR (ddPCR) assays to quantify HHV-6B genome copy number per cell (Figure 4A). Using this sensitive approach, low-level HHV-6B was detected in 44 samples (84.6%) with a mean value 0.00145 copies per cell (range 0.0000233–0.0125). Two kidney DNA samples, K1 and K10, were also positive for HHV-6B at 0.000525 and 0.0124 copies per cell, respectively (Figure 4A, D).

Previously we used Single TElomere Length Analysis (STELA), a PCR-based method, to detect and measure the length of iciHHV-6A/6B-associated telomeres at DR_L-T1 (Huang *et al.*, 2014). To determine whether some copies of acqHHV-6B are integrated into telomeres, we aimed to detect these potentially rare events using STELA. The first step involved STELA of genomic DNA from saliva samples that had low but measurable levels of HHV-6B DNA. The STELA PCR products were then diluted and subjected to a second round of PCR with primers TJ1F and DR421R to amplify DR_L-pvT1. Successful amplification in the second round was taken as evidence that an HHV-6B-associated telomere had been amplified in the primary STELA round (Figure 4B-C). Sanger sequencing was used to confirm DR_L-pvT1 amplified from STELA products matched that amplified from genomic DNA from each individual. Various steps were taken to avoid false positive results. These include the use of newly designed STELA primers for these experiments (Figure 4B) and conducting STELA on genomic DNA from the HT1080 cell line (HHV-6A/6B negative) to check for potential non-specific amplification from another telomere or elsewhere in the human genome. No STELA products were generated from HT1080 among 900 STELA reactions, total 4.5μg DNA screened. This two-step STELA procedure, conducted on DNA from six saliva and two kidney samples identified a small number of amplicons from some samples with acqHHV-6B (Supplementary Table 3). The proportion of HHV-6B genomes from which a telomere was amplified was estimated using the HHV-6B copy number per cell (determined by ddPCR) and by estimating the number of cell equivalents of DNA used per STELA reaction, assuming 6.6 pg DNA per cell (Figure 4D, Supplementary Table 3). For the eight samples analysed, an average of 0.95% (range 0–1.98%) of HHV-6B genomes resulted in pvT1 amplification, indicative of telomeric integration. The low copy number of HHV-6B in these samples, combined with reduced PCR amplification efficiency of longer molecules (telomeres in this case), has a stochastic effect on the potential to detect an HHV-6B-associated telomere in each STELA reaction therefore, the integration frequencies should be interpreted cautiously.

We then sought to measure the proportion of acqHHV-6B genomes that are *not* integrated in saliva samples, using ddPCR to quantify the copy numbers of DR and PAC1. PAC1 and PAC2 are genome packaging signals located at the end of T1 and T2, respectively (Figure 4B). The linear, unintegrated genome has two copies of DR and two copies of PAC1 and PAC2, whereas the integrated genome has two copies of DR but retains only a single copy of PAC1 and PAC2 (Figure 4B) (Arbuckle *et al.*, 2010) (Huang *et al.*, 2014). As expected, the ratio of DR:PAC1 in an iciHHV-6B sample (4B-11p15.5) was approximately 2:1, whereas the ratio in acqHHV6-B samples in saliva samples was approximately 2:2 (Figure 4E). This shows that most acqHHV-6B genomes in saliva samples are not integrated, consistent with the STELA data that revealed only low level telomeric integration of acqHHV-6B genomes in saliva DNA samples.

287

288 **Partial excision of iciHHV-6B genomes and novel telomere formation at DR_L-T2**

289 We showed previously that iciHHV-6A/6B genomes in lymphoblastoid cell lines (LCLs) can be
290 truncated at DR_L-T2, resulting in loss of the terminal DR_L and formation of a novel short telomere at
291 the breakpoint (Huang *et al.*, 2014; Wood & Royle, 2017). We proposed that truncation is achieved
292 through a t-loop-driven mechanism in which the 3′ G-rich overhang at the end of the telomere
293 strand invades DR_L-T2, facilitating excision of the terminal DR_L as a DR-containing t-circle and leaving
294 a novel telomere at the excision point. Here, we measured the frequency of iciHHV-6B truncations at
295 DR_L-T2 in seven LCLs, nine blood DNAs (from white blood cells), two pluripotent cell lines, three
296 sperm DNA samples and saliva DNA (Figure 5A-C, Supplementary Table 4). The average frequency of
297 DR_L-T2 truncations with novel telomere formation was 1 in 120 cells, but there were significant
298 differences between DNAs from different cell types. The number of truncations per cell was lowest
299 in blood and saliva DNA, with an average of 1 in 300 (0.0033 per cell) and 1 in 320 (0.0031),
300 respectively, and approximately double this in sperm at 1 in 160 cells (0.00627 per cell). An
301 astonishingly high number of DR_L-T2 truncations were observed in LCLs (0.015 per cell) and
302 pluripotent cells (0.014 per cell), equating to approximately one in every 70 cells. Furthermore,
303 released circular DR molecules were detected using an inverse PCR approach (Figure 5 – figure
304 supplement 1).
305 The histone deacetylase inhibitor, trichostatin-A (TSA) has been shown to promote iciHHV-
306 6A reactivation in cell lines and cultured T cells from iciHHV-6A/6B individuals (Arbuckle *et al.*, 2010;
307 Arbuckle *et al.*, 2013), and also to increase the abundance of t-circles (Zhang *et al*, 2019). To explore
308 whether the frequency of truncations with short telomere formation at DR_L-T2 could be influenced
309 by the chromatin state of the iciHHV-6B genome, the 4B-11p15.5 lymphoblastoid cell line was
310 treated with TSA. The cells were grown in medium supplemented with various concentrations of TSA
311 for approximately 5 days, and the DR_L-T2 truncation assay (DR_L-T2-STELA) was conducted on DNA
312 extracted from TSA-treated and control cells (Figure 5D). The frequency of truncation events at DR_L-
313 T2 increased significantly from 0.0162 to 0.0290 per cell at the highest TSA concentration. This
314 suggests that iciHHV-6B chromatin conformation influences the chance of t-loop formation at the
315 telomere-like repeats within the viral genome and subsequent excision events.
316 Loss of the terminal DR_L via t-loop formation and excision at DR_L-T2 was expected to
317 generate a short novel telomere detected as a STELA fragment consisting of a flanking region of DR_L
318 of approximately 600 bp plus a telomere repeat array limited to the length of the DR_L-T2 (Figure 5A).
319 Some of the DR_L-T2-STELA amplicons were larger than the expected 0.7-0.9 kb (Figure 5B). We
320 showed that these amplicons lack DR3 or DR8 sequences (Figure 5E), thus indicating they are not

molecules truncated at different sites within DR_L. We hypothesized that the intermediate length amplicons (longer than 0.7-0.9kb, Figure 5B) could have arisen by telomerase-mediated lengthening of newly formed telomeres at the DR_L-T2 truncation site. To address this, six of the lengthened amplicons from three DNA samples (4B-11p15.5, d56 and NWA008) were sequenced. All comprised the expected flanking sequence followed by a uniform array of (TTAGGG) repeats exceeding the known length of DR_L-T2 for the sample, thus showing that some of the novel telomeres formed at DR_L-T2 had been lengthened (Figure 5 – figure supplement 1). Telomerase activity was detected at a low level in the 4B-11p15.5 and other iciHHV-6B LCLs (Figure 5 – figure supplement 1), consistent with a telomerase-mediated lengthening of newly formed telomeres.

The percentage of DR_L-T2 telomeres that had undergone lengthening varied between the iciHHV-6B samples and cell types (Figure 5F). The proportion of lengthened telomeres was higher in the pluripotent cell lines, blood DNA and saliva samples, and lower in the LCLs and sperm samples. This may reflect the level of telomerase activity in the cells or their progenitors, but it may also indicate variable responses to extremely short telomeres.

Partial excision of iciHHV-6B genomes and novel telomere formation at DR_R-T1

Processes driven by t-loop formation can also facilitate the release of U in its entirety with a single DR from iciHHV-6B (reconstituted with both PAC1 and PAC2) as a circular (U-DR) molecule (Arbuckle *et al.*, 2013; Borenstein & Frenkel, 2009; Huang *et al.*, 2014; Wood & Royle, 2017). The reciprocal product of U-DR excision is expected to be a truncation of the iciHHV-6B genome at DR_R-T1 with new telomere formation. To explore this, we exploited the variable nature of pvT1. Differences between DR_R-pvT1 and DR_L-pvT1 within a single iciHHV-6B genome were found in many of the iciHHV-6B samples analysed (24/35, 68.6%) (Figure 6A, Figure 6 – figure supplement 1). These differences were usually a consequence of loss or gain of a small number of repeats, although in some cases they involved single base substitutions that converted one repeat type to another. These differences made it possible to measure the frequency of truncations and new telomere formation at DR_R-T1 via a two-step process.

First, the iciHHV-6B-associated telomeres were amplified using STELA with the DR1R primer that can generate products from a telomere at DR_L-T1 (from normal, full-length iciHHV-6B) or DR_R-T1 (following U-DR excision). Second, to distinguish between these STELA products, the PCR amplicons were subjected to nested PCR to amplify DR_L-pvT1 and DR_R-pvT1 (Figure 6A). The sizes of the pvT1 amplicons indicated whether the STELA products in the primary PCR had been derived from telomeres at DR_L or DR_R (Figure 6B), and selected sequencing was used to confirm. Truncations at

354 DR_R-T1 were detected in all ten iciHHV-6B samples analysed, and the frequency of newly formed
355 telomeres at DR_R-T1 was estimated to be 0.0002–0.0029 per cell (Figure 6C, Supplementary Table 5).

356

357 **Generation of DR-only iciHHV-6B by partial excision of full-length iciHHV6-B genomes in the**
358 **germline**

359 The frequency of truncations and new telomere formation at DR_R-T1 in sperm DNA from
360 iciHHV-6B carriers raised the strong possibility that such events could explain how individuals may
361 inherit integrations consisting only of DR (DR-only iciHHV-6A/6B) (Huang *et al.*, 2014; Liu *et al.*, 2020;
362 Ohye *et al*, 2014). To date, we have identified three individuals (308006 and SAL018 in the present
363 study, and KEN071 (Huang *et al.*, 2014)) who carry iciHHV-6B DR-only. Comparison of pvT1 repeat
364 patterns in these samples with DR_R-pvT1/DR_L-pvT1 repeat patterns in full length iciHHV-6B
365 suggested shared ancestry between these individuals with DR-only iciHHV-6B and those with full
366 length iciHHV-6B (Figure 3A). To investigate this, attempts were made to amplify and sequence the
367 subtelomere-iciHHV-6B junction, based on previously described junction fragments (Tweedy *et al.*,
368 2016; Zhang *et al.*, 2017) and using primers that anneal in the subtelomeric regions of various
369 chromosomes (Figure 3B). Using this approach, we found that the DR-only iciHHV-6B in SAL018 and
370 KEN071 share the common 17p (major) subtelomere-iciHHV-6B junction that is also found in
371 801018, d44 and others (Figure 3C). Similarly, the pattern of telomere and degenerate repeats
372 across a subtelomere-iciHHV-6B junction (amplified by subtelomere primer 2p2) in the DR-only
373 iciHHV-6B sample 308006, closely matched those in full length iciHHV-6B individuals 401027 and
374 410005 (Figure 3C). The existence of shared integration sites for the full-length and DR-only iciHHV-
375 6B carriers at two different chromosome ends clearly establishes that the DR-only status has arisen
376 independently, on at least two occasions, by loss of U and one copy of DR in the germline of an
377 ancestor with a full-length iciHHV-6B genome.

378

379 **Evidence of viral transmission from iciHHV-6B carrier mother to non-iciHHV-6B son**

380 It has been shown that iciHHV-6A can reactivate in an immune-compromised setting (Endo
381 *et al.*, 2014) and there is evidence of transplacental transmission of reactivated iciHHV-6A/6B
382 (Gravel *et al.*, 2013). Despite these examples, the high prevalence of HHV-6B in populations has
383 made it difficult to determine how often iciHHV-6B reactivation occurs. The evidence for frequent
384 partial or complete release of iciHHV-6B genomes in somatic cells and the germline presented above
385 suggests that opportunities for reactivation may be more common than currently appreciated. To

explore this, we used DR_R-pvT1 analysis to investigate the relationship between strains of iciHHV-6B and low-level acqHHV-6B within families. In one family (Rx-F6a), the mother (G3P1) had a low acqHHV-6B load in saliva (0.00035 copies per cell), but both her children were iciHHV-6B carriers. The DR_R-pvT1 repeat patterns in the children were identical and presumed to have been inherited from the father, who was not available for testing. Clearly the mother in this family had a different HHV-6B strain with a distinct DR_R-pvT1 repeat pattern (Figure 7).

Quantification of HHV-6B in saliva samples from another family (Rx-F3a) showed that the mother (G3P2) was an iciHHV-6B carrier and that her daughter (G4P3) had approximately 2 copies of iciHHV-6B per cell. Identical DR_R-pvT1 repeat patterns between the mother and daughter proved maternal inheritance of one iciHHV-6B copy. A second, distinct DR_R-pvT1 repeat pattern in the daughter was assumed to represent iciHHV-6B inherited from the father, who was not available for testing. The son (G4P1) had 0.00025 copies of HHV-6B per cell in saliva DNA, consistent with the level expected from acqHHV-6B infection. Importantly, the DR_R-pvT1 repeat pattern in the son (G4P1) was identical to that in the mother and one copy of iciHHV-6B in his sister. This repeat pattern was not seen outside this family among 102 DR_R-pvT1 repeat patterns (Figure 1 – figure supplement 1). These observations strongly suggest that iciHHV-6B genome excision occurred in the mother and that the reactivated HHV-6B was then transmitted to the non-iciHHV-6B son, who retained residual viral sequences in his saliva.

Discussion

The discovery of germline transmission of chromosomally-integrated HHV-6A/6B genomes has raised questions about the possible relationship between iciHHV-6A/6B carrier status and lifelong disease risk (Gravel *et al.*, 2015) (Gaccioli *et al.*, 2020; Hill *et al.*, 2017). Events that could have deleterious consequences include full viral reactivation (Endo *et al.*, 2014; Gravel *et al.*, 2013; Hall *et al.*, 2010), intermittent expression of iciHHV-6A/6B genes that may elicit intermittent immune and inflammatory responses over a lifetime (Peddu *et al.*, 2019), and an impact on telomere stability and function (Huang *et al.*, 2014; Prusty *et al.*, 2013; Wood & Royle, 2017; Zhang *et al.*, 2017).

Progress towards understanding the potential impact of iciHHV-6A/6B carrier status has been advanced by the recent increase in the number of HHV-6A/6B genome sequences available (Aswad *et al.*, 2021; Greninger *et al.*, 2018; Zhang *et al.*, 2017). This has shown that most iciHHV-6A/6B genomes in populations are derived from a small number of ancient telomere-integration events. Here we have expanded the number of sequenced iciHHV-6A/6B genomes from individuals

in Europe and North America and developed a web-based HHV-6 Explorer that can be used to interrogate diversity and functionality between inherited and acquired HHV-6A or HHV-6B genomes. The HHV-6 Explorer includes the sequence of 84 complete or nearly complete iciHHV-6A/6B genomes representative of the various known clades in the phylogenetic network and genome sequences from 28 HHV-6A/6B viruses circulating in populations. Using the HHV-6 Explorer we displayed two mutations that introduced stop codons in U79 in three of 14 iciHHV-6A samples in the 17p clade and in U14 in one of three iciHHV-6B samples in the 17p (minor) clade (Figure 2 – figure supplement 1) so demonstrating that each mutation arose after integration. The presence of an inactivating iciHHV-6A/6B mutation in some but not all descendants of a particular ancestral integration event adds a further complication to understanding the potential lifetime risk for individual iciHHV-6A/6B carriers.

The relationship between iciHHV-6A/6B carrier status and potential associated disease risk may also be influenced by interactions between the integrated viral genome and genes or chromatin on the chromosome carrying the viral genome (Gravel *et al.*, 2015; Wood & Royle, 2017). It is therefore important to have a rapid method to distinguish between viral strains and integration sites, which is offered by the hypervariable pvT1 region in HHV-6B. Length variation across pvT1 is mostly attributable to the diverse interspersion of (CTAGGG) and canonical (TTAGGG) telomere repeat sequences in the middle of pvT1 amplicons. Notably, short blocks of $(CTAGGG)_n$ repeats are highly unstable in human telomeres in somatic and germline cells, probably due to replication errors and *in vitro* studies showed that $(CTAGGG)_n$ repeats bind efficiently to POT1, a component of Shelterin (Barrientos *et al*, 2008; Baumann & Cech, 2001; de Lange, 2018; Lim *et al*, 2009; Loayza *et al*, 2004; Mendez-Bermudez *et al*, 2009). In many cases analysis of the DR_R-pvT1 repeat pattern alone can be used as a rapid and inexpensive way to predict the phylogenetic clade and integration site of an iciHHV-6B genome.

DR_R-pvT1 analysis is also an excellent tool for tracking acqHHV-6B transmission in families as shown by the evidence that community-acquired HHV-6 transmission usually occurs between family members, with maternal transmission most common. We showed that DR_R-pvT1 repeat patterns can be used effectively to discriminate between HHV-6B strains circulating in communities (61/63 different pvT1 sequences in saliva from healthy non-iciHHV-6B donors in the UK). In the future, pvT1 analysis could be used to trace patterns of transmission more generally. This may be particularly important in the setting of organ and tissue transplants (Hill, 2019). For example, reactivation of iciHHV-6B from a donor tissue could be monitored and differentiated from HHV-6B acquired by the recipient in early childhood or to identify cases of multiple infections by different strains of HHV-6B.

The iciHHV-6B and free HHV-6B viruses in communities must have evolutionary histories that are interlaced but these are difficult to disentangle as there is little understanding of HHV-6 telomeric integration and iciHHV-6B excision and reactivation. The current picture indicates a modest number of ancient iciHHV-6B clades (in Europe and North America at least) some of which are accumulating mutations that would prevent full reactivation (discussed above). There is also at least one example of an iciHHV-6B genome with high sequence homology to a group of genome sequences from acqHHV-6B (Aswad *et al.*, 2021; Greninger *et al.*, 2018), which complicates interpretation of HHV-6B phylogenetic relationships (Forni *et al*, 2020). Indirectly this suggests that some modern circulating strains retain the capacity for germline integration into telomeres and to be passed on or that iciHHV-6B can reactive and be transmitted, re-entering the reservoir of circulating strains. We demonstrated that some copies of HHV-6B in saliva acquire a telomere, indicative of integration in somatic cells *in vivo* and as previously detected *in vitro* (Arbuckle *et al.*, 2010). The viral load in the saliva samples was low, as seen in some other studies (Leibovitch *et al*, 2014; Leibovitch *et al*, 2019; Turriziani *et al*, 2014), and the number of HHV-6B genomes with a telomere was small (Figure 4, Supplementary Table 3), which is consistent with the majority of HHV-6B genomes present as viral particles in saliva (Jarrett *et al*, 1990). The approach we used to detect telomeric integration in saliva could, in principle, be used to detect HHV-6B integration events in sperm from healthy non-iciHHV-6B men (Neofytou *et al*, 2009) (Godet *et al*, 2015; Kaspersen *et al*, 2012). This would address the outstanding question of whether current HHV-6B strains circulating in communities can integrate in the germline.

Previously we have proposed that iciHHV6A/6B genomes can be excised from telomeres in a one or two-step process as by-products of t-loop processing (Huang *et al.*, 2014; Wood & Royle, 2017). In this study we measured the frequency of iciHHV-6B excision events, by detection of novel telomeres at DR_L-T2 and for the first time at DR_R-T1, in unrelated iciHHV-6B carriers and in different tissues and cell types. The frequencies of iciHHV-6B truncations at DR_L-T2 (range, 0.014 - 0.0031 per cell) and DR_R-T1 (range, 0.0002-0.0029 per cell) are not directly comparable because they were ascertained by different approaches but both are surprisingly high *in vivo* (Figure 5, Figure 6). This demonstrates that tissues in iciHHV-6B carriers must be mosaic for different compositions of the iciHHV-6B genome. The telomeres formed at DR_L-T2 were expected to be particularly short, limited to the length of the (TTAGGG) repeat array at T2. However, a cell with a small number of very short telomeres will elicit a telomere-mediated DNA damage response and entry into cellular senescence (Cesare *et al*, 2013; d'Adda di Fagagna *et al*, 2003; de Lange, 2018; Takai *et al*, 2003) so preventing proliferation of a cell with a potentially unstable residual iciHHV-6B genome. It is therefore remarkable that a high percentage of newly formed telomeres at DR_L-T2 were lengthened. The

frequency of DR_L-T2 telomere lengthening was highest in circulating white blood cells and in two pluripotent cell lines (Figure 5) consistent with lengthening by telomerase. From these observations and the increase in viral genome excision events in TSA treated cells, we also propose that iciHHV-6A/6B genomes are more likely to be excised and reactivated in undifferentiated or pluripotent cells. By extrapolation, the potential for iciHHV-6A/6B genome excision, viral gene expression or full reactivation has the potential to be deleterious during early development (Miura *et al.*, 2020).

Finally, we present two lines of evidence that iciHHV-6B genome can be excised and re-enter the reservoir of circulating HHV-6B strains. First, we identified individuals with full-length iciHHV-6B or DR-only genomes that fall into the same clade in the phylogenetic tree (Figure 3). These integrated full-length iciHHV-6B or DR-only genomes share similar pvT1 repeat patterns and subterminal-iciHHV-6B junction sequences. This demonstrates that the different iciHHV-6B structures are carried in the same telomere-allele at the particular chromosome end and it proves that these DR-only carriers have arisen by germline excision of U-DR in an ancestor. The fact that this has occurred independently at least twice suggests this is a relatively common event, and this is supported by our evidence that new telomere formation at DR_R-T1 occurs at a measurable frequency in sperm DNA. Second, we show an example of probable reactivation of iciHHV-6B in a mother with transmission to her son, who carries a very low load of acqHHV-6B with the same distinctive DR_R-pvT1 repeat pattern in his saliva. This observation warrants further research to determine how frequently HHV-6B is transmitted from iciHHV-6B parent to their non-iciHHV-6B children but it requires the use of a hypervariable marker, such as pvT1, that has the power to discriminate between HHV-6B strains.

Materials and Methods

Saliva collection and DNA extraction

The study was conducted in accordance with the Declaration of Helsinki and with the approval of the University of Leicester's Research Ethics Committee (refs: 10553-njr-genetics; njr-61d3). Saliva samples were donated by individuals and members of families (all 18 years or older) with informed consent and were given anonymous identifiers at the point of collection (Garrido-Navas *et al*, 2020). Approximately 1.5 ml of saliva was collected in a OraGEN saliva collection tube (Genotek, Ottawa, Canada), and DNA was extracted from 500 µl following the manufacturer's instructions.

Identification of DNA samples and cell lines with iciHHV-6A/6B or acqHHV-6B

The full list of iciHHV-6A/6B-positive DNA samples and cell lines used in this study is given in Supplementary Table 1 with available information on donor ethnicity and iciHHV-6A/6B chromosomal location. To interrogate any relationship between iciHHV-6A/6B carrier status and heart failure, the BIOlogy Study to TAilored Treatment in Chronic Heart Failure (BIOSTAT-CHF) cohort (Voors *et al*, 2016) was screened. The BIOSTAT-CHF study complied with the Declaration of Helsinki and was approved by the relevant ethics committee in each centre, while all participants gave their written, informed consent to participate. The 2470 blood DNAs from Europeans in the BIOSTAT-CHF cohort was screened using PCR assays to detect various regions of the viral genome (U11, DR3 and DR5 in HHV-6A, and DR7 in HHV-6B) (Huang *et al.*, 2014; Zhang *et al.*, 2017). This identified 19 iciHHV-6A/6B positive samples (nine iciHHV-6A, 0.36%, and ten iciHHV-6B, 0.40%, one of which was iciHHV-6B DR-only). Four iciHHV-6B carriers were identified among the saliva donors: two with a single copy of iciHHV-6B, one with two copies of iciHHV-6B, and one with iciHHV-6B DR-only. The saliva samples were also screened for acqHHV-6B using ddPCR, described below. Additionally, two kidney DNA samples (part of the TRANScriptome of renaL humAn TissuE (TRANSLATE) study (Marques *et al*, 2015; Rowland *et al*, 2019)) were positive for DR3 by PCR assay and were confirmed as acqHHV-6B by ddPCR.

HHV-6B quantification by ddPCR

HHV-6B copy number was estimated by ddPCR as describe previously (Bell *et al*, 2014). Hydrolysis probe ddPCRs (20 μl volumes) consisted of 1 x ddPCR Supermix for probes without dUTP (Bio-Rad Laboratories), virus-specific primers (HHV-6B POL F and HHV-6B POL R) and FAM-labelled HHV-6B POL (U38) probe (Eurogentec; Supplementary Table 6) at 300 nM and 200 nM respectively, 1 x RPP30 primer/HEX labelled probe mix (Bio-Rad Laboratories), 1μl XhoI digestion mix consisting of 5U XhoI restriction enzyme and 1 x NEB buffer 2.1 (New England Biolabs), and 10 ng genomic DNA for iciHHV-6B samples or 200 ng DNA for non-iciHHV-6B samples. Assays to quantify acqHHV-6B were carried out in triplicate. DNA from the HT1080 osteosarcoma-derived, established cell line was used as a negative control to detect non-specific amplification or contamination, and water was used as a no-template control. As very low viral copy number were expected, the ddPCR reactions were set up in a PCR-clean room where no HHV-6 PCR had previously been conducted. Droplets were generated using QX200 Droplet Generator (Bio-Rad Laboratories) with 70 μl Droplet Generation Oil for Probes or 70 μl Droplet Generation Oil for Evegreen, as appropriate (Bio-Rad Laboratories). Thermocycling was carried out according to the manufacturer's instructions on a Veriti (Bio-Rad Laboratories). QX200 Droplet Reader and QuantaSoft analysis software (Bio-Rad

Laboratories) were used to count droplets and to calculate the estimated copy number. The number of DR copies per cell in iciHHV-6B DNA was determine by ddPCR with primers DR6B-F and DR6B-R and DR6B FAM-labelled hydrolysis probe (Eurogentec, Liège, Belgium) together with the HEX-labelled RPP30 reference probe (Bell *et al.*, 2014).

Absolute quantification of DR and PAC1 was determined by ddPCR using DNA intercalating dye, EvaGreen. EvaGreen ddPCRs (20 μl volumes) consisted of 1 x ddPCR EvaGreen Supermix (Bio-Rad Laboratories), virus-specific primers for DR (DR6B-F and DR6B-R) or PAC1 (PAC1F and PAC1R-33) at 300 nM, 1μl XhoI digestion mix consisting of 5U XhoI restriction enzyme and 1 x NEB buffer 2.1 (New England Biolabs, Ipswich, Massachusetts), and 10 ng genomic DNA for iciHHV-6B samples or 200 ng DNA for non-iciHHV-6B samples.

Cell culture and TSA treatment

LCLs with iciHHV-6B were cultured in RPMI 1640 medium as described previously (Huang *et al.*, 2014). The CRL-1730 adherent human vascular endothelial cell line derived from umbilical cord vein (ATCC, (Shioda *et al.*, 2018)) was cultured in F-12K medium (Gibco/ThermoFisher Scientific) supplemented with 10% heat inactivated foetal bovine serum (Gibco/ThermoFisher Scientific), 0.1 mg/ml heparin (Sigma-Aldrich, Darmstadt, Germany) and 1% endothelial growth supplement (BD Biosciences). The adherent mesenchymal stem cell line derived by explant culture from umblical cord, d37 (gifted by Dr Sukhvir Rai, University of Leicester), was cultured in human mesenchymal stem cell growth media (MSCBM hMSC Basal Medium, Lonza, Basel, Switzerland) supplemented with mesenchymal stem cell growth supplements (MSCGM hMSC SingleQuot Kit, Lonza, Basel, Switzerland).

For TSA treatment, 2 x 10^6 cells from the 4B-11p15.5 iciHHV-6B LCL were suspended in RPMI 1640 medium supplemented with 0, 100 or 200 ng/ml Trichostatin A (Sigma-Aldrich, Darmstadt, Germany) in three biological replicates. After 124 h (5 days), cells were pelleted at 1200 rpm for 8 min, washed twice with phosphate-buffered saline and snap-frozen on dry ice. DNA was extracted using phenol-chloroform and precipitated using ethanol. The DNA pellet was washed with 80% ethanol, briefly air-dried and dissolved in nuclease-free water. DR_L-T2 STELA (see below) was conducted on extracted DNA using primer UDL6R to detect telomeres at DR_L T2, as described previously (Huang *et al.*). STELA was carried out two times on DNA from each treatment from three biological replicates.

Whole iciHHV-6A/6B genome sequencing

582 Ten iciHHV-6A and five iciHHV-6B genomes were sequenced and annotated as described previously
583 (Huang *et al.*, 2014; Zhang *et al.*, 2017). Pooled, overlapping PCR amplicons (100 ng) were sheared
584 using a Covaris S220 sonicator to an approximate size of 450 bp. Sequencing libraries were prepared
585 using the LTP library preparation kit for Illumina platforms (Kapa Biosystems, Germany). The libraries
586 were then processed for PCR (7 cycles) using the LTP library preparation kit and employing NEBNext
587 multiplex oligos for Illumina index primer pairs set 1 (New England Biolabs, Ipswich, Massachusetts).
588 Sequencing was performed using a NextSeq 500/550 mid-output v2.5 300 cycle cartridge (Illumina,
589 San Diego, California) to produce 6-9 million paired-end 150 base reads per sample. The annotated
590 sequences were deposited in NCBI GenBank under accession numbers: MW049313-MW049327.

591

592 **Genome sequence analysis**

593 94 complete or near-complete HHV-6A/6B sequences were downloaded from NCBI GenBank
594 (Supplementary Table 1) and, together with the 15 newly sequenced genomes, were aligned using
595 MAFFT (v7.407, (Katoh & Standley, 2013)) with default parameters. The alignment was trimmed
596 using trimAl (v1.4.1, (Capella-Gutierrez *et al*, 2009)) to remove gaps. Phylogenetic networks were
597 inferred using FastME (v2.1.6.1), a distance-based algorithm, with bootstrap values calculated from
598 100 replicates. Phylogenetic networks were plotted using Interactive Tree of Life browser application
599 (https://itol.embl.de, v6.1) (Letunic & Bork, 2016). The time to the most recent common ancestor
600 was estimated using Network 10.0 (Fluxus-engineering, Colchester, United Kingdom) using rho
601 values calculated by Network (Forster *et al*, 1996) and an assumed mutation rate of 0.5×10^{-9}
602 substitutions per base per year (Scally & Durbin, 2012; Zhang *et al.*, 2017).

603

604 **Development of the HHV-6 explorer**

605 The HHV-6 Counter takes a fasta multiple alignment and compares each sequence to a selected
606 reference HHV-6 strain to generate counts of genetic variation (substitutions, insertions, deletions)
607 from overlapping or non-overlapping windows across the HHV-6 genome. If a corresponding
608 genbank file for the reference is present, HHV-6 Counter will also provide windowed counts for
609 coding sequence and amino acid variation across the genome and for each gene. This includes
610 missense/nonsense changes, in-frame insertions/deletions, nonsense insertions, potential splice site
611 changes, loss of start or stop and tracking of frameshift changes. Windows which contain non-
612 standard base characters or have sequence gaps due to method failures are flagged but their counts

are still retained in the results. HHV-6 Counter exports the count windows both as a series of Excel files and as a python panda pickle file for use in the HHV-6 Explorer.

The HHV-6 Explorer is based on plotly Dash (https://dash.plotly.com/) and, using the output from HHV-6 Counter, allows the graphical display of variation counts for different strains across the HHV-6 genomes and/or on a per gene basis compared against a selected reference HHV-6 strain. It also displays a multiple alignment for the selected gene. A pre-populated version of HHV-6 Explorer containing the data from this manuscript can be found at https://www.hhv6explorer.org/ . The source code for HHV-6 Explorer and HHV-6 Counter is available from https://github.com/colinveal/HHV6-Explorer.

PCR primers and other oligonucleotides.

The primer sequences used in this study and the Taqman hydrolysis probes are listed in Supplementary Table 6.

Amplification and analysis of subtelomere-iciHHV-6B junctions

Subtelomere-iciHHV-6B junctions were amplified by PCR (33 cycles) using a trial an error approach with primer DR8F(A/B) and various primers known to anneal to chromosomal subtelomere regions (Zhang *et al.*, 2017). Amplicons were purified using a Zymoclean gel DNA recovery kit (Zymo Research, Irvine, California) and sequenced using primer DR8FT2 or the appropriate subtelomere primer (Supplementary Table 6). The number and pattern of telomere repeats (TTAGGG) and degenerate telomere-like repeats across the subtelomere-iciHHV-6B junction amplicons were identified and colour-coded manually to generate repeat patterns.

Amplification and analysis of HHV-6B DR_R-pvT1 and DR_L-pvT1

DR_R- pvT1 was amplified by PCR using primers DR1R and U100Fw2 in the first round (94°C, 1.5 min; 25 cycles 94°C 15 s, 62°C 30 s, 68°C 10 min; 68°C 2 min) and primers DR421R and TJ1F in the second round (94°C, 1.5 min; 25 cycles 94°C 15 s, 64°C 30 s, 68°C 1.5 min; 68°C 2 min). DR_L-pvT1 was amplified by STELA (see below) followed by a secondary PCR using primers DR421R and TJ1F. The short pvT1 amplicons were size-separated by electrophoresis in a 3% NuSieve (Lonza, Basel, Switzerland) agarose gel, extracted and Sanger sequenced using primer TJ1F. The number and

pattern of (TTAGGG) and degenerate telomere-like repeats were identified and colour-coded manually to generate repeat maps.

STELA and detection of newly formed telomeres at DR_R-T1 and DR_L-T2

The telomere at the end of the iciHHV-6B genome was amplified by STELA using the DR1R primer and Telorette2/Teltail essentially as described previously (Huang *et al.*, 2014) (Jeyapalan *et al*, 2008). DNA was diluted to 250-1000 pg/µl for cell line DNA, 500 pg/µl for saliva DNA, 600 pg/µl for blood DNA and 1000 pg/µl for sperm DNA. The primer concentrations in each 10 µl STELA reaction were 0.3 µM DR1R, 0.225 µM Telorette2 and 0.05 µM Teltail. *Taq* polymerase (Kapa Biosystems, Germany) was used at 0.04 U/µl and *Pwo* (Genaxxon Bioscience, Ulm, Germany) at 0.025 U/µl. The STELA PCRs were cycled 25 times.

To detect telomeres at DR_R-T1, STELA was conducted as above using primers DR1R and Telorette2/Teltail on iciHHV-6B DNA samples that showed a length difference between DR_L-pvT1 and DR_R-pvT1. Next the STELA reaction product (1µl) was diluted 1:10 in water and used as input for PCR of pvT1 using primers DR421R and TJ1F (25 cycles). The amplicons were size-separated by agarose gel electrophoresis to distinguish DR_R-T1-associated telomeres from the majority of DR_L-T1-associated telomeres. The remainder of the undiluted STELA product was size-separated by agarose gel electrophoresis and amplified telomeres detected by Southern blot hybridisation to a radiolabelled $(TTAGGG)_n$ probe.

To detect telomeres at DR_L-T2, primer UDL6R was used in STELA reactions instead of primer DR1R with 250-1000 pg genomic DNA per reaction and cycled 26 times. Amplicons hybridising to the radiolabelled $(TTAGGG)_n$ probe that migrated at less than 900 bp were counted as unlengthened truncations, those between 900 bp and 8.6 kb were counted as lengthened truncations, and those larger than 8.6 kb were not counted as truncations. The number of truncations per cell was estimated by converting the amount of input DNA to cell equivalents on the assumption that a cell contains 6.6 pg DNA (or 3.3 pg for a haploid sperm cell) and dividing the number of truncations (lengthened and unlengthened) by the number of cells screened. To sequence DR_L-T2-associated telomeres, STELA products were extracted from agarose gel slices using repeated freeze-thawing and reamplified using primers DR8RT2 and Telorette2. The recovered amplicons were Sanger sequenced.

Detection of integrated HHV-6B in individuals with acqHHV-6B

675 STELA was carried out on genomic DNA from individuals with a known copy number of acqHHV-6B,
676 measured by ddPCR. As the copy number of acqHHV-6B was low and telomere integration events
677 expected to be lower, various precautions were introduced for these experiments. STELA reactions
678 were set up in a room previously unused for any STELA or HHV-6 experiments. In addition to avoid
679 contamination with previously generated iciHHV-6A/6B STELA products, STELA primers with new
680 barcodes (Telorette2BC28/Teltail2BC38) and a new a flanking primer (DR2RSTELA) were used. The
681 DR2RSTELA primer anneals upstream of the DR1R primer used for other iciHHV-6A/6B STELA
682 reactions. STELA reactions were set up as explained above, but with 2-5 ng genomic DNA per
683 reaction and cycles 25 times. Next 1 µl of STELA reaction product was diluted 1:10 in water and used
684 as input for amplification of DR_L-pvT1, using primers DR421R and TJ1F (25 cycles). The amplicons
685 were sequenced using TJ1F to confirm that the DR_L-pvT1 sequence in the amplified telomere was the
686 same HHV-6B strain as present in that saliva sample. The remainder of the undiluted STELA product
687 was size-separated by agarose gel electrophoresis and detected by Southern blot hybridisation to a
688 radiolabelled $(TTAGGG)_n$ probe. As a control for non-specific amplification from another telomere or
689 elsewhere in the human genome, 900 STELA reactions were conducted each with 5 ng genomic DNA
690 from a HHV-6A/6B free cell line, HT1080 (4500 ng total). No STELA amplicons were generated from
691 the HT1080 control reactions.

692

693 **DR circles**

694 Double restriction digests were carried out at 37C for 1 hour using 10 U of each enzyme (XbaI and
695 ScaI-HF, or PstI and SacI) and 1x NEB CutSmart Buffer (New England Biolabs, Ipswich, Massachusetts)
696 in 500 uL reactions containing 10 µg 4B-11p15.5 or 1B-HHV-6B DNA. Enzymes were heat inactivated
697 at 80C for 20 minutes. Control DNA was treated without any restriction enzymes. Diluted DNA was
698 amplified using PCR with primers DR8F(A/B) and DR3R with a 10 minute extension time (26 cycles).
699 PCR products were size-separated on a 0.8% agarose gel with electrophoresis and amplicons were
700 detected by Southern blot hybridisation to a radiolabelled telomere $(TTAGGG)_n$ probe.
701

702 **Statistical analysis**

703 Data are expressed as means ± standard error of the mean (SEM). Mann-Whitney test was used to
704 compare unpaired groups of ranked data obtained from assays conducted on DNA derived from the
705 same biological sample type (Figure 4C, 4F). The Wilcoxon test was used to compare paired groups
706 of data obtained from treated and untreated samples. Statistical analyses were performed using

Prism software (Version 9.0, Graphpad Software). Outliers were not removed from data sets. Samples sizes were based on availability of suitable biological materials.

Acknowledgements

We thank Dr Sukhvir Rai (University of Leicester) for the gift of the d37 mesenchymal stem cell line; Dr Yan Huang, Dr Enjie Zhang, Dilan Patel and Ryan Mate for preliminary work that contributed the initiation of this study; and Drs Chiara Batini, Celia May and Jon Wetton for their advice on phylogenetics and hypervariable markers. We also thank Matthew Denniff and Charlotte Hogg for help with sample acquisition and TRAP assays respectively. We also acknowledge the contribution of members of the BIOSTAT-CHF consortium.

Funding

MLW was funded UK Biotechnology and Biological Sciences Research Council (BBSRC) and the Midlands Integrative Biosciences Training Partnership (MIBTP 1645656). The work was supported in part by the UK Medical Research Council (G0901657 to N.J.R.); also the Canadian Institutes of Health Research grants (MOP_123214). The BIOSTAT-CHF project was funded by a grant from the European Commission (FP7-242209- BIOSTAT-CHF).

Competing interests: none of the authors have competing interests

References

Ablashi D, Agut H, Alvarez-Lafuente R, Clark DA, Dewhurst S, DiLuca D, Flamand L, Frenkel N, Gallo R, Gompels UA *et al* (2014) **Classification of HHV-6A and HHV-6B as distinct viruses**. *Arch Virol* **159**: 863-870. https://doi.org/10.1007/s00705-013-1902-5

Achour A, Malet I, Deback C, Bonnafous P, Boutolleau D, Gautheret-Dejean A, Agut H (2009) **Length variability of telomeric repeat sequences of human herpesvirus 6 DNA**. *J Virol Methods* **159**: 127-130. https://doi.org/10.1016/j.jviromet.2009.03.002

Aihara Y, Ito SI, Kobayashi Y, Yamakawa Y, Aihara M, Yokota S (2003) **Carbamazepine-induced hypersensitivity syndrome associated with transient hypogammaglobulinaemia and reactivation of human herpesvirus 6 infection demonstrated by real-time quantitative polymerase chain reaction**. *Br J Dermatol* **149**: 165-169. https://doi.org/10.1046/j.1365-2133.2003.05368.x

Arbuckle JH, Medveczky MM, Luka J, Hadley SH, Luegmayr A, Ablashi D, Lund TC, Tolar J, De Meirleir K, Montoya JG *et al* (2010) **The latent human herpesvirus-6A genome specifically integrates in telomeres of human chromosomes in vivo and in vitro**. *Proc Natl Acad Sci U S A* **107**: 5563-5568. https://doi.org/10.1073/pnas.0913586107

Arbuckle JH, Pantry SN, Medveczky MM, Prichett J, Loomis KS, Ablashi D, Medveczky PG (2013) **Mapping the telomere integrated genome of human herpesvirus 6A and 6B**. *Virology* https://doi.org/10.1016/j.virol.2013.03.030

Asano Y, Yoshikawa T, Suga S, Kobayashi I, Nakashima T, Yazaki T, Kajita Y, Ozaki T (1994) **Clinical features of infants with primary human herpesvirus 6 infection (exanthem subitum, roseola infantum)**. *Pediatrics* **93**: 104-108.

Aswad A, Aimola G, Wight D, Roychoudhury P, Zimmermann C, Hill J, Lassner D, Xie H, Huang ML, Parrish NF *et al* (2021) **Evolutionary History of Endogenous Human Herpesvirus 6 Reflects Human Migration out of Africa**. *Mol Biol Evol* **38**: 96-107. https://doi.org/10.1093/molbev/msaa190

Barrientos KS, Kendellen MF, Freibaum BD, Armbruster BN, Etheridge KT, Counter CM (2008) **Distinct functions of POT1 at telomeres**. *Mol Cell Biol* **28**: 5251-5264. https://doi.org/10.1128/MCB.00048-08

Baumann P, Cech TR (2001) **Pot1, the putative telomere end-binding protein in fission yeast and humans**. *Science* **292**: 1171-1175.

Bell AJ, Gallagher A, Mottram T, Lake A, Kane EV, Lightfoot T, Roman E, Jarrett RF (2014) **Germ-line transmitted, chromosomally integrated HHV-6 and classical Hodgkin lymphoma**. *PLoS One* **9**: e112642. https://doi.org/10.1371/journal.pone.0112642

Bonnafous P, Marlet J, Bouvet D, Salame E, Tellier AC, Guyetant S, Goudeau A, Agut H, Gautheret-Dejean A, Gaudy-Graffin C (2018) **Fatal outcome after reactivation of inherited chromosomally integrated HHV-6A (iciHHV-6A) transmitted through liver transplantation**. *Am J Transplant* **18**: 1548-1551. https://doi.org/10.1111/ajt.14657

Bonnafous P, Phan TL, Himes R, Eldin K, Gautheret-Dejean A, Prusty BK, Agut H, Munoz FM (2020) **Evaluation of liver failure in a pediatric transplant recipient of a liver allograft with inherited chromosomally integrated HHV-6B**. *J Med Virol* **92**: 241-250. https://doi.org/10.1002/jmv.25600

Borenstein R, Frenkel N (2009) **Cloning human herpes virus 6A genome into bacterial artificial chromosomes and study of DNA replication intermediates**. *Proc Natl Acad Sci U S A* **106**: 19138-19143. https://doi.org/10.1073/pnas.0908504106

Capella-Gutierrez S, Silla-Martinez JM, Gabaldon T (2009) **trimAl: a tool for automated alignment trimming in large-scale phylogenetic analyses**. *Bioinformatics* **25**: 1972-1973. https://doi.org/10.1093/bioinformatics/btp348

Cesare AJ, Hayashi MT, Crabbe L, Karlseder J (2013) **The telomere deprotection response is functionally distinct from the genomic DNA damage response**. *Mol Cell* **51**: 141-155. https://doi.org/10.1016/j.molcel.2013.06.006

Collin V, Gravel A, Kaufer BB, Flamand L (2020) **The Promyelocytic Leukemia Protein facilitates human herpesvirus 6B chromosomal integration, immediate-early 1 protein multiSUMOylation and its localization at telomeres**. *PLoS Pathog* **16**: e1008683. https://doi.org/10.1371/journal.ppat.1008683

d'Adda di Fagagna F, Reaper PM, Clay-Farrace L, Fiegler H, Carr P, Von Zglinicki T, Saretzki G, Carter NP, Jackson SP (2003) **A DNA damage checkpoint response in telomere-initiated senescence**. *Nature* **426**: 194-198.

Daibata M, Taguchi T, Nemoto Y, Taguchi H, Miyoshi I (1999) **Inheritance of chromosomally integrated human herpesvirus 6 DNA**. *Blood* **94**: 1545-1549.

de Lange T (2018) **Shelterin-Mediated Telomere Protection**. *Annu Rev Genet* **52**: 223-247. https://doi.org/10.1146/annurev-genet-032918-021921

Deng Z, Glousker G, Molczan A, Fox AJ, Lamm N, Dheekollu J, Weizman OE, Schertzer M, Wang Z, Vladimirova O *et al* (2013) **Inherited mutations in the helicase RTEL1 cause telomere dysfunction and Hoyeraal-Hreidarsson syndrome**. *Proc Natl Acad Sci U S A* **110**: E3408-3416. https://doi.org/10.1073/pnas.1300600110

Doksani Y, Wu JY, de Lange T, Zhuang X (2013) **Super-resolution fluorescence imaging of telomeres reveals TRF2-dependent T-loop formation**. *Cell* **155**: 345-356. https://doi.org/10.1016/j.cell.2013.09.048

Endo A, Watanabe K, Ohye T, Suzuki K, Matsubara T, Shimizu N, Kurahashi H, Yoshikawa T, Katano H, Inoue N *et al* (2014) **Molecular and virological evidence of viral activation from chromosomally**

integrated human herpesvirus 6A in a patient with X-linked severe combined immunodeficiency. *Clin Infect Dis* **59**: 545-548. https://doi.org/10.1093/cid/ciu323

Eshki M, Allanore L, Musette P, Milpied B, Grange A, Guillaume JC, Chosidow O, Guillot I, Paradis V, Joly P *et al* (2009) **Twelve-year analysis of severe cases of drug reaction with eosinophilia and systemic symptoms: a cause of unpredictable multiorgan failure**. *Arch Dermatol* **145**: 67-72. https://doi.org/10.1001/archderm.145.1.67

Fekairi S, Scaglione S, Chahwan C, Taylor ER, Tissier A, Coulon S, Dong MQ, Ruse C, Yates JR, 3rd, Russell P *et al* (2009) **Human SLX4 is a Holliday junction resolvase subunit that binds multiple DNA repair/recombination endonucleases**. *Cell* **138**: 78-89. https://doi.org/10.1016/j.cell.2009.06.029

Forni D, Pontremoli C, Clerici M, Pozzoli U, Cagliani R, Sironi M (2020) **Recent Out-of-Africa Migration of Human Herpes Simplex Viruses**. *Mol Biol Evol* **37**: 1259-1271. https://doi.org/10.1093/molbev/msaa001

Forster P, Harding R, Torroni A, Bandelt HJ (1996) **Origin and evolution of Native American mtDNA variation: a reappraisal**. *Am J Hum Genet* **59**: 935-945.

Gaccioli F, Lager S, de Goffau MC, Sovio U, Dopierala J, Gong S, Cook E, Sharkey A, Moffett A, Lee WK *et al* (2020) **Fetal inheritance of chromosomally integrated human herpesvirus 6 predisposes the mother to pre-eclampsia**. *Nat Microbiol* **5**: 901-908. https://doi.org/10.1038/s41564-020-0711-3

Garrido-Navas MC, Tippins F, Barwell J, Hoffman J, Codd V, Royle NJ (2020) **Telomere Instability in Lynch Syndrome Families Leads to Some Shorter Telomeres in MSH2+/- Carriers**. *Life (Basel)* **10** https://doi.org/10.3390/life10110265

Gilbert-Girard S, Gravel A, Artusi S, Richter SN, Wallaschek N, Kaufer BB, Flamand L (2017) **Stabilization of Telomere G-Quadruplexes Interferes with Human Herpesvirus 6A Chromosomal Integration**. *J Virol* **91** https://doi.org/10.1128/JVI.00402-17

Gilbert-Girard S, Gravel A, Collin V, Wight DJ, Kaufer BB, Lazzerini-Denchi E, Flamand L (2020) **Role for the shelterin protein TRF2 in human herpesvirus 6A/B chromosomal integration**. *PLoS Pathog* **16**: e1008496. https://doi.org/10.1371/journal.ppat.1008496

Godet AN, Soignon G, Koubi H, Bonnafous P, Agut H, Poirot C, Gautheret-Dejean A (2015) **Presence of HHV-6 genome in spermatozoa in a context of couples with low fertility: what type of infection?** *Andrologia* **47**: 531-535. https://doi.org/10.1111/and.12299

Gravel A, Dubuc I, Morissette G, Sedlak RH, Jerome KR, Flamand L (2015) **Inherited chromosomally integrated human herpesvirus 6 as a predisposing risk factor for the development of angina pectoris**. *Proc Natl Acad Sci U S A* **112**: 8058-8063. https://doi.org/10.1073/pnas.1502741112

Gravel A, Dubuc I, Wallaschek N, Gilbert-Girard S, Collin V, Hall-Sedlak R, Jerome KR, Mori Y, Carbonneau J, Boivin G *et al* (2017) **Cell Culture Systems To Study Human Herpesvirus 6A/B Chromosomal Integration**. *J Virol* **91** https://doi.org/10.1128/JVI.00437-17

Gravel A, Hall CB, Flamand L (2013) **Sequence analysis of transplacentally acquired human herpesvirus 6 DNA is consistent with transmission of a chromosomally integrated reactivated virus**. *J Infect Dis* **207**: 1585-1589. https://doi.org/10.1093/infdis/jit060

Greninger AL, Knudsen GM, Roychoudhury P, Hanson DJ, Sedlak RH, Xie H, Guan J, Nguyen T, Peddu V, Boeckh M *et al* (2018) **Comparative genomic, transcriptomic, and proteomic reannotation of human herpesvirus 6**. *BMC Genomics* **19**: 204. https://doi.org/10.1186/s12864-018-4604-2

Griffith JD, Comeau L, Rosenfield S, Stansel RM, Bianchi A, Moss H, deLange T (1999) **Mammalian telomeres end in a large duplex loop**. *Cell* **97**: 503-514.

Hall CB, Caserta MT, Schnabel KC, Shelley LM, Carnahan JA, Marino AS, Yoo C, Lofthus GK (2010) **Transplacental congenital human herpesvirus 6 infection caused by maternal chromosomally integrated virus**. *J Infect Dis* **201**: 505-507. https://doi.org/10.1086/650495

Hall CB, Long CE, Schnabel KC, Caserta MT, McIntyre KM, Costanzo MA, Knott A, Dewhurst S, Insel RA, Epstein LG (1994) **Human herpesvirus-6 infection in children. A prospective study of complications and reactivation**. *N Engl J Med* **331**: 432-438. https://doi.org/10.1056/NEJM199408183310703

Hill JA (2019) **Human herpesvirus 6 in transplant recipients: an update on diagnostic and treatment strategies**. *Curr Opin Infect Dis* **32**: 584-590. https://doi.org/10.1097/QCO.0000000000000592

Hill JA, Magaret AS, Hall-Sedlak R, Mikhaylova A, Huang ML, Sandmaier BM, Hansen JA, Jerome KR, Zerr DM, Boeckh M (2017) **Outcomes of hematopoietic cell transplantation using donors or recipients with inherited chromosomally integrated HHV-6**. *Blood* **130**: 1062-1069. https://doi.org/10.1182/blood-2017-03-775759

Huang Y, Hidalgo-Bravo A, Zhang E, Cotton VE, Mendez-Bermudez A, Wig G, Medina-Calzada Z, Neumann R, Jeffreys AJ, Winney B *et al* (2014) **Human telomeres that carry an integrated copy of human herpesvirus 6 are often short and unstable, facilitating release of the viral genome from the chromosome**. *Nucleic Acids Res* **42**: 315-327. https://doi.org/10.1093/nar/gkt840

Jarrett RF, Clark DA, Josephs SF, Onions DE (1990) **Detection of human herpesvirus-6 DNA in peripheral blood and saliva**. *J Med Virol* **32**: 73-76.

Jeyapalan JN, Mendez-Bermudez A, Zaffaroni N, Dubrova YE, Royle NJ (2008) **Evidence for alternative lengthening of telomeres in liposarcomas in the absence of ALT-associated PML bodies**. *Int J Cancer* **122**: 2414-2421. https://doi.org/10.1002/ijc.23412

Kaspersen MD, Larsen PB, Kofod-Olsen E, Fedder J, Bonde J, Hollsberg P (2012) **Human herpesvirus-6A/B binds to spermatozoa acrosome and is the most prevalent herpesvirus in semen from sperm donors**. *PLoS One* **7**: e48810. https://doi.org/10.1371/journal.pone.0048810

Katoh K, Standley DM (2013) **MAFFT multiple sequence alignment software version 7: improvements in performance and usability**. *Mol Biol Evol* **30**: 772-780. https://doi.org/10.1093/molbev/mst010

Kawamura Y, Ohye T, Miura H, Ihira M, Kato Y, Kurahashi H, Yoshikawa T (2017) **Analysis of the origin of inherited chromosomally integrated human herpesvirus 6 in the Japanese population**. *J Gen Virol* https://doi.org/10.1099/jgv.0.000834

Kondo K, Nagafuji H, Hata A, Tomomori C, Yamanishi K (1993) **Association of human herpesvirus 6 infection of the central nervous system with recurrence of febrile convulsions**. *J Infect Dis* **167**: 1197-1200. https://doi.org/10.1093/infdis/167.5.1197

Leibovitch EC, Brunetto GS, Caruso B, Fenton K, Ohayon J, Reich DS, Jacobson S (2014) **Coinfection of human herpesviruses 6A (HHV-6A) and HHV-6B as demonstrated by novel digital droplet PCR assay**. *PLoS One* **9**: e92328. https://doi.org/10.1371/journal.pone.0092328

Leibovitch EC, Lin CM, Billioux BJ, Graves J, Waubant E, Jacobson S (2019) **Prevalence of salivary human herpesviruses in pediatric multiple sclerosis cases and controls**. *Mult Scler* **25**: 644-652. https://doi.org/10.1177/1352458518765654

Leong HN, Tuke PW, Tedder RS, Khanom AB, Eglin RP, Atkinson CE, Ward KN, Griffiths PD, Clark DA (2007) **The prevalence of chromosomally integrated human herpesvirus 6 genomes in the blood of UK blood donors**. *J Med Virol* **79**: 45-51.

Letunic I, Bork P (2016) **Interactive tree of life (iTOL) v3: an online tool for the display and annotation of phylogenetic and other trees**. *Nucleic Acids Res* **44**: W242-245. https://doi.org/10.1093/nar/gkw290

Lim KW, Alberti P, Guedin A, Lacroix L, Riou JF, Royle NJ, Mergny JL, Phan AT (2009) **Sequence variant (CTAGGG)n in the human telomere favors a G-quadruplex structure containing a G{middle dot}C{middle dot}G{middle dot}C tetrad**. *Nucleic Acids Res* **37**: 6239 - 6248.

Lindquester GJ, Pellett PE (1991) **Properties of the human herpesvirus 6 strain Z29 genome: G + C content, length, and presence of variable-length directly repeated terminal sequence elements**. *Virology* **182**: 102-110.

Liu S, Huang S, Chen F, Zhao L, Yuan Y, Francis SS, Fang L, Li Z, Lin L, Liu R *et al* (2018) **Genomic Analyses from Non-invasive Prenatal Testing Reveal Genetic Associations, Patterns of Viral Infections, and Chinese Population History**. *Cell* **175**: 347-359 e314. https://doi.org/10.1016/j.cell.2018.08.016

Liu X, Kosugi S, Koide R, Kawamura Y, Ito J, Miura H, Matoba N, Matsuzaki M, Fujita M, Kamada AJ *et al* (2020) **Endogenization and excision of human herpesvirus 6 in human genomes**. *PLoS Genet* **16**: e1008915. https://doi.org/10.1371/journal.pgen.1008915

Loayza D, Parsons H, Donigian J, Hoke K, de Lange T (2004) **DNA binding features of human POT1: a nonamer 5'-TAGGGTTAG-3' minimal binding site, sequence specificity, and internal binding to multimeric sites**. *J Biol Chem* **279**: 13241-13248.

Luppi M, Barozzi P, Morris CM, Merelli E, Torelli G (1998) **Integration of human herpesvirus 6 genome in human chromosomes**. *Lancet* **352**: 1707-1708.

Marques FZ, Romaine SP, Denniff M, Eales J, Dormer J, Garrelds IM, Wojnar L, Musialik K, Duda-Raszewska B, Kiszka B *et al* (2015) **Signatures of miR-181a on the Renal Transcriptome and Blood Pressure**. *Mol Med* **21**: 739-748. https://doi.org/10.2119/molmed.2015.00096

Mendez-Bermudez A, Hills M, Pickett HA, Phan AT, Mergny JL, Riou JF, Royle NJ (2009) **Human telomeres that contain (CTAGGG)n repeats show replication dependent instability in somatic cells and the male germline**. *Nucleic Acids Res* **37**: 6225 - 6238.

Miura H, Kawamura Y, Hattori F, Kozawa K, Ihira M, Ohye T, Kurahashi H, Yoshikawa T (2018) **Chromosomally integrated human herpesvirus 6 in the Japanese population**. *J Med Virol* **90**: 1636-1642. https://doi.org/10.1002/jmv.25244

Miura H, Kawamura Y, Ohye T, Hattori F, Kozawa K, Ihira M, Yatsuya H, Nishizawa H, Kurahashi H, Yoshikawa T (2020) **Inherited chromosomally integrated human herpesvirus 6 is a risk factor for spontaneous abortion**. *J Infect Dis* https://doi.org/10.1093/infdis/jiaa606

Morris C, Luppi M, McDonald M, Barozzi P, Torelli G (1999) **Fine mapping of an apparently targeted latent human herpesvirus type 6 integration site in chromosome band 17p13.3**. *J Med Virol* **58**: 69-75.

Moustafa A, Xie C, Kirkness E, Biggs W, Wong E, Turpaz Y, Bloom K, Delwart E, Nelson KE, Venter JC *et al* (2017) **The blood DNA virome in 8,000 humans**. *PLoS Pathog* **13**: e1006292. https://doi.org/10.1371/journal.ppat.1006292

Nacheva EP, Ward KN, Brazma D, Virgili A, Howard J, Leong HN, Clark DA (2008) **Human herpesvirus 6 integrates within telomeric regions as evidenced by five different chromosomal sites**. *J Med Virol* **80**: 1952-1958.

Neofytou E, Sourvinos G, Asmarianaki M, Spandidos DA, Makrigiannakis A (2009) **Prevalence of human herpes virus types 1-7 in the semen of men attending an infertility clinic and correlation with semen parameters**. *Fertil Steril* **91**: 2487-2494. https://doi.org/10.1016/j.fertnstert.2008.03.074

Ohye T, Inagaki H, Ihira M, Higashimoto Y, Kato K, Oikawa J, Yagasaki H, Niizuma T, Takahashi Y, Kojima S *et al* (2014) **Dual roles for the telomeric repeats in chromosomally integrated human herpesvirus-6**. *Sci Rep* **4**: 4559. https://doi.org/10.1038/srep04559

Peddu V, Dubuc I, Gravel A, Xie H, Huang ML, Tenenbaum D, Jerome KR, Tardif JC, Dube MP, Flamand L *et al* (2019) **Inherited Chromosomally Integrated Human Herpesvirus 6 Demonstrates Tissue-Specific RNA Expression In Vivo That Correlates with an Increased Antibody Immune Response**. *J Virol* **94** https://doi.org/10.1128/JVI.01418-19

Petit V, Bonnafous P, Fages V, Gautheret-Dejean A, Engelmann I, Baras A, Hober D, Gerard R, Gibier JB, Leteurtre E *et al* (2020) **Donor-to-recipient transmission and reactivation in a kidney transplant recipient of an inherited chromosomally integrated HHV-6A: Evidence and outcomes**. *Am J Transplant* **20**: 3667-3672. https://doi.org/10.1111/ajt.16067

Pickett HA, Cesare AJ, Johnston RL, Neumann AA, Reddel RR (2009) **Control of telomere length by a trimming mechanism that involves generation of t-circles**. *EMBO J* **28**: 799-809. https://doi.org/10.1038/emboj.2009.42

Pickett HA, Henson JD, Au AY, Neumann AA, Reddel RR (2011) **Normal mammalian cells negatively regulate telomere length by telomere trimming**. *Hum Mol Genet* **20**: 4684-4692.

Pritchett JC, Nanau RM, Neuman MG (2012) **The Link between Hypersensitivity Syndrome Reaction Development and Human Herpes Virus-6 Reactivation**. *Int J Hepatol* **2012**: 723062. https://doi.org/10.1155/2012/723062

Prusty BK, Gulve N, Chowdhury SR, Schuster M, Strempel S, Descamps V, Rudel T (2018) **HHV-6 encoded small non-coding RNAs define an intermediate and early stage in viral reactivation**. *NPJ Genom Med* **3**: 25. https://doi.org/10.1038/s41525-018-0064-5

Prusty BK, Krohne G, Rudel T (2013) **Reactivation of chromosomally integrated human herpesvirus-6 by telomeric circle formation**. *PLoS Genet* **9**: e1004033. https://doi.org/10.1371/journal.pgen.1004033

Riethman H (2008) **Human telomere structure and biology**. *Annu Rev Genomics Hum Genet* **9**: 1-19.

Rivera T, Haggblom C, Cosconati S, Karlseder J (2017) **A balance between elongation and trimming regulates telomere stability in stem cells**. *Nat Struct Mol Biol* **24**: 30-39. https://doi.org/10.1038/nsmb.3335

Rowland J, Akbarov A, Eales J, Xu X, Dormer JP, Guo H, Denniff M, Jiang X, Ranjzad P, Nazgiewicz A *et al* (2019) **Uncovering genetic mechanisms of kidney aging through transcriptomics, genomics, and epigenomics**. *Kidney Int* **95**: 624-635. https://doi.org/10.1016/j.kint.2018.10.029

Sarek G, Vannier JB, Panier S, Petrini JH, Boulton SJ (2015) **TRF2 recruits RTEL1 to telomeres in S phase to promote t-loop unwinding**. *Mol Cell* **57**: 622-635. https://doi.org/10.1016/j.molcel.2014.12.024

Scally A, Durbin R (2012) **Revising the human mutation rate: implications for understanding human evolution**. *Nat Rev Genet* **13**: 745-753. https://doi.org/10.1038/nrg3295

Schmutz I, Timashev L, Xie W, Patel DJ, de Lange T (2017) **TRF2 binds branched DNA to safeguard telomere integrity**. *Nat Struct Mol Biol* **24**: 734-742. https://doi.org/10.1038/nsmb.3451

Shioda S, Kasai F, Ozawa M, Hirayama N, Satoh M, Kameoka Y, Watanabe K, Shimizu N, Tang H, Mori Y *et al* (2018) **The human vascular endothelial cell line HUV-EC-C harbors the integrated HHV-6B genome which remains stable in long term culture**. *Cytotechnology* **70**: 141-152. https://doi.org/10.1007/s10616-017-0119-y

Stansel RM, de Lange T, Griffith JD (2001) **T-loop assembly in vitro involves binding of TRF2 near the 3' telomeric overhang**. *EMBO J* **20**: 5532-5540. https://doi.org/10.1093/emboj/20.19.5532

Strenger V, Caselli E, Lautenschlager I, Schwinger W, Aberle SW, Loginov R, Gentili V, Nacheva E, DiLuca D, Urban C (2014) **Detection of HHV-6-specific mRNA and antigens in PBMCs of individuals with chromosomally integrated HHV-6 (ciHHV-6)**. *Clin Microbiol Infect* **20**: 1027-1032. https://doi.org/10.1111/1469-0691.12639

Takai H, Smogorzewska A, de Lange T (2003) **DNA damage foci at dysfunctional telomeres**. *Curr Biol* **13**: 1549-1556.

Tanaka-Taya K, Sashihara J, Kurahashi H, Amo K, Miyagawa H, Kondo K, Okada S, Yamanishi K (2004) **Human herpesvirus 6 (HHV-6) is transmitted from parent to child in an integrated form and characterization of cases with chromosomally integrated HHV-6 DNA**. *J Med Virol* **73**: 465-473.

Telford M, Navarro A, Santpere G (2018) **Whole genome diversity of inherited chromosomally integrated HHV-6 derived from healthy individuals of diverse geographic origin**. *Sci Rep* **8**: 3472. https://doi.org/10.1038/s41598-018-21645-x

Tomaska L, Nosek J, Kar A, Willcox S, Griffith JD (2019) **A New View of the T-Loop Junction: Implications for Self-Primed Telomere Extension, Expansion of Disease-Related Nucleotide Repeat Blocks, and Telomere Evolution**. *Front Genet* **10**: 792. https://doi.org/10.3389/fgene.2019.00792

Turriziani O, Falasca F, Maida P, Gaeta A, De Vito C, Mancini P, De Seta D, Covelli E, Attanasio G, Antonelli G (2014) **Early collection of saliva specimens from Bell's palsy patients: quantitative analysis of HHV-6, HSV-1, and VZV**. *J Med Virol* **86**: 1752-1758. https://doi.org/10.1002/jmv.23917

Tweedy J, Spyrou MA, Pearson M, Lassner D, Kuhl U, Gompels UA (2016) **Complete Genome Sequence of Germline Chromosomally Integrated Human Herpesvirus 6A and Analyses Integration Sites Define a New Human Endogenous Virus with Potential to Reactivate as an Emerging Infection**. *Viruses* **8** https://doi.org/10.3390/v8010019

995 Van Ly D, Low RRJ, Frolich S, Bartolec TK, Kafer GR, Pickett HA, Gaus K, Cesare AJ (2018) **Telomere**
996 **Loop Dynamics in Chromosome End Protection**. *Mol Cell* **71**: 510-525 e516.
997 https://doi.org/10.1016/j.molcel.2018.06.025
998 Vannier JB, Pavicic-Kaltenbrunner V, Petalcorin MI, Ding H, Boulton SJ (2012) **RTEL1 dismantles T**
999 **loops and counteracts telomeric G4-DNA to maintain telomere integrity**. *Cell* **149**: 795-806.
1000 https://doi.org/10.1016/j.cell.2012.03.030
1001 Voors AA, Anker SD, Cleland JG, Dickstein K, Filippatos G, van der Harst P, Hillege HL, Lang CC, Ter
1002 Maaten JM, Ng L *et al* (2016) **A systems BIOlogy Study to TAilored Treatment in Chronic Heart**
1003 **Failure: rationale, design, and baseline characteristics of BIOSTAT-CHF**. *Eur J Heart Fail* **18**: 716-726.
1004 https://doi.org/10.1002/ejhf.531
1005 Wallaschek N, Gravel A, Flamand L, Kaufer BB (2016a) **The putative U94 integrase is dispensable for**
1006 **human herpesvirus 6 (HHV-6) chromosomal integration**. *J Gen Virol*
1007 https://doi.org/10.1099/jgv.0.000502
1008 Wallaschek N, Sanyal A, Pirzer F, Gravel A, Mori Y, Flamand L, Kaufer BB (2016b) **The Telomeric**
1009 **Repeats of Human Herpesvirus 6A (HHV-6A) Are Required for Efficient Virus Integration**. *PLoS*
1010 *Pathog* **12**: e1005666. https://doi.org/10.1371/journal.ppat.1005666
1011 Wan B, Yin J, Horvath K, Sarkar J, Chen Y, Wu J, Wan K, Lu J, Gu P, Yu EY *et al* (2013) **SLX4 assembles**
1012 **a telomere maintenance toolkit by bridging multiple endonucleases with telomeres**. *Cell Rep* **4**:
1013 861-869. https://doi.org/10.1016/j.celrep.2013.08.017
1014 Wang RC, Smogorzewska A, de Lange T (2004) **Homologous recombination generates T-loop-sized**
1015 **deletions at human telomeres**. *Cell* **119**: 355-368.
1016 Ward KN, Gray JJ (1994) **Primary human herpesvirus-6 infection is frequently overlooked as a cause**
1017 **of febrile fits in young children**. *J Med Virol* **42**: 119-123. https://doi.org/10.1002/jmv.1890420204
1018 Weschke DP, Leisenring WM, Lawler RL, Stevens-Ayers T, Huang ML, Jerome KR, Zerr DM, Hansen JA,
1019 Boeckh M, Hill JA (2020) **Inflammatory Cytokine Profile in Individuals with Inherited**
1020 **Chromosomally Integrated Human Herpesvirus 6**. *Biol Blood Marrow Transplant* **26**: 254-261.
1021 https://doi.org/10.1016/j.bbmt.2019.10.023
1022 Wight DJ, Aimola G, Aswad A, Jill Lai CY, Bahamon C, Hong K, Hill JA, Kaufer BB (2020) **Unbiased**
1023 **optical mapping of telomere-integrated endogenous human herpesvirus 6**. *Proc Natl Acad Sci U S A*
1024 **117**: 31410-31416. https://doi.org/10.1073/pnas.2011872117
1025 Wight DJ, Wallaschek N, Sanyal A, Weller SK, Flamand L, Kaufer BB (2018) **Viral Proteins U41 and**
1026 **U70 of Human Herpesvirus 6A Are Dispensable for Telomere Integration**. *Viruses* **10**
1027 https://doi.org/10.3390/v10110656
1028 Wood ML, Royle NJ (2017) **Chromosomally Integrated Human Herpesvirus 6: Models of Viral**
1029 **Genome Release from the Telomere and Impacts on Human Health**. *Viruses* **9**
1030 https://doi.org/10.3390/v9070184
1031 Yao K, Crawford JR, Komaroff AL, Ablashi DV, Jacobson S (2010) **Review part 2: Human herpesvirus-6**
1032 **in central nervous system diseases**. *J Med Virol* **82**: 1669-1678. https://doi.org/10.1002/jmv.21861
1033 Yoshikawa T, Fujita A, Yagami A, Suzuki K, Matsunaga K, Ihira M, Asano Y (2006) **Human herpesvirus**
1034 **6 reactivation and inflammatory cytokine production in patients with drug-induced**
1035 **hypersensitivity syndrome**. *J Clin Virol* **37 Suppl 1**: S92-96. https://doi.org/10.1016/S1386-
1036 6532(06)70019-1
1037 Zerr DM, Meier AS, Selke SS, Frenkel LM, Huang ML, Wald A, Rhoads MP, Nguy L, Bornemann R,
1038 Morrow RA *et al* (2005) **A population-based study of primary human herpesvirus 6 infection**. *N Engl*
1039 *J Med* **352**: 768-776. https://doi.org/10.1056/NEJMoa042207
1040 Zhang E, Bell AJ, Wilkie GS, Suarez NM, Batini C, Veal CD, Armendariz-Castillo I, Neumann R, Cotton
1041 VE, Huang Y *et al* (2017) **Inherited Chromosomally Integrated Human Herpesvirus 6 Genomes Are**
1042 **Ancient, Intact, and Potentially Able To Reactivate from Telomeres**. *J Virol* **91**
1043 https://doi.org/10.1128/JVI.01137-17
1044 Zhang E, Cotton VE, Hidalgo-Bravo A, Huang Y, J. Bell A, F. Jarrett R, Wilkie GS, Davison AJ, P.
1045 Nacheva E, Siebert R *et al* (2016) **HHV-8-unrelated primary effusion-like lymphoma associated with**

clonal loss of inherited chromosomally-integrated human herpesvirus-6A from the telomere of chromosome 19q. *Scientific Reports* **6**: 22730. https://doi.org/10.1038/srep22730

http://www.nature.com/articles/srep22730#supplementary-information

Zhang Z, Zhang T, Ge Y, Tang M, Ma W, Zhang Q, Gong S, Wright WE, Shay J, Liu H *et al* (2019) **2D gel electrophoresis reveals dynamics of t-loop formation during the cell cycle and t-loop in maintenance regulated by heterochromatin state**. *J Biol Chem* **294**: 6645-6656. https://doi.org/10.1074/jbc.RA119.007677

Figure legends

Figure 1. Characterisation of the highly variable DR_R-pvT1 in iciHHV-6B and acqHHV-6B genomes. (A) Diagram showing the locations of PCR primers used to amplify the DR_R-T1 region specifically (U100Fw2 and DR1R) and the nested primers used to reamplify and sequence pvT1 (DR421R and TJ1F) in the iciHHV-6B genome (left) and in the acqHHV-6B genome (right). (B) DR_R-pvT1 repeat patterns are shown to demonstrate diversity among a subset of iciHHV-6B (inherited) and acqHHV-6B (acquired) genomes from various individuals. Telomere-like and degenerate repeats present in the HHV-6B pvT1 region are colour-coded: Dark green, TTAGGG; brown, CTAGGG; cyan, TTAGTG; yellow, TTACTG; dark yellow, ATAGAC; teal, CTAAGG; pink, CTATGG; lime green, TTATGG; blue, GTAGTG; peach, TTAGAG; red, GTCTGG. Black squares represent other less common degenerate repeats, white squares show where the sequence could not be determined accurately. Dashes between repeats were added to maximize alignment and to allow comparison between the left, middle (highly variable) and right (highly conserved) sections of DR_R-pvT1 in different samples. (C) DR_R-pvT1 repeat patterns from acqHHV-6B in two families. None of the family members were iciHHV-6 carriers. In both families the HHV-6B DR_R-pvT1 region in the two children was the same as one parent, indicating the children carried the same strain of the virus, whereas the second parent carried a different strain. Blue shapes indicate that the child had acqHHV-6B with the same pvT1 repeat map as the mother. Analysis of DR_R-pvT1 in the CEPH1375 family showed stable inheritance of the same pvT1 repeat pattern across three generations. iciHHV-6B carriers in the CEPH1375 family are shown as filled black symbols

Figure 2. Distance-based phylogenetic networks for HHV-6A and HHV-6B. (A) A phylogenetic network of 41 HHV-6A viral genome sequences. High sequence homology to iciHHV-6A genomes for which the integration site had already been established allowed all but one (GLA_4298) iciHHV-6A genomes to be assigned to a telomeric integration site. The colours indicate an chromosomal integration as follows: Green, 19q; Orange, 18q; Purple, 10q; Yellow-green, 22q; Blue, 17p. The name in black identifies the iciHHV-6A strain without a predicted chromosomal location. Non-inherited, acqHHV-6A strains are shown in red. iciHHV-6A genomes sequenced as part of this study are identified by a black asterisk. (B) A phylogenetic tree of 68 HHV-6B genome sequences (51 iciHHV-6B and 17 acqHHV-6B). iciHHV-6B genomes sequenced as part of this study are identified by a black asterisk. High sequence homology to iciHHV-6B genomes with a known integration site (already established by FISH) allowed the majority of iciHHV-6B genomes to be assigned a telomeric chromosomal location. From the newly sequenced iciHHV-6B genomes two new clades were identified and provisionally labelled as: 17p (minor) and 2p. The 17p (minor) clade includes the 1B-

1089 iciHHV-6B genome, previously a singleton in HHV-6B networks, and the iciHHV-6B genomes in
1090 704021 and 704016. The subtelomere-iciHHV-6B junction sequences, amplified with the 17p311 and
1091 DR8F(A/B) primers, are similar for all three samples and distinct form the 17p (major) clade. The
1092 other new clade is characterised by the iciHHV-6B genome (401027). This group is provisionally
1093 labelled 2p because the subtelomere-iciHHV-6B junction was amplified by the 2p2 and DR8F(A/B)
1094 primers in 401027, and two other samples (410005 and 308006, see Figure 3C).

1095

1096 **Figure 3.** pvT1 repeat patterns are similar between strains of iciHHV-6B known to have the same
1097 ancestral integration site and those predicted to share that integration site. (A) Distance-based
1098 phylogenetic tree of selected iciHHV-6B (black names) and acquired HHV-6B (red names) genomes.
1099 Where DNA was available, DR_R-pvT1 repeat patterns from 19 iciHHV-6B samples in the phylogenetic
1100 tree are shown. The repeats in the pvT1 region are colour-coded: Dark green, TTAGGG; brown,
1101 CTAGGG; cyan, TTAGTG; yellow, TTACTG; dark yellow, ATAGAC; teal, CTAAGG; pink, CTATGG; lime
1102 green, TTATGG; blue, GTAGTG; peach, TTAGAG; red, GTCTGG. Black vertical bars on the right
1103 indicate groups of iciHHV-6Bs for which the integration site has been determined by FISH,
1104 phylogeny, subtelomere-iciHHV-6B junction analysis or a combination of these. DR_R-pvT1 repeat
1105 patterns within black boxes identify iciHHV-6B samples for which the integration site has been
1106 predicted based on DR_R-pvT1 similarity. For some of these samples the integration site has been
1107 validated by subtelomere-iciHHV-6B junction analysis (410005, 308006, d44, SAL018, NWA008 and
1108 KEN071). (B) Line diagram showing the position of DR8F(A/B) and potential subtelomere primers
1109 used to amplify and sequence subtelomere-iciHHV-6B junctions. The subtelomere-iciHHV-6B
1110 integration site can be amplified whether the integrated viral genome is full length or iciHHV-6B-DR
1111 only. (C) Diagram showing of the pattern of canonical (TTAGGG) and degenerate telomere-like
1112 repeat maps across the subtelomere-HHV-6B junction from two different chromosome ends. The
1113 subtelomere-HHV-6B repeat maps from the 401027, 410005 and 308006 were generated following
1114 amplification with primers 2p2 and DR8F(A/B). They are very similar demonstrating common
1115 ancestry (top three maps). The subtelomere-HHV-6B repeat maps from the 801018, d44, SAL018 and
1116 KEN071 generated by amplification with 17p311 and DR8F(A/B) (bottom four maps) are very similar
1117 to the group of iciHHV-6B genomes in the 17p (major) clade some of which have been shown to be
1118 integrated in 17p. The 308006, SAL018 and KEN071 samples contain iciHHV-6B DR-only.

1119

1120 **Figure 4.** Evidence of telomere formation at the distal end of HHV-6B genomes in individuals with
1121 community-acquired HHV-6B. (A) Graph showing HHV-6B copy number per cell estimated from HHV-

6B *POL* (U38) and RPP30 copy number by ddPCR. Triplicate results are shown for saliva DNA from 52 individuals and kidney samples from two individuals. Crosses show where zero copies per cell were estimated for a single replicate and black crosses indicate that zero copies per cell were estimated from all three replicates. The mean and standard error are shown. (B) STELA primers, DR2RSTELA and Telorette2BC38/TeltailBC38, that were used to amplify HHV-6B associated telomeres are shown on an integrated HHV-6B genome. DR421R and TJ1F primers were used to amplify DR_L-pvT1 in secondary nested PCRs. In non-integrated HHV-6B STELA products cannot be generated as there is no HHV-6B-associated telomere. The copies of PAC1 (P1) and PAC2 (P2) are shown. (C) STELA blots from two DNA samples (SAL039 and K10) are shown. In a small number of reactions an amplified HHV-6B-associated telomere was detected with a radiolabeled $(TTAGGG)_n$ telomere-repeat probe. Diluted STELA PCR products were used as input for secondary, nested PCRs to amplify DR_L-pvT1 as shown in the agarose gel photograph below. The 6-iciHHV-6B DNA was used as a positive control (+) for STELA and DR_L-pvT1 secondary PCR. (D) Graph showing the total copy number of HHV-6B per cell measured by ddPCR (filled diamonds); the estimated number of copies of integrated HHV-6B per cell from STELA and pvT1 PCR (open circles). (E) Measuring the DR:PAC1 ratio by ddPCR. 1D EvaGreen ddPCR plots of one iciHHV-6B (4B-11p15.5) cell line and acqHHV-6B in three saliva samples (SAL035, SAL044 and SAL050). Triplicate reactions for a DR amplicon (DR6B-F and DR6B-R primers) and a PAC1 amplicon (PAC1F and PAC1R-33 primers) are shown. The absolute copy number of each amplicon per μl ddPCR reaction and the ratio between DR and PAC1 amplicons are shown below each plot.

Figure 5. Quantifying iciHHV-6B truncations at DR_L-T2 and assessment of the newly formed telomere length. (A) Diagram showing the loss of DR_L from iciHHV-6B, formation of a novel telomere at DR_L-T2 and the potential lengthening of the newly formed telomere by a telomere maintenance mechanism. STELA primers (Teltail and Telorette2) and the primer UDL6R, in the unique region of the iciHHV-6B genome, were used to amplify HHV-6B-associated telomeres. Long STELA products (>8.6kb) are generated from intact copies of the iciHHV-6B genome and include amplification through DR_L to the end of the telomere. Short STELA products (0.6 - 0.9 kb) are generated when DR_L has been lost and a novel telomere has formed at DR_L-T2. Intermediate sized STELA products are generated when the novel telomere formed at DRL-T2 has been lengthened. All three types of STELA amplicons contain TTAGGG telomere repeats and hybridise to a telomere repeat probe. The relative positions of the DR3 and DR8 probes used to detect DR sequences are shown. (B) Representative HHV-6B STELA blots generated from different cell-types from iciHHV-6B carriers or derived cell lines. These include a lymphoblastoid cell line (LCL) from individual 4B-11p15.5; white blood cells from individual 607009; a pluripotent cell line d37; sperm DNA d56. Bands between the mauve and yellow

lines are short STELA products. The bands detected between the yellow and green lines are intermediate length STELA products, representative of newly formed telomeres at DR_L-T2 that have been lengthened. Long STELA amplicons, above the green line, are products generated from full-length copies of iciHHV-6B and include DR_L. (C) Graph showing the estimated number of DR_L-T2 truncations per cell, including those that have been lengthened, in DNA from different iciHHV-6B individuals and cell types. Means with standard error and the p-values from a Mann-Whitney ranked sum test to compare truncation frequencies (LCL vs other cell-types) are shown. (D) Representative UDL6R-STELA blots from the 4B-11p15.5 cell line treated with 0, 100 and 200 ng/mL of trichostatin-A and a graph showing the frequency of truncations per cell (mean and standard error). Data were derived from UDL6R-STELA conducted twice (technical replicates) using DNA extracted from treated and untreated cells grown in triplicate (biological replicates). p-values were from a Wilcoxon test. (E) DR_L-T2 truncation assay on blood DNA from the 401027 iciHHV-6B carrier demonstrating that the long STELA products (above the green line) contain DR sequences that hybridise to the telomere repeat probe (left panel) and the combined DR3/DR8 probe (right panel). Whereas the intermediate length amplicons (below the green line) only hybridise to the telomere repeat probe (left panel) demonstrating that each amplicon represents newly formed telomere at DR_L-T2 that has been lengthened. (F) The graph shows the percentage of newly formed telomeres at DR_L-T2 that were lengthened in samples from various unrelated iciHHV-6B carriers and cell types. Means with standard error and the p-values from a Mann-Whitney ranked sum test to compare truncation frequencies (LCL vs other cell-types) are shown.

Figure 6. Measuring the frequency of iciHHV-6B truncations at DR_R-T1 associated with novel telomere formation. (A) Schematic of the two-step assay used to differentiate between iciHHV-6B associated telomeres at DR_R-T1 and DR_L-T1. Telomeres at DR_R-T1 and DR_L-T1 were PCR amplified using the STELA primers, DR1R with Telorette2/Teltail. Subsequently, secondary nested PCRs were used to amplify pvT1 (primers DR421 and TJ1F) followed by size separation to distinguish pvT1 from DR_R-T1 or DR_L-T1. (B) Detection of telomeres at DR_R-T1 or DR_L -T1 in two iciHHV-6B samples (NWA008 and 401027) with known length differences between pvT1 in the DRs. Top images show telomeres at DR_L and DR_R in the iciHHV-6B samples amplified by STELA and detected by Southern blot hybridization to a radiolabeled $(TTAGGG)_n$ probe. Lower images show ethidium bromide-stained agarose gels of size separated pvT1 sequences amplified from the corresponding STELA reaction in the panel above. White dots identify the PCR reactions that contain pvT1 from DR_R-T1. Below each set of panels are the pvT1 repeat maps from DR_R-T1 or DR_L-T1 for the corresponding sample, highlighting the differences. (C) Graph showing the frequency of truncations and new telomere

formation at DR_R-T1 in iciHHV-6B samples from unrelated individuals and cell types. The number of truncations per cell was calculated using the number of reactions from which DR_R-pvT1 was amplified divided by the cell equivalents estimated from the total quantity of DNA screened (6.6 pg or 3.3 pg DNA per cell was assumed for diploid and haploid cells respectively).

Figure 7. HHV-6B copy number and DR_R-pvT1-repeat patterns can be used to identify potential iciHHV-6B reactivation and transmission within families. (A) In family Rx-F6a both children are iciHHV-6B carriers with approximately one copy per cell. They share the same DR_R-pvT1 repeat map, presumably inherited from the father (grey filled square, not available for testing). The mother has a low level of acqHHV-6B in her saliva (0.00035 copies per cell) and the DR_R-pvT1 repeat map is different from her children. (B) Evidence of iciHHV-6B reactivation in family Rx-F3a and transmission to non-iciHHV-6B son. Left shows the Rx-F3a family tree with HHV-6 copy number per cell in saliva DNA and iciHHV-6B carrier status. Father (grey filled square) was not available for testing. Right, the DR_R-pvT1 repeat maps from family members. Daughter (G4P3) has two copies of iciHHV-6B, one copy shares the same DR_R-pvT1 as seen in her mother (G3P2) and a second copy has a different DR_R-pvT1 repeat pattern assumed to have been inherited from her father. The son (G4P1) has a very low level of HHV-6B in his saliva with the same pvT1 repeat pattern as the maternal iciHHV-6B genome. The DR_R-pvT1 repeat patterns are also labeled with m (present in mother); d (present in daughter) and s (present in son).

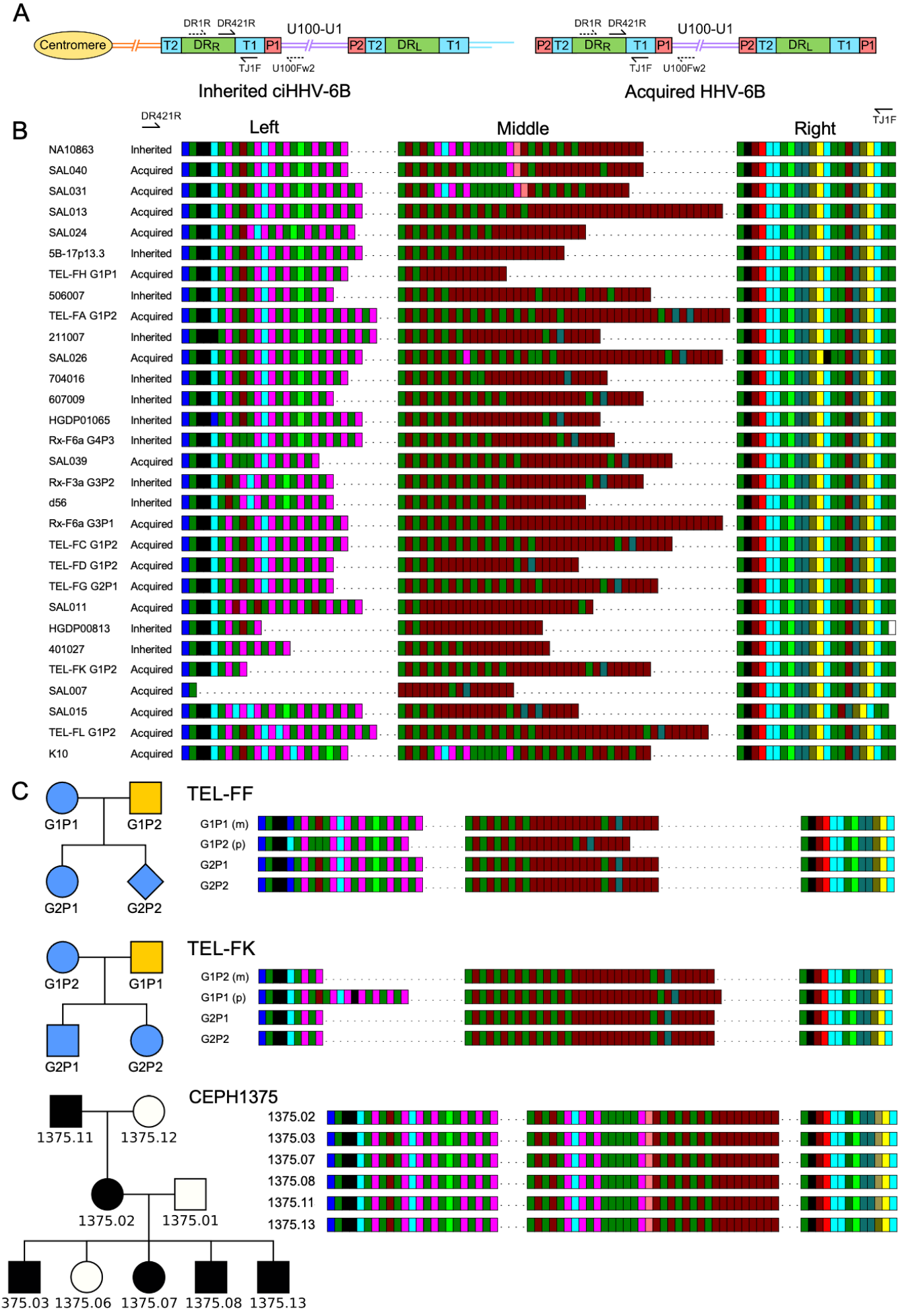
A
Centromere
T2
DRR
T1
P1
U100-U1
P2
T2
DRL
T1
DR1R
DR421R
TJ1F
U100Fw2
Inherited ciHHV-6B
Acquired HHV-6B
B
DR421R
Left
Middle
Right
TJ1F
NA10863 Inherited
SAL040 Acquired
SAL031 Acquired
SAL013 Acquired
SAL024 Acquired
5B-17p13.3 Inherited
TEL-FH G1P1 Acquired
506007 Inherited
TEL-FA G1P2 Acquired
211007 Inherited
SAL026 Acquired
704016 Inherited
607009 Inherited
HGDP01065 Inherited
Rx-F6a G4P3 Inherited
SAL039 Acquired
Rx-F3a G3P2 Inherited
d56 Inherited
Rx-F6a G3P1 Acquired
TEL-FC G1P2 Acquired
TEL-FD G1P2 Acquired
TEL-FG G2P1 Acquired
SAL011 Acquired
HGDP00813 Inherited
401027 Inherited
TEL-FK G1P2 Acquired
SAL007 Acquired
SAL015 Acquired
TEL-FL G1P2 Acquired
K10 Acquired
C
TEL-FF
G1P1
G1P2
G2P1
G2P2
G1P1 (m)
G1P2 (p)
G2P1
G2P2
TEL-FK
G1P2
G1P1
G2P1
G2P2
G1P2 (m)
G1P1 (p)
G2P1
G2P2
CEPH1375
1375.11
1375.12
1375.02
1375.01
1375.03
1375.06
1375.07
1375.08
1375.13
1375.02
1375.03
1375.07
1375.08
1375.11
1375.13

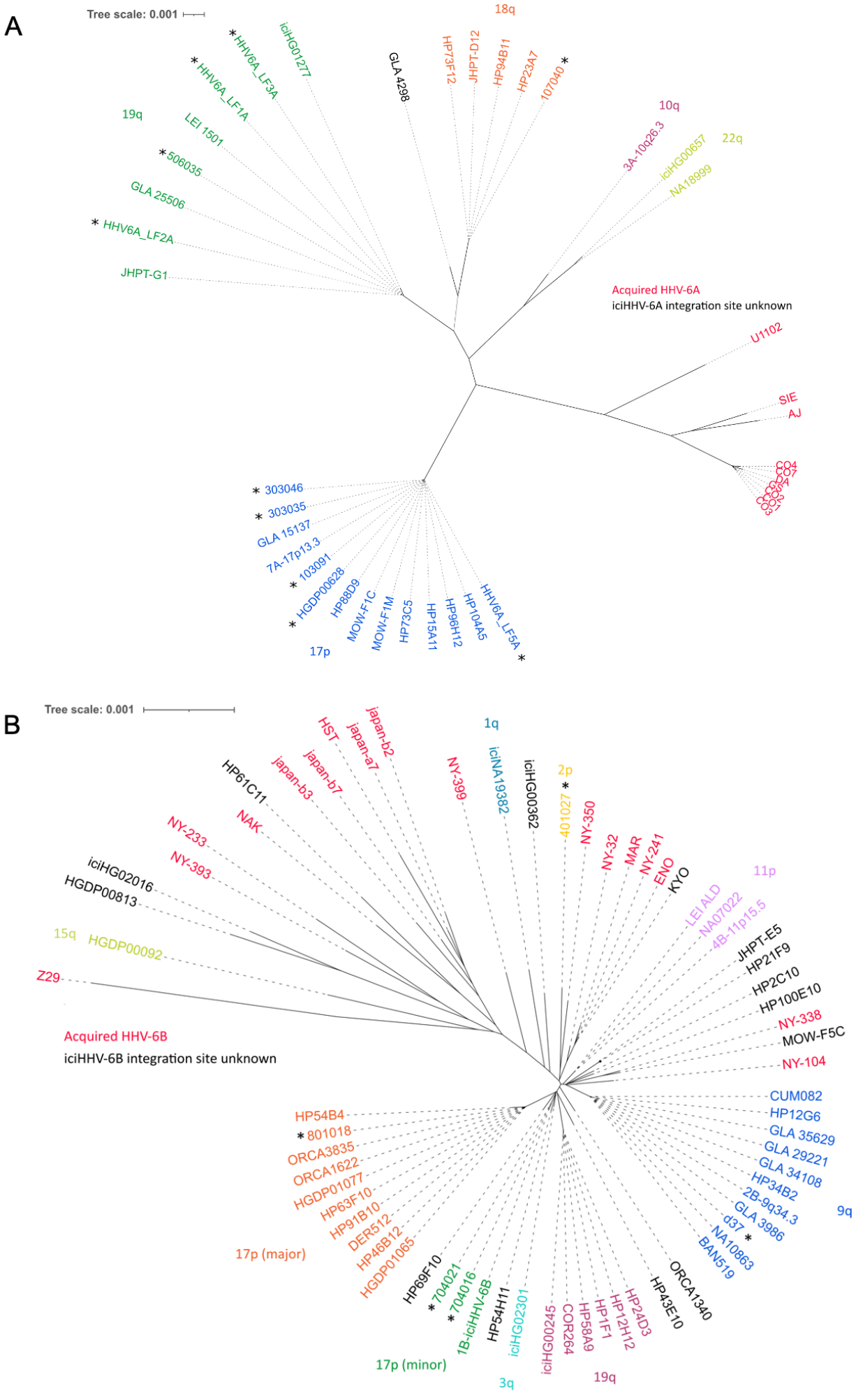
A
Tree scale: 0.001
18q
HP73F12
JHPT-D12
HP94B11
HP23A7
107040 *
GLA 4298
iciHG01277
*HHV6A_LF3A
*HHV6A_LF1A
19q
LEI 1501
*506035
GLA 25506
* HHV6A_LF2A
JHPT-G1
10q
3A-10q26.3
22q
iciHG00657
NA18999
Acquired HHV-6A
iciHHV-6A integration site unknown
U1102
SIE
AJ
CO4
CO7
* 303046
* 303035
GLA 15137
7A-17p13.3
* 103091
* HGDP00628
HP88D9
MOW-F1C
MOW-F1M
HP73C5
HP15A11
HP96H12
HP104A5
HHV6A_LF5A *
17p
B
Tree scale: 0.001
1q
japan-b2
japan-a7
HST
japan-b7
japan-b3
HP61C11
NAK
NY-233
NY-393
iciHG02016
HGDP00813
15q
HGDP00092
Z29
NY-399
iciNA19382
iciHG00362
2p
401027 *
NY-350
NY-32
MAR
NY-241
ENO
KYO
11p
LEI ALD
NA07022
4B-11p15.5
JHPT-E5
HP21F9
HP2C10
HP100E10
NY-338
MOW-F5C
NY-104
Acquired HHV-6B
iciHHV-6B integration site unknown
HP54B4
* 801018
ORCA3835
ORCA1622
HGDP01077
HP63F10
HP91B10
DER512
HP46B12
HGDP01065
17p (major)
HP69F10
* 704021
* 704016
1B-iciHHV-6B
HP54H11
iciHG02301
iciHG00245
COR264
HP58A9
HP1F1
HP12H12
HP24D3
HP43E10
ORCA1340
17p (minor)
3q
19q
CUM082
HP12G6
GLA 35629
GLA 29221
GLA 34108
HP34B2
2B-9q34.3
GLA 3986
d37 *
NA10863
BAN519
9q

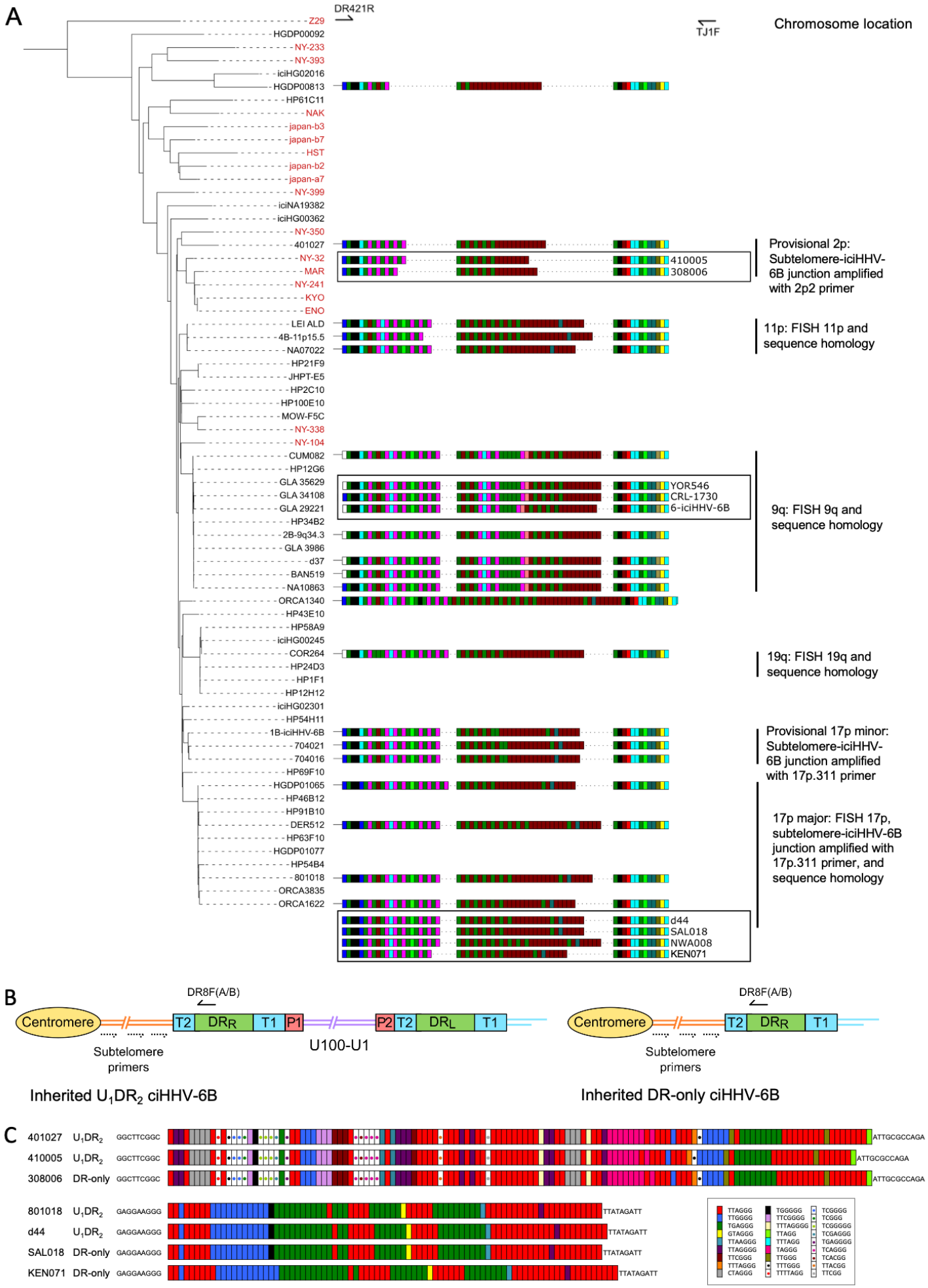
A
DR421R
TJ1F
Chromosome location
Z29
HGDP00092
NY-233
NY-393
iciHG02016
HGDP00813
HP61C11
NAK
japan-b3
japan-b7
HST
japan-b2
japan-a7
NY-399
iciNA19382
iciHG00362
NY-350
401027
NY-32
MAR
NY-241
KYO
ENO
LEI ALD
4B-11p15.5
NA07022
HP21F9
JHPT-E5
HP2C10
HP100E10
MOW-F5C
NY-338
NY-104
CUM082
HP12G6
GLA 35629
GLA 34108
GLA 29221
HP34B2
2B-9q34.3
GLA 3986
d37
BAN519
NA10863
ORCA1340
HP43E10
HP58A9
iciHG00245
COR264
HP24D3
HP1F1
HP12H12
iciHG02301
HP54H11
1B-iciHHV-6B
704021
704016
HP69F10
HGDP01065
HP46B12
HP91B10
DER512
HP63F10
HGDP01077
HP54B4
801018
ORCA3835
ORCA1622
410005
308006
YOR546
CRL-1730
6-iciHHV-6B
d44
SAL018
NWA008
KEN071
Provisional 2p: Subtelomere-iciHHV-6B junction amplified with 2p2 primer
11p: FISH 11p and sequence homology
9q: FISH 9q and sequence homology
19q: FISH 19q and sequence homology
Provisional 17p minor: Subtelomere-iciHHV-6B junction amplified with 17p.311 primer
17p major: FISH 17p, subtelomere-iciHHV-6B junction amplified with 17p.311 primer, and sequence homology
B
DR8F(A/B)
Centromere
T2
DRR
T1
P1
P2
DRL
U100-U1
Subtelomere primers
Inherited U1DR2 ciHHV-6B
Inherited DR-only ciHHV-6B
C
401027 U1DR2 GGCTTCGGC ATTGCGCCAGA
410005 U1DR2 GGCTTCGGC ATTGCGCCAGA
308006 DR-only GGCTTCGGC ATTGCGCCAGA
801018 U1DR2 GAGGAAGGG TTATAGATT
d44 U1DR2 GAGGAAGGG TTATAGATT
SAL018 DR-only GAGGAAGGG TTATAGATT
KEN071 DR-only GAGGAAGGG TTATAGATT

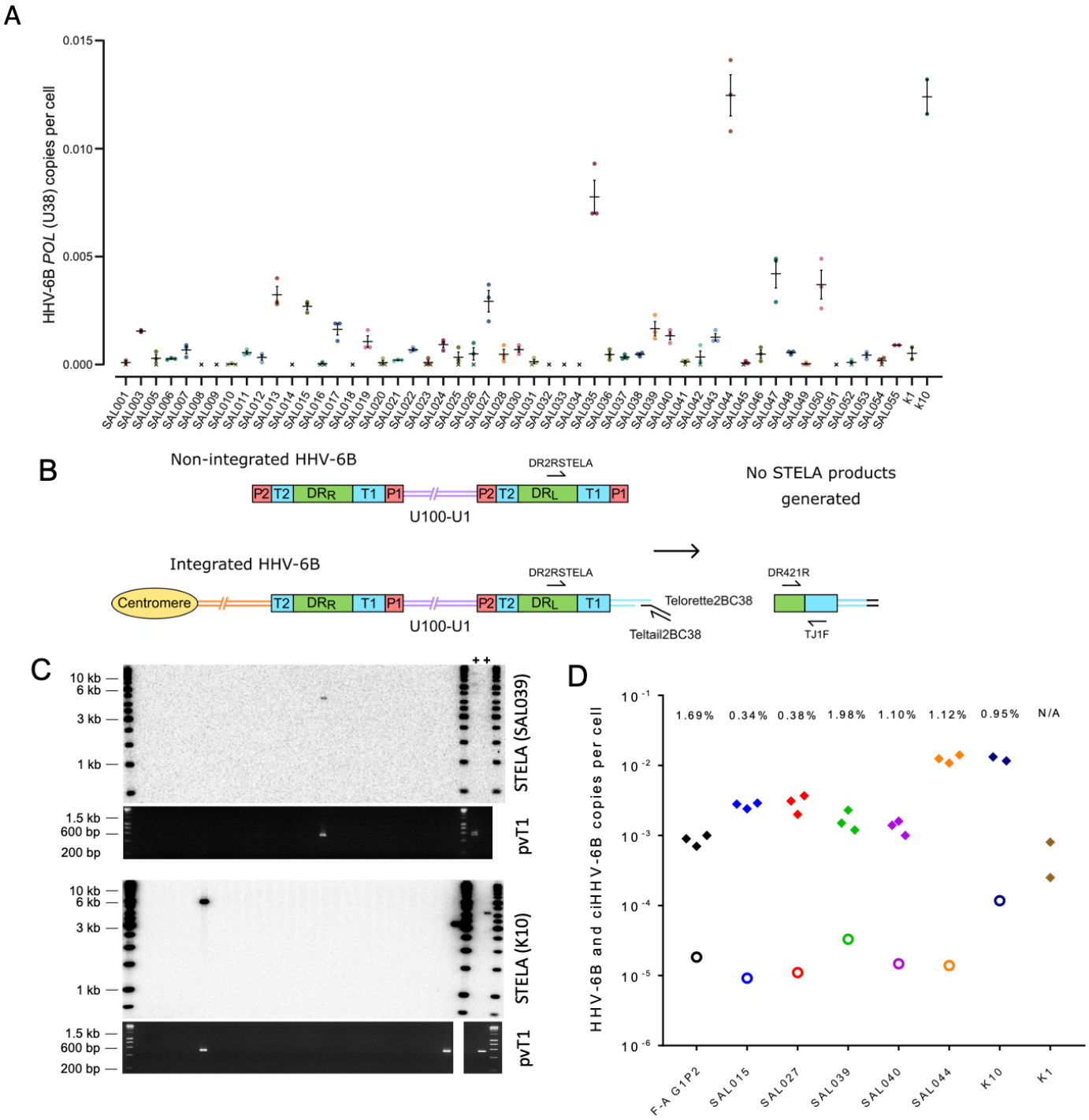

Region	DR	PAC1	DR	PAC1	DR	PAC1	DR	PAC1
Copies per uL	83.1	48.7	4.2	4.9	8.1	8.8	1.64	1.86
DR:PAC1	2:1.17		2: 2.34		2 : 2.18		2: 2.26	

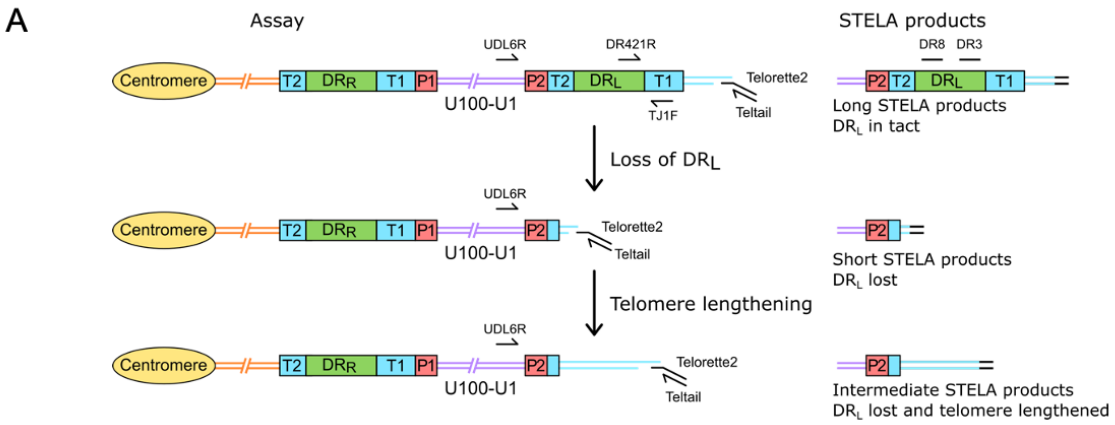
A
Assay
STELA products
UDL6R
DR421R
Centromere
T2
DRR
T1
P1
P2
T2
DRL
T1
Telorette2
U100-U1
TJ1F
Teltail
DR8
DR3
Long STELA products
DRL in tact
Loss of DRL
Short STELA products
DRL lost
Telomere lengthening
Intermediate STELA products
DRL lost and telomere lengthened

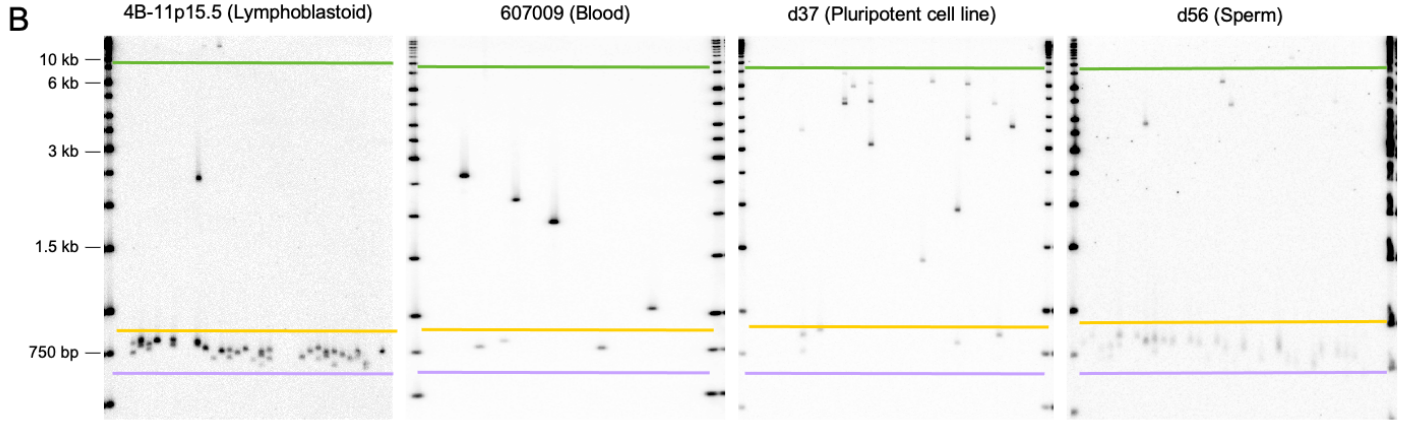
B
4B-11p15.5 (Lymphoblastoid)
607009 (Blood)
d37 (Pluripotent cell line)
d56 (Sperm)
10 kb
6 kb
3 kb
1.5 kb
750 bp

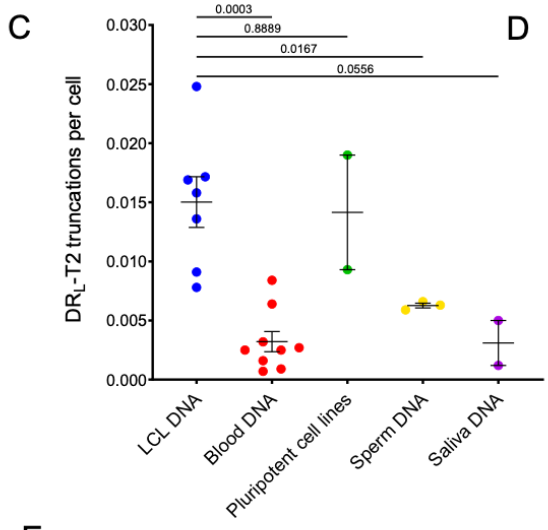
C
DRL-T2 truncations per cell
0.0003
0.8889
0.0167
0.0556
LCL DNA
Blood DNA
Pluripotent cell lines
Sperm DNA
Saliva DNA

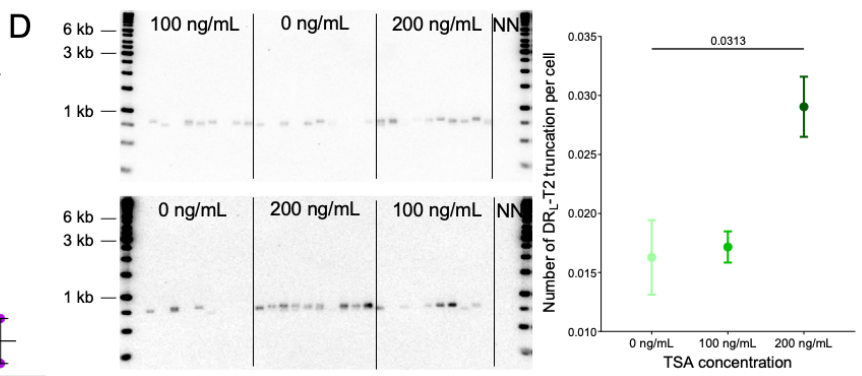
D
6 kb
3 kb
1 kb
100 ng/mL
0 ng/mL
200 ng/mL
NN
Number of DRL-T2 truncation per cell
0.0313
TSA concentration

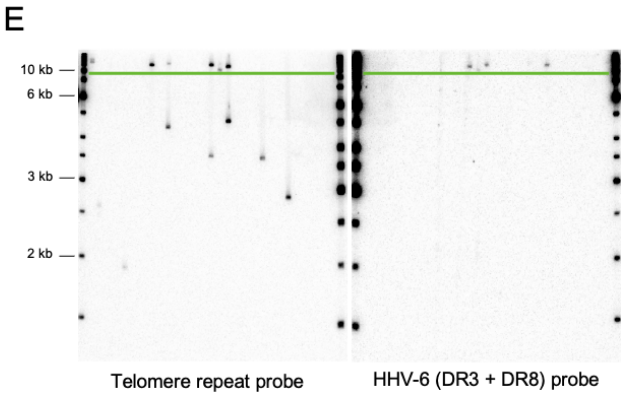
E
10 kb
6 kb
3 kb
2 kb
Telomere repeat probe
HHV-6 (DR3 + DR8) probe

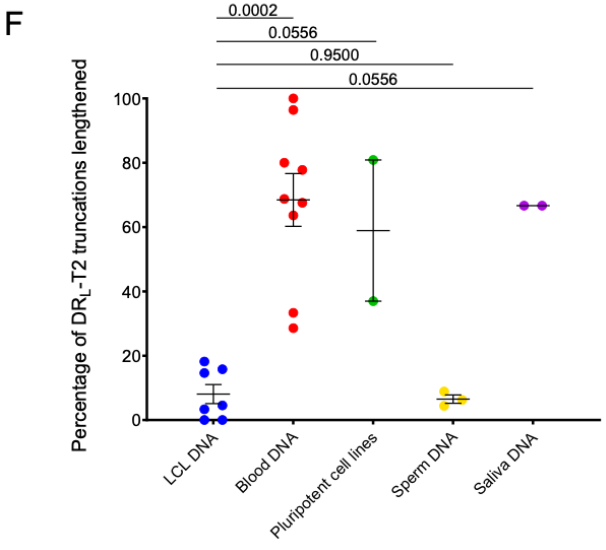
F
Percentage of DRL-T2 truncations lengthened
0.0002
0.0556
0.9500
0.0556
LCL DNA
Blood DNA
Pluripotent cell lines
Sperm DNA
Saliva DNA

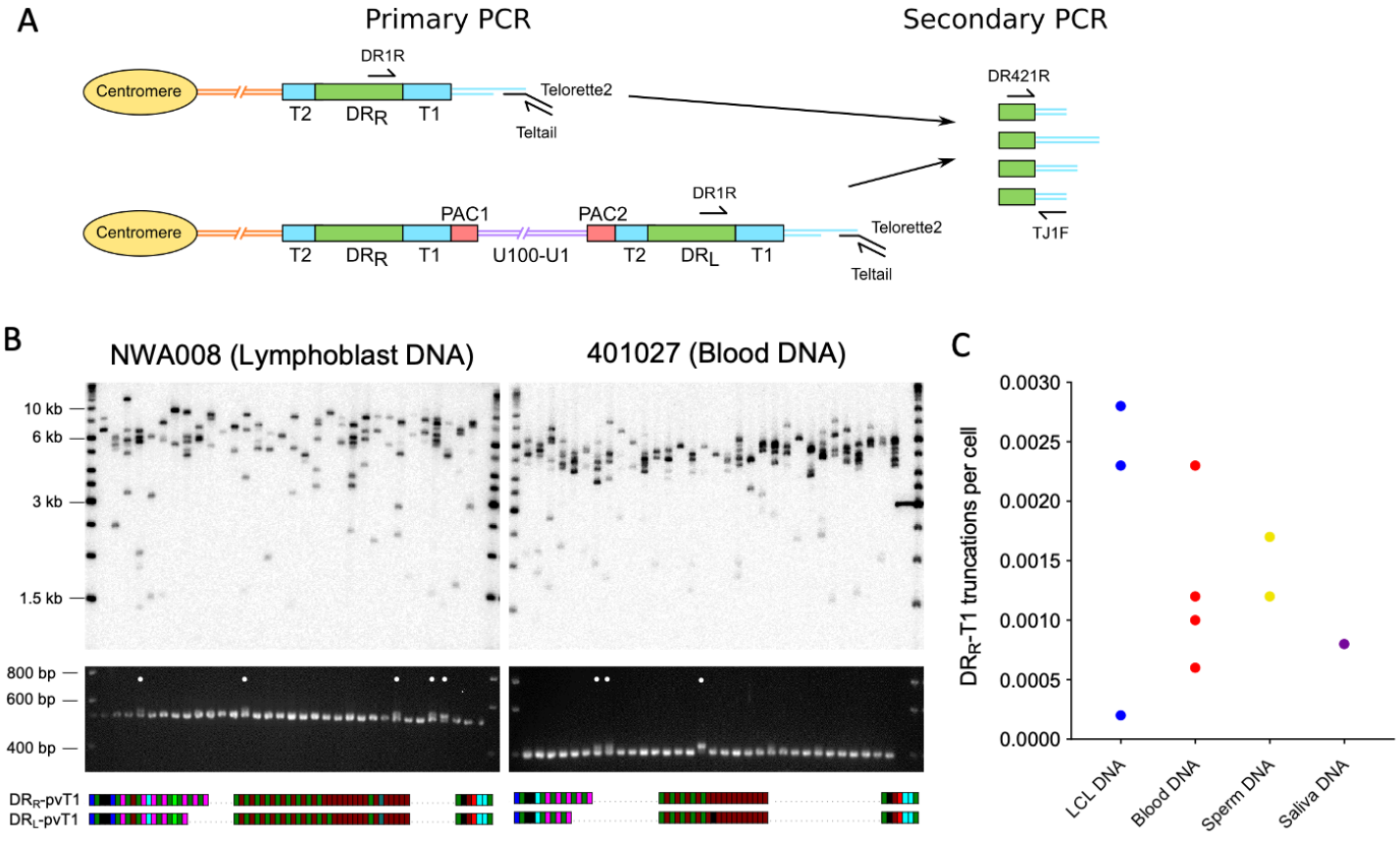
A
Primary PCR
Secondary PCR
DR1R
Centromere
T2
DRR
T1
Telorette2
Teltail
DR421R
TJ1F
PAC1
PAC2
U100-U1
DRL
B
NWA008 (Lymphoblast DNA)
401027 (Blood DNA)
10 kb
6 kb
3 kb
1.5 kb
800 bp
600 bp
400 bp
DRR-pvT1
DRL-pvT1
C
DRR-T1 truncations per cell
0.0030
0.0025
0.0020
0.0015
0.0010
0.0005
0.0000
LCL DNA
Blood DNA
Sperm DNA
Saliva DNA

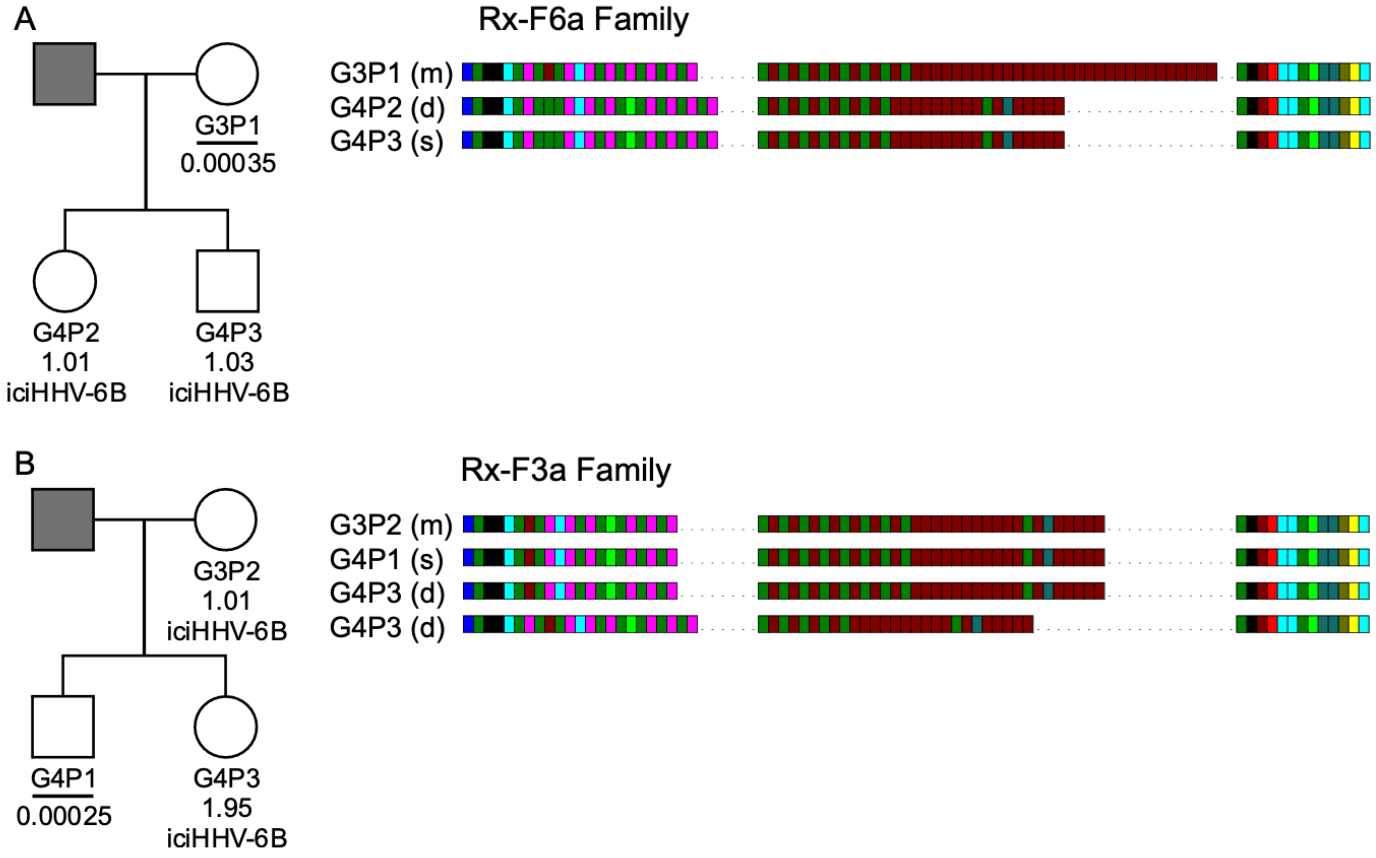
A
G3P1
0.00035
G4P2
1.01
iciHHV-6B
G4P3
1.03
iciHHV-6B
Rx-F6a Family
G3P1 (m)
G4P2 (d)
G4P3 (s)
B
G3P2
1.01
iciHHV-6B
G4P1
0.00025
G4P3
1.95
iciHHV-6B
Rx-F3a Family
G3P2 (m)
G4P1 (s)
G4P3 (d)
G4P3 (d)

Figure Supplements and Supplementary Tables

Figure 1 – figure supplement 1. Complete set of pvT1 interspersion maps from DR_R in iciHHV-6B (inherited) and acquired HHV-6B (non-inherited) strains

Figure 1 – figure supplement 2. HHV-6B strain identification using DR_R pvT1 repeat patterns in eight families, suggests that transmission of acquired HHV-6B is predominantly from parents

Figure 2 – figure supplement 1. Examples of views taken from the HHV-6 Explorer.

Figure 5 – figure supplement**.** Detect of excised circular DR-only molecules, sequencing of a lengthened new telomere at DR_L-T2 and detection of telomerase activity.

Figure 6 – figure supplement. The majority of iciHHV-6B genomes show sequence differences between DR_R-pvT1 and DR_L-pvT1

Supplementary Table 1. AcqHHV-6A/6B and iciHHV-6A/6B genomes included in study

Supplementary Table 2. Estimated Time to Most Recent Common Ancestor (TMRCA) for carriers of iciHHV-6A and iciHHV-6B with different chromosomal locations.

Supplementary Table 3. Measuring the percentage of acquired HHV-6B with a telomere, as an indicator of integration

Supplementary Table 4. Variation in the frequency of truncations at DR_L-T2 and percentage lengthened between samples

Supplementary Table 5. Measuring the frequency of truncations at DR_R-T1 in various samples

Supplementary Table 6. Primers used in this study, including primers used to generate overlapping amplicons for iciHHV-6A/6B genome sequencing

Figure 1 – figure supplement 1. Complete set of pvT1 interspersion maps from DR_R in iciHHV-6B (inherited) and acquired HHV-6B (non-inherited) strains.

The 102 DR_R-pvT1 repeat patterns shown demonstrate the diversity among iciHHV-6B (inherited) and HHV-6B (acquired) genomes. Ninety of the repeat patterns were unique. Degenerate, telomere-like repeats present in the HHV-6B pvT1 region are colour-coded: Dark green, TTAGGG; brown, CTAGGG; cyan, TTAGTG; yellow, TTACTG; dark yellow, ATAGAC; teal, CTAAGG; pink, CTATGG; lime green, TTATGG; blue, GTAGTG; peach, TTAGAG; red, GTCTGG. Black squares represent other, less common degenerate repeats and white squares show where the sequence could not be determined accurately. Dashes between repeats were added to maximize alignment between samples allowing comparison between the left, middle (highly variable) and right (highly conserved) sections of DR_R-pvT1. Repeat maps were grouped primarily based on the left section, then on less common features within the middle or right region, and finally by the length of the middle region. Ninety eight of the 102 DR_R-pvT1 repeat patterns are from unrelated individuals and four are from children who have an acqHHV-6B that has a different DR_R-pvT1 repeat pattern from their parents (blue diamonds). Coloured arrows identify 12 repeats patterns found more than once in donors not known to be related. Among eight of the identical DR_R-pvT1 repeat patterns (blue arrows), seven are in iciHHV-6B genomes predicted to be integrated in the 9q telomere and one in an acquired HHV-6B in SAL030. Two others, in NWA008 and DER512 from the UK, have a 17p iciHHV-6B integration and share identical DR_R-pvT1 repeat patterns. In addition, the acquired HHV-6B strains in SAL023 and TEL-FA G1P1 share the same DR_R-pvT1 repeat pattern.

Black boxes surround repeat maps from iciHHV-6Bs predicted to have the same integration site, by whole viral genome sequence homology, FISH, or subtelomere-iciHHV-6B junction sequence. Notably within integration groups there are often shared characteristic features in the DR_R-pvT1 repeat patterns.

Black dots indicate iciHHV-6B samples where DR_R-pvT1 could not be used to predict the integration site confidently. For example, the DR_R-pvT1 in iciHHV-6B in d32 has a unique right section and is unlikely to share common ancestry with any of the other iciHHV-6B carriers analysed.

Yellow diamond identifies the DR_R-pvT1 repeat pattern in family Rx-F3a, transmitted from iciHHV-6B mother to non-carrier son. This pvT1 repeat map is different from the other 101 maps shown here.

Figure 1 – figure supplement 1

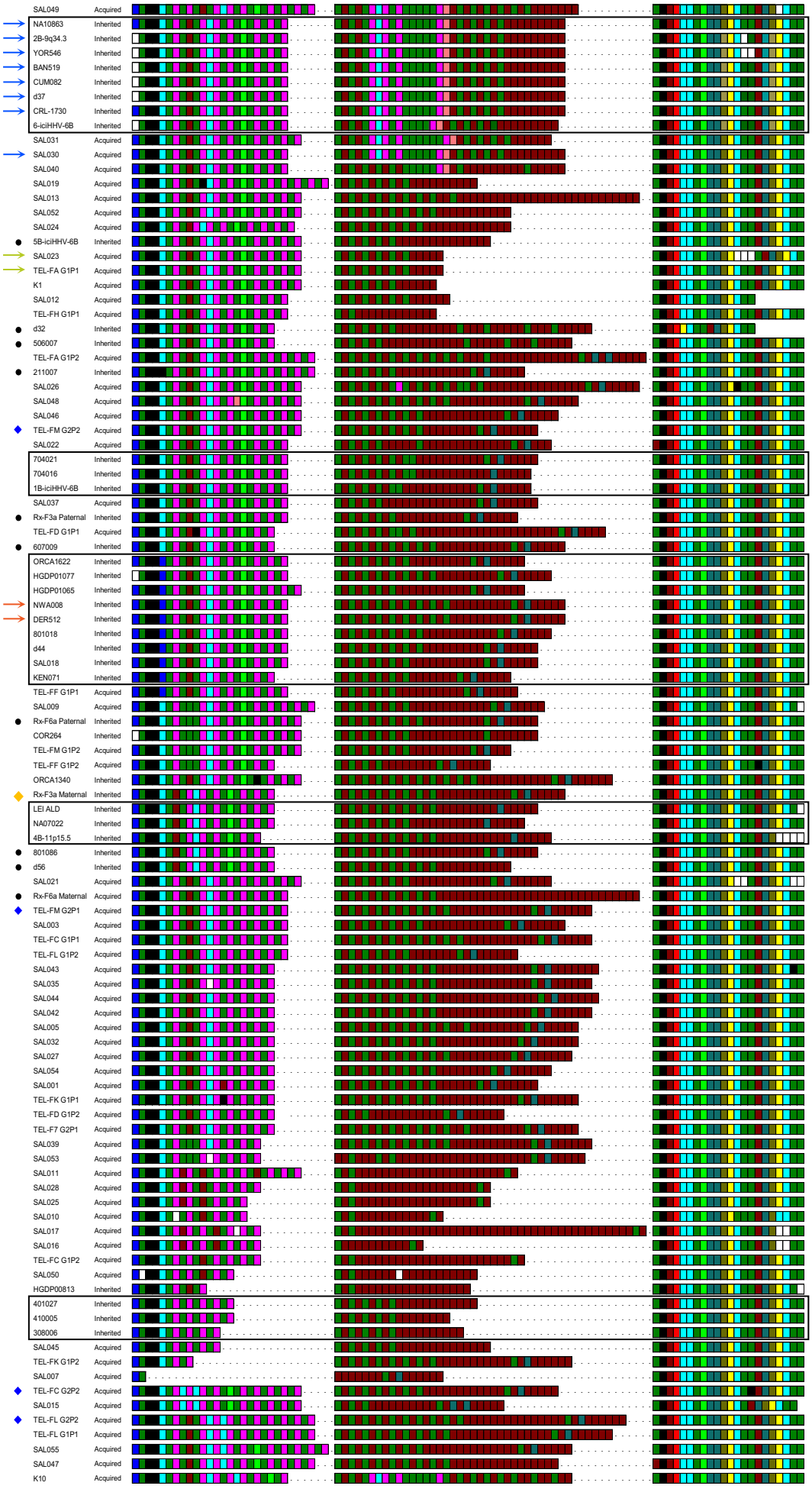

Figure 1 – figure supplement 2. HHV-6B strain identification using DR_R-pvT1 repeat patterns in eight families, suggests that transmission of acqHHV-6B is predominantly from parents.

The key to the repeat pattern is the same as in Figure 1. Pedigree symbols shaded blue indicate the child(ren) had the same acqHHV-6B DR_R-pvT1 repeat pattern as their mother and yellow indicates it was the same as their father. The pedigree symbols shaded grey identify individuals from whom the pvT1 region could not be amplified. The green symbols identify children that do not share a DR_R-pvT1 map with either parent and the dark green symbol for TEL-FM G2P1 indicates that this individual had a DR_R-pvT1 that was different to their siblings and parents. TEL-FL G2P2 (asterisk) has a DR_R-pvT1 repeat pattern that differs from that in their mother by a gain of two repeats (CTAGGG-TTAGGG) in the middle section.

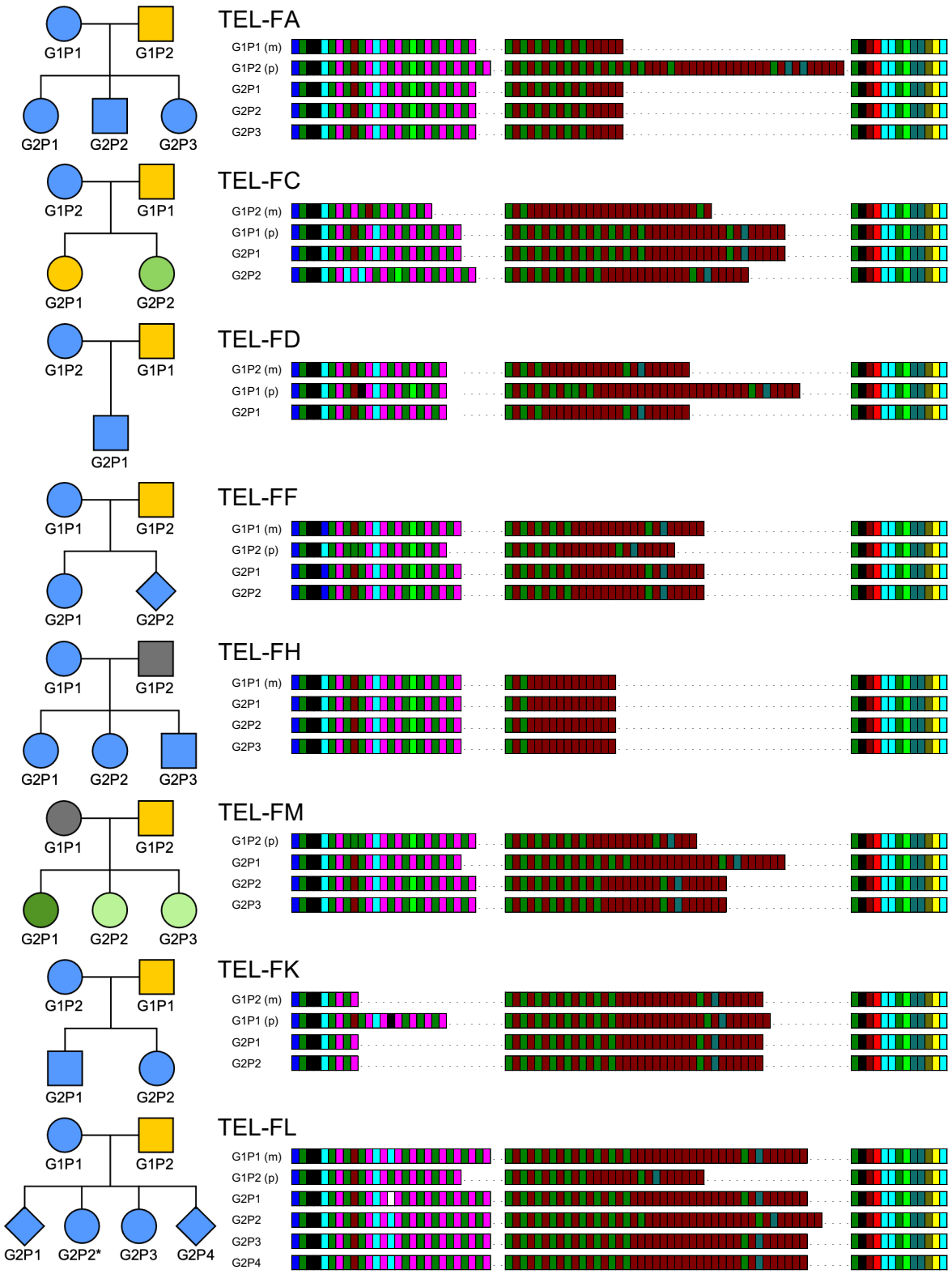

Figure 2 – figure supplement 1. Examples of views taken from the HHV-6 Explorer.

The HHV-6 explorer allows different types of variation across iciHHV-6A/6B and acquired HHV-6A/6B genomes from different individuals to be compared against a reference genome. The user can select the size of overlapping or non-overlapping sliding windows in an upper and lower graph to allow easier comparison when a larger number of genomes are selected from the drop-down menus. After selecting the type(s) of variation and genomes to be explored, a lower and upper Genome View graph will be generated based on the user-selected sliding window size. The Genome View shows the specified type(s) of variation across the whole genome as a count of mutations per window size (100 bp, non-overlapping in the examples shown here). Cumulative mutations per window size are shown if multiple types of variation are selected. Each genome is assigned a unique colour and where part of sequence is missing, a value of negative one will be assigned for that particular window and the bar on the graph will be red.

In the examples shown, iciHHV-6A and acquired HHV-6A genomes have been compared to GLA_25506 (19q iciHHV-6A) as the reference, and iciHHV-6B and acquired HHV-6B genomes have been compared to HST (acquired HHV-6B). In both examples, truncations (i.e. a nonsense mutation encoding a premature stop codon) are displayed. For HHV-6A, seven 17p iciHHV-6A genomes have been selected to be displayed on the lower graph and a variety of acquired HHV-6A and 18q, 19q and 22q iciHHV-6A genomes have been selected to be displayed on the upper graph. The Genome View is zoomed in to show a region displaying truncations in U79 in three 17p iciHHV-6A genomes (303-046, 303-035 and GLA_15137). In the HHV-6 Explorer the next graph generated is the Gene View where a single gene of interest can be selected to view variation at the amino acid level, U79 in this case. The final plot on the HHV-6 Explorer is the Gene Alignment, based on an alignment of all iciHHV-6A and acquired HHV-6A (or iciHHV-6B and acquired HHV-6B) used to generate the phylogenetic networks. In this region of U79, the sequence assemblies are missing data in 13 of the viral genomes (dashes). The exact amino acid position of the premature stop codon for 303-035 is highlighted, underscore at amino acid 431. All other iciHHV-6A/HHV-6A genomes (for which sequence is available) lack this premature stop codon, including other 17p iciHHV-6A genomes (e.g. 7A-17p13.3) indicating that this mutation arose after integration.

In the right-hand column, members of the iciHHV-6B 17p (minor) integration group are displayed in the upper graphs and a variety of other iciHHV-6B integrations and acquired HHV-6B genomes are displayed on the lower graphs. HST was used as the reference strain here. A premature stop codon is present at position 116 in U14 in 1B-iciHHV-6B but not in 704-021 or 704-016, which share the same common ancestor. Again, this indicates that the nonsense mutation arose after integration.

Figure 2 – figure supplement 1.

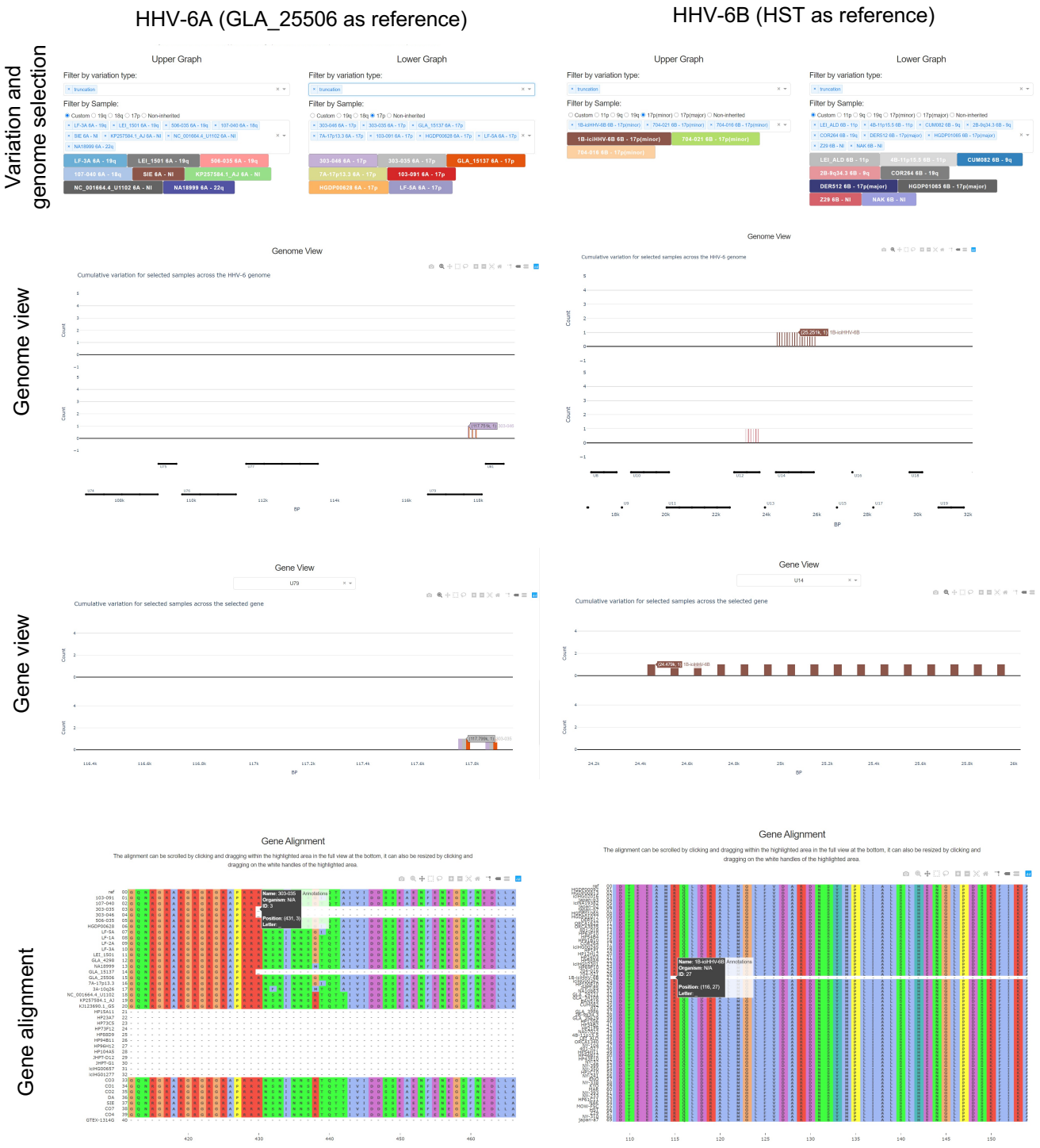

Figure 5 – figure supplement 1. Detect of excised circular DR-only molecules, sequencing of a lengthened new telomere at DR_L-T2 and detection of telomerase activity.

(A) Schematic of DR-circle assay. DR-circles were amplified using primers (DR8F(A/B) and DR3R) that should not generate a PCR product from full-length iciHHV-6B but should amplify across telomere repeats in a DR-circle, the predicted reciprocal product of a t-loop mediated excision event at DR_L-T2. Genomic DNA from two iciHHV-6B individuals (1B-iciHHV-6B and 4B-11p15.5) was digested with combinations of restriction enzymes that cut in the unique region and DR (X: SacI and PstI), only the unique region (Y: XbaI and ScaHF) or were not treated with restriction enzymes. Treated DNA was amplified using DR8F(A/B) and DR3R, and PCR products were size separated and detected by Southern blot hybridized to a radiolabelled $(TTAGGG)_n$ telomere probe. Amplicons of variable length were detected reflecting different lengths of telomere repeat arrays expected in individual DR-circles. Restriction digestion with SacI/PstI, including between DR8F(A/B) and T2, prevents amplification from DR-circles. Importantly, the minimal size of amplicons detected was greater than the combined length of the flanking regions. Full length 4B-11p15.5 had longer average telomere length at DR_L-T1 than 1B-iciHHV-6B, which is consistent with the longer products generated in the DR-circle assay.
(B) The schematic shows how newly formed telomeres at DR_L-T2 were detected and sequenced. UDL6R-STELA was used to amplify telomeres at DR_L-T2 and it occasionally amplified telomeres that were longer than the length of DR_L-T2. Six of these intermediate length STELA products from three different DNA samples were re-amplified in a semi-nested, secondary PCR using primer DR8RT2 and Telorette2. Following gel extraction these products were Sanger sequenced using DR8RT2 or Telorette2. The TTAGGG repeats were visualized with FinchTV and counted manually. Electropherograms from one reamplified molecule from NWA008 are shown. As expected, the PAC2 motif was present (boxed sequence). A black line at base 273 shows where DR_L-T2 in this sample was expected to end (after 18 TTAGGG repeats). Over 100 telomere repeats were counted from Telorette 2, considerably more than the length of T2 showing that this telomere has been lengthened.
(C) Detecting telomerase activity in iciHHV-6B lymphoblastoid cell lines. Telomere repeat amplification protocol (TRAP) was used to detect low levels of telomerase activity in various iciHHV-6B lymphoblastoid cell lines. Water and CHAPS were used as negative controls and cell lysate from a telomerase positive HUV-EC cell line was used as a positive control.

Figure 5 – figure supplement 1

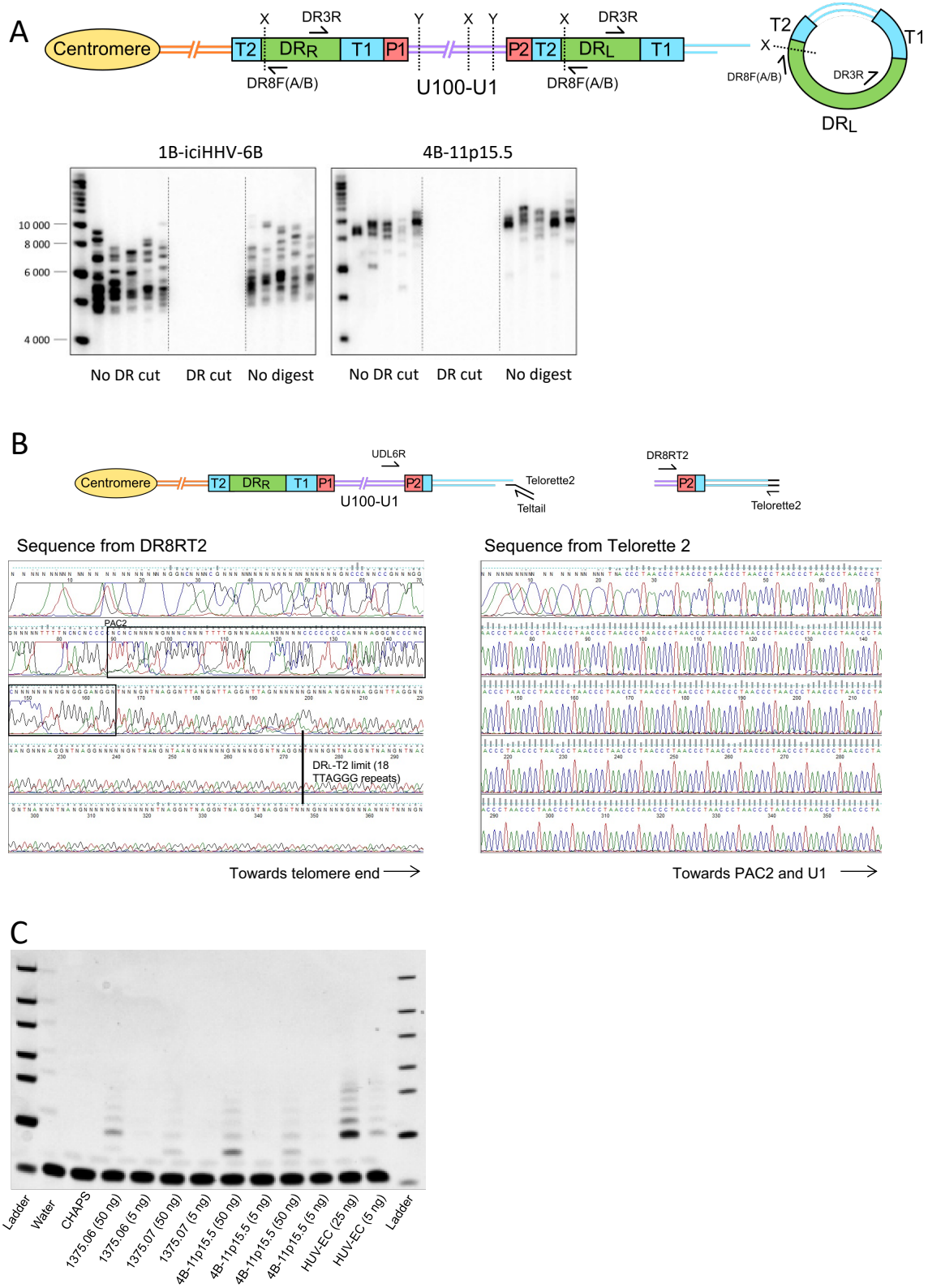

Figure 6 – figure supplement 1. The majority of iciHHV-6B genomes show sequence differences between DR_R-pvT1 and DR_L-pvT1.

DR_R-T1 and DR_L-T1 were specifically amplified by PCR using DR1R and U100Fw2 for DR_R-T1, or by STELA using DR1R and STELA oligonucleotides (Teltail and Telorette 2) for DR_L-T1. The products from DR_R-T1 and DR_L-T1 specific PCRs were used as input for secondary, nested PCR using DR421R and TJ1F to specifically amplify DR_R-pvT1 and DR_L-pvT1. Sanger sequencing was carried out using the TJ1F primer. Sequences were manually examined to generate pvT1 repeat maps. Repeats maps were colour coded and aligned as in Figure 1 – figure supplement 1. The majority of iciHHV-6B genomes (24/35, 68.6%) showed differences between DR_R-pvT1 and DR_L-pvT1, usually as loss or gain of a small number of hexameric telomere (TTAGGG) or degenerate telomere-like repeats. In a smaller number of cases, a single base change converted one repeat type to another. Regions containing CTAGGG repeats were most prone to loss or gain of repeats. Where differences between DR_R-pvT1 and DR_L-pvT1 were detected in multiple iciHHV-6B genomes from the same integration group (boxed) the differences were rarely the same between individuals. This indicates that the differences arose after integration. Interestingly, 9q iciHHV-6B genomes did not display any variation between DR_R-pvT1 and DR_L-pvT1.

Figure 6 – figure supplement 1. Comparison of pvT1 repeat patterns in DR_R and DR_L pvT1-L

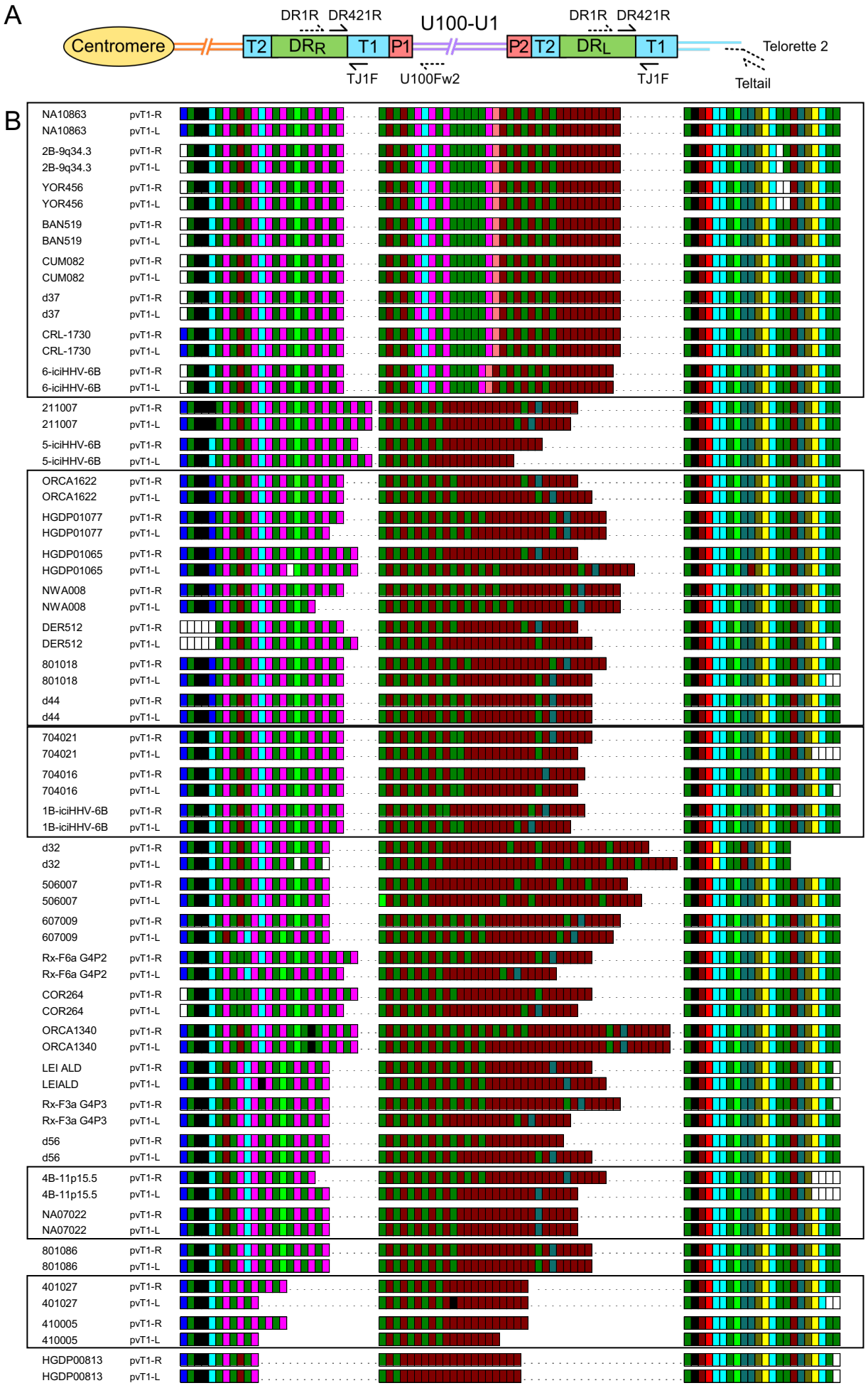

Supplementary Table 1. AcqHHV-6A/6B and iciHHV-6A/6B genomes included in study

AcqHHV-6A and iciHHV-6A genomes

Genomes in network	HHV-6A	Accession	From/Reference	Chr	Location based on:	Nationality/Ethnicity
U1102	Acquired	X83413	Gompels U. A. et. al., Virology 1995	Exogenous		Uganda
SIE	Acquired	MF994828.1	Greninger AL, et al. JVI. 92 (2018)	Exogenous		Cote d'Ivoire
AJ	Acquired	KP257584	Tweedy	Exogenous		Gambia
CO4	Acquired	MF994818.1	Greninger AL, et al. JVI. 92 (2018)	Exogenous		Germany
CO7	Acquired	MF994819.1	Greninger AL, et al. JVI. 92 (2018)	Exogenous		Germany
DA	Acquired	MF994820.1	Greninger AL, et al. JVI. 92 (2018)	Exogenous		USA
GS	Acquired	KJ123690	Unpublished	Exogenous		USA
CO2	Acquired	MF994816.1	Greninger AL, et al. JVI. 92 (2018)	Exogenous		Germany
CO1	Acquired	MF994815.1	Greninger AL, et al. JVI. 92 (2018)	Exogenous		Germany
CO3	Acquired		Greninger AL, et al. JVI. 92 (2018)	Exogenous		Germany
3A-10q26.3	Inherited	KY316049	Zhang E, et al. J Virol. 91:JVI.01137-17 (2017)	10q	FISH (Nacheva EP, et al. J Med Virol 80(11):1952-8 (2008)) and subtelomere junction (10qF primer)	UK
iciHG00657	Inherited	MG894370	Telford M, Navarro A, Santpere G. Sci Rep. 8:3472 (2018)	22q	Long read sequencing (Liu X, et al. PLOS Genet 16(8):e1008915 (2020))	Han Chinese
NA18999	Inherited	KY316047.1	Zhang E, et al. J Virol. 91:JVI.01137-17 (2017)	22q	Long read sequencing (Liu X, et al. PLOS Genet 16(8):e1008915 (2020))	Japanese
107040	Inherited		BIOSTAT-CHF cohort	18q	Homology to HP73F12	Netherlands
HP23A7	Inherited	KY315531.2	Greninger AL, et al. BMC Genomics 19:204 (2018)	18q	Homology to HP73F12	
HP94B11	Inherited	KY315549.2	Greninger AL, et al. BMC Genomics 19:204 (2018)	18q	Homology to HP73F12	
JHPT-D12	Inherited	KY315555	Greninger AL, et al. BMC Genomics 19:204 (2018)	18q	Homology to HP73F12	
HP73F12	Inherited	KY315540.2	Greninger AL, et al. BMC Genomics 19:204 (2018)	18q	FISH (Aswad A, et al. Mol Biol Evol 38(1):96-107 (2021))	
GLA 4298	Inherited	KY316056.1	Zhang E, et al. J Virol. 91:JVI.01137-17 (2017)	Unknown		UK
iciHG01277	Inherited	MG894371.1	Telford M, Navarro A, Santpere G. Sci Rep. 8:3472 (2018)	19q/p?	FISH (Aswad A, et al. Mol Biol Evol 38(1):96-107 (2021))	Colombia
HHV6A_LF3A	Inherited		Louis Flamand	19q	Homology to LEI 1501	Canadian
HHV6A_LF1A	Inherited		Louis Flamand	19q	Homology to LEI 1501	Canadian
LEI 1501	Inherited	KT355575.1	Zhang E, et al. Sci Rep. 6:22730 (2016)	19q	FISH (Zhang E, et al. Sci Rep. 6:22730 (2016))	UK
506035	Inherited		BIOSTAT-CHF cohort	19q	Homology to LEI 1501	Italy
GLA 25506	Inherited	KY316054.1	Zhang E, et al. J Virol. 91:JVI.01137-17 (2017)	19q	Homology to LEI 1501	UK
HHV6A_LF2A	Inherited		Louis Flamand	19q	Homology to LEI 1501	Canadian
JHPT-G1	Inherited	KY315558.2	Greninger AL, et al. BMC Genomics 19:204 (2018)	19q	Homology to LEI 1501	
303046	Inherited		BIOSTAT-CHF cohort	17p	Subtelomere junction (17p.311 primer) and homology to 7A-17p13.3 and HP73C5	Serbia
303035	Inherited		BIOSTAT-CHF cohort	17p	Subtelomere junction (17p.311 primer) and homology to 7A-17p13.3 and HP73C5	Serbia
GLA 15137	Inherited	KY316055.1	Zhang E, et al. J Virol. 91:JVI.01137-17 (2017)	17p	Subtelomere junction (17p.311 primer) and homology to 7A-17p13.3 and HP73C5	UK
7A-17p13.3	Inherited	KY316048.1	Zhang E, et al. J Virol. 91:JVI.01137-17 (2017)	17p	FISH (Zhang E, et al. J Virol. 91:JVI.01137-17 (2017))	UK
103091	Inherited		BIOSTAT-CHF cohort	17p	Subtelomere junction (17p.311 primer) and homology to 7A-17p13.3 and HP73C5	Netherlands
HGDP00628	Inherited		Huang Y, et al. Nucleic Acids Res 42(1):315-327 (2014)	17p	Subtelomere junction (17p.311 primer) and homology to 7A-17p13.3 and HP73C5	
HP88D9	Inherited	KY315545.2	Greninger AL, et al. BMC Genomics 19:204 (2018)	17p	Homology to 7A-17p13.3 and HP73C5	
MOW-F1C	Inherited	MK630133.1	Lysenkova M Y, et al. Children Infections 18(1):11-16 (2019)	17p	Homology to 7A-17p13.3 and HP73C5	
MOW-F1M	Inherited	MK630134.1	Lysenkova M Y, et al. Children Infections 18(1):11-16 (2019)	17p	Homology to 7A-17p13.3 and HP73C5	
HP73C5	Inherited	KY290183.2	Greninger AL, et al. BMC Genomics 19:204 (2018)	17p	FISH (Aswad A, et al. Mol Biol Evol 38(1):96-107 (2021))	
HP15A11	Inherited	KY274508.2	Greninger AL, et al. BMC Genomics 19:204 (2018)	17p	Homology to 7A-17p13.3 and HP73C5	
HP96H12	Inherited	KY315552.2	Greninger AL, et al. BMC Genomics 19:204 (2018)	17p	Homology to 7A-17p13.3 and HP73C5	
HP104A5	Inherited	KY290185.2	Greninger AL, et al. BMC Genomics 19:204 (2018)	17p	Homology to 7A-17p13.3 and HP73C5	
HHV6A_LF4A	Inherited		Louis Flamand	17p	Subtelomere junction (17p.311 primer) and homology to 7A-17p13.3 and HP73C5	Canadian
HHV6A_LF5A	Inherited	Not sequenced	Louis Flamand	17p	Subtelomere junction (17p.311 primer)	Canadian
HHV6A_LF6A	Inherited	Not sequenced	Louis Flamand	17p	Subtelomere junction (17p.311 primer)	Canadian
303046	Inherited		BIOSTAT-CHF cohort	17p	Subtelomere junction (17p.311 primer) and homology to 7A-17p13.3 and HP73C5	Serbia
303035	Inherited		BIOSTAT-CHF cohort	17p	Subtelomere junction (17p.311 primer) and homology to 7A-17p13.3 and HP73C5	Serbia
107040	Inherited		BIOSTAT-CHF cohort	18q	Homology to HP73F12	Netherlands
301005	Inherited	Not sequenced	BIOSTAT-CHF cohort	17p	Subtelomere junction (17p.311 primer) and T1 sizing	German
311033	Inherited	Not sequenced	BIOSTAT-CHF cohort	17p	Subtelomere junction (17p.311 primer) and T1 sizing	Slovenian
701042	Inherited	Not sequenced	BIOSTAT-CHF cohort	17p	Subtelomere junction (17p.311 primer) and T1 sizing	Polish
801015	Inherited	Not sequenced	BIOSTAT-CHF cohort	Not tested		British

Supplementary Table 1 (Continued).

AcqHHV-6B and iciHHV-6B genomes

Genomes in network	HHV-6B	Accession	From/Reference	Chr	Location based on:	Nationality/Ethnicity
Z29	Acquired	AF157706	Dominguez G, et al. J Virol. 73:8040–52 (1999).	Exogenous		Democratic Republic of Congo
HP61C11	Inherited	KY290178.2	Greninger AL, et al. BMC Genomics 19:204 (2018)	Unknown		White
NAK	Acquired	MF994827	Greninger AL, et al. J Virol. 92 (2018)	Exogenous		Japanese
HGDP00092	Inherited	KY316037	Zhang E, et al. J Virol. 91:JVI.01137-17 (2017)	15q	FISH (Aswad A, et al. Mol Biol Evol 38(1):96-107 (2021))	Pakistan
NY-233	Acquired	KY290195.2	Greninger AL, et al. BMC Genomics 19:204 (2018)	Exogenous		Hispanic
NY-393	Acquired	KY290215.2	Greninger AL, et al. BMC Genomics 19:204 (2018)	Exogenous		White
iciHG02016	Inherited	MG894372	Telford M, Navarro A, Santpere G. Sci Rep. 8:3472 (2018)	Unknown		Vietnam
HGDP00813	Inherited	KY316036	Zhang E, et al. J Virol. 91:JVI.01137-17 (2017)	Unknown		Han Chinese
japan-b3	Acquired	KY274498.2	Greninger AL, et al. BMC Genomics 19:204 (2018)	Exogenous		Japanese
japan-b7	Acquired	KY274501.2	Greninger AL, et al. BMC Genomics 19:204 (2018)	Exogenous		Japanese
HST	Acquired	AB021506	Isegawa Y, et al. J Virol. 73:8053–8063 (1999).	Exogenous		Uganda
japan-b2	Acquired	KY274497.2	Greninger AL, et al. BMC Genomics 19:204 (2018)	Exogenous		Japanese
japan-a7	Acquired	KY274491.2	Greninger AL, et al. BMC Genomics 19:204 (2018)	Exogenous		Japanese
NY-399	Acquired	KY290218.2	Greninger AL, et al. BMC Genomics 19:204 (2018)	Exogenous		White
iciNA19382	Inherited	MG894376	Telford M, Navarro A, Santpere G. Sci Rep. 8:3472 (2018)	1q	FISH (Aswad A, et al. Mol Biol Evol 38(1):96-107 (2021))	Kenya
iciHG00362	Inherited	MG894369	Telford M, Navarro A, Santpere G. Sci Rep. 8:3472 (2018)	Unknown		Finland
NY-350	Acquired	KY290207.2	Greninger AL, et al. BMC Genomics 19:204 (2018)	Exogenous		White
401027	Inherited		BIOSTAT-CHF cohort	provisional 2p	Subtelomere junction (2p2 primer)	Greece
NY-32	Acquired	KY290187.2	Greninger AL, et al. BMC Genomics 19:204 (2018)	Exogenous		White
MAR	Acquired	MF994826	Greninger AL, et al. JVI. 92 (2018)	Exogenous		France
NY-241	Acquired	KY290197.2	Greninger AL, et al. BMC Genomics 19:204 (2018)	Exogenous		USA
KYO	Acquired	MF994825	Greninger AL, et al. JVI. 92 (2018)	Exogenous		Japanese
ENO	Acquired	MF994821	Greninger AL, et al. JVI. 92 (2018)	Exogenous		Japanese
LEI ALD	Inherited	KY316033	Zhang E, et al. J Virol. 91:JVI.01137-17 (2017)	11p	Homology with 4B-11p15.5	UK
4B-11p15.5	Inherited	KY316044	Zhang E, et al. J Virol. 91:JVI.01137-17 (2017)	11p	FISH (Nacheva EP, et al. J Med Virol 80(11):1952-8 (2008))	UK
NA07022	Inherited	KY316039	Zhang E, et al. J Virol. 91:JVI.01137-17 (2017)	11p	Homology with 4B-11p15.5	USA
JHPT-E5	Inherited	KY315557.2	Greninger AL, et al. BMC Genomics 19:204 (2018)	Unknown		White
HP2C10	Inherited	KY315522.2	Greninger AL, et al. BMC Genomics 19:204 (2018)	Unknown		White
HP100E10	Inherited	KY290184.2	Greninger AL, et al. BMC Genomics 19:204 (2018)	Exogenous		White
MOW-F5C	Inherited	MN242397	Lysenkova M Y, et al. Children Infections 18(1):11-16 (2019)	Unknown		Russian
NY-338	Acquired	KY290206.2	Greninger AL, et al. BMC Genomics 19:204 (2018)	Exogenous		Black
NY-104	Acquired	KY290189.2	Greninger AL, et al. BMC Genomics 19:204 (2018)	Exogenous		USA
CUM082	Inherited	KY316041	Zhang E, et al. J Virol. 91:JVI.01137-17 (2017)	9q	Homology with 2B-9q34.3 and pvT1 CRL-1730	UK
HP12G6	Inherited	KY315529.2	Greninger AL, et al. BMC Genomics 19:204 (2018)	9q	Homology with 2B-9q34.3	White
GLA 35629	Inherited	KY316050	Zhang E, et al. J Virol. 91:JVI.01137-17 (2017)	9q	Homology with 2B-9q34.3	UK
GLA 34108	Inherited	KY316051	Zhang E, et al. J Virol. 91:JVI.01137-17 (2017)	9q	Homology with 2B-9q34.3	UK
GLA 29221	Inherited	KY316052	Zhang E, et al. J Virol. 91:JVI.01137-17 (2017)	9q	Homology with 2B-9q34.3	UK
HP34B2	Inherited	KY274520.2	Greninger AL, et al. BMC Genomics 19:204 (2018)	9q	Homology with 2B-9q34.3	White
2B-9q34.3	Inherited	KY316045	Zhang E, et al. J Virol. 91:JVI.01137-17 (2017)	9q	FISH (Nacheva EP, et al. J Med Virol 80(11):1952-8 (2008))	UK
GLA 3986	Inherited	KY316053	Zhang E, et al. J Virol. 91:JVI.01137-17 (2017)	9q	Homology with 2B-9q34.3	UK
d37	Inherited		This paper	9q	Homology with 2B-9q34.3 and pvT1 CRL-1730	Unknown
BAN519	Inherited	KY316043	Zhang E, et al. J Virol. 91:JVI.01137-17 (2017)	9q	Homology with 2B-9q34.3 and pvT1 CRL-1730	UK
NA10863	Inherited	KY316038	Zhang E, et al. J Virol. 91:JVI.01137-17 (2017)	9q	Homology with 2B-9q34.3 and pvT1 CRL-1730	USA
ORCA1340	Inherited	KY316032	Zhang E, et al. J Virol. 91:JVI.01137-17 (2017)	Unknown		UK
HP43E10	Inherited	KY315535.2	Greninger AL, et al. BMC Genomics 19:204 (2018)	Unknown		White
HP58A9	Inherited	KY290176.2	Greninger AL, et al. BMC Genomics 19:204 (2018)	19q	Homology with iciHG00245 and HP24D3	White
iciHG00245	Inherited	MG894368	Telford M, Navarro A, Santpere G. Sci Rep. 8:3472 (2018)	19q	FISH (Aswad A, et al. Mol Biol Evol 38(1):96-107 (2021))	UK
COR264	Inherited	KY316042	Zhang E, et al. J Virol. 91:JVI.01137-17 (2017)	19q	Homology with iciHG00245 and HP24D3	UK
HP24D3	Inherited	KY274514.2	Greninger AL, et al. BMC Genomics 19:204 (2018)	19q	FISH (Aswad A, et al. Mol Biol Evol 38(1):96-107 (2021))	White
HP1F1	Inherited	KY315521.2	Greninger AL, et al. BMC Genomics 19:204 (2018)	19q	Homology with iciHG00245 and HP24D3	White
HP12H12	Inherited	KY315530.2	Greninger AL, et al. BMC Genomics 19:204 (2018)	19q	Homology with iciHG00245 and HP24D3	White
iciHG02301	Inherited	MG894373	Telford M, Navarro A, Santpere G. Sci Rep. 8:3472 (2018)	3q	FISH (Aswad A, et al. Mol Biol Evol 38(1):96-107 (2021))	Peru
HP54H11	Inherited	KY290175.2	Greninger AL, et al. BMC Genomics 19:204 (2018)	Unknown		USA
1B-iciHHV-6B	Inherited	KY316046	Zhang E, et al. J Virol. 91:JVI.01137-17 (2017)	provisional 17p (min	Subtelomere junction (17p.311 primer)	UK
704021	Inherited		BIOSTAT-CHF cohort	provisional 17p (min	Subtelomere junction (17p.311 primer)	Poland
704016	Inherited		BIOSTAT-CHF cohort	provisional 17p (min	Subtelomere junction (17p.311 primer)	Poland
HP69F10	Inherited	KY290182.2	Greninger AL, et al. BMC Genomics 19:204 (2018)	Unknown		USA
HGDP01065	Inherited	KY316035	Zhang E, et al. J Virol. 91:JVI.01137-17 (2017)	17p (major)	Subtelomere junction (17p.311 primer) and homology to HP46B12	Italy
HP46B12	Inherited	KY315536.2	Greninger AL, et al. BMC Genomics 19:204 (2018)	17p (major)	FISH (Aswad A, et al. Mol Biol Evol 38(1):96-107 (2021))	Black
DER512	Inherited	KY316040	Zhang E, et al. J Virol. 91:JVI.01137-17 (2017)	17p (major)	Subtelomere junction (17p.311 primer) and homology to HP46B12	UK
HGDP01077	Inherited	KY316034	Zhang E, et al. J Virol. 91:JVI.01137-17 (2017)	17p (major)	Subtelomere junction (17p.311 primer) and homology to HP46B12	Italy
801018	Inherited		BIOSTAT-CHF cohort	17p (major)	Subtelomere junction (17p.311 primer) and homology to HP46B12	
ORCA3835	Inherited	KY316030	Zhang E, et al. J Virol. 91:JVI.01137-17 (2017)	17p (major)	Subtelomere junction (17p.311 primer) and homology to HP46B12	UK
ORCA1622	Inherited	KY316031	Zhang E, et al. J Virol. 91:JVI.01137-17 (2017)	17p (major)	Subtelomere junction (17p.311 primer) and homology to HP46B12	UK
HP54B4	Inherited	KY290174.2	Greninger AL, et al. BMC Genomics 19:204 (2018)	17p (major)	Homology to HP46B12	White
HP63F10	Inherited	KY290179.2	Greninger AL, et al. BMC Genomics 19:204 (2018)	17p (major)	Homology to HP46B12	White
HP91B10	Inherited	KY315547.2	Greninger AL, et al. BMC Genomics 19:204 (2018)	17p (major)	Homology to HP46B12	White
HP21F9	Inherited	KY274512.2	Greninger AL, et al. BMC Genomics 19:204 (2018)	Unknown		White

Supplementary Table 1 (Continued).

AcqHHV-6B and iciHHV-6B genomes (continued)

Genomes not in network	HHV-6B	Accession	From/Reference	Chr	Location based on:	Nationality/Ethnicity
410005	Inherited	Not sequenced	BIOSTAT-CHF cohort	provisional 2p	Subtelomere junction (2p2 primer)	Greece
308006	Inherited	Not sequenced	BIOSTAT-CHF cohort	provisional 2p	Subtelomere junction (2p2 primer)	Serbia
d56	Inherited	Not sequenced	Jeffreys AJ, et al. Nat Genet 31:267-271 (2002)	Unknown		UK
YOR546	Inherited	Not sequenced	Huang Y, et al. Nucleic Acids Res 42(1):315-327 (2014)	9q	pvT1 2B-9q34.3 and pvT1 CRL-1730	UK
CRL-1730	Inherited	Not sequenced	Shioda S, et al. Cytotechnology 70:141-152 (2018)	9q	FISH (Shioda S, et al. Cytotechnology 70:141-152 (2018))	Unknown
6-iciHHV-6B	Inherited	Not sequenced	Nacheva EP, et al. J Med Virol 80(11):1952-8 (2008)	9q	pvT1 2B-9q34.3 and pvT1 CRL-1730	UK
d44	Inherited	Not sequenced	Jeffreys AJ, et al. Nat Genet 31:267-271 (2002)	17p	Subtelomere junction (17p.311 primer) and homology to HP46B12	UK
NWA008	Inherited	Not sequenced	Zhang E, et al. J Virol. 91:JVI.01137-17 (2017)	17p	Subtelomere junction (17p.311 primer) and homology to HP46B12	UK
801086	Inherited	Not sequenced	BIOSTAT-CHF cohort	Unknown		UK
5B-iciHHV-6B	Inherited	Not sequenced	Nacheva EP, et al. J Med Virol 80(11):1952-8 (2008)	Unknown		UK
d32	Inherited	Not sequenced	Jeffreys AJ, et al. Nat Genet 31:267-271 (2002)	Unknown		UK
506007	Inherited	Not sequenced	BIOSTAT-CHF cohort	Unknown		Italy
211007	Inherited	Not sequenced	BIOSTAT-CHF cohort	Unknown		France
607009	Inherited	Not sequenced	BIOSTAT-CHF cohort	Unknown		Norway
KEN071	Inherited	Not sequenced	Huang Y, et al. Nucleic Acids Res 42(1):315-327 (2014)	17p	Subtelomere junction (17p.311 primer)	UK
SAL001	Acquired	Not sequenced	SAL saliva this study	Exogenous		White British
SAL003	Acquired	Not sequenced	SAL saliva this study	Exogenous		White British
SAL005	Acquired	Not sequenced	SAL saliva this study	Exogenous		White British
SAL006	Acquired	Not sequenced	SAL saliva this study	Exogenous		White British
SAL007	Acquired	Not sequenced	SAL saliva this study	Exogenous		White British
SAL008	Acquired	Not sequenced	SAL saliva this study	Exogenous		White British
SAL009	Acquired	Not sequenced	SAL saliva this study	Exogenous		White British
SAL010	Acquired	Not sequenced	SAL saliva this study	Exogenous		Asian European
SAL011	Acquired	Not sequenced	SAL saliva this study	Exogenous		Spanish
SAL012	Acquired	Not sequenced	SAL saliva this study	Exogenous		Polish
SAL013	Acquired	Not sequenced	SAL saliva this study	Exogenous		Indian
SAL014	Acquired	Not sequenced	SAL saliva this study	Exogenous		French
SAL015	Acquired	Not sequenced	SAL saliva this study	Exogenous		White British
SAL016	Acquired	Not sequenced	SAL saliva this study	Exogenous		White British
SAL017	Acquired	Not sequenced	SAL saliva this study	Exogenous		White British
SAL018	Inherited	Not sequenced	SAL saliva this study	Exogenous		White British
SAL019	Acquired	Not sequenced	SAL saliva this study	Exogenous		Polish
SAL020	Acquired	Not sequenced	SAL saliva this study	Exogenous		Dutch
SAL021	Acquired	Not sequenced	SAL saliva this study	Exogenous		Italian
SAL022	Acquired	Not sequenced	SAL saliva this study	Exogenous		White British
SAL023	Acquired	Not sequenced	SAL saliva this study	Exogenous		White British
SAL024	Acquired	Not sequenced	SAL saliva this study	Exogenous		Spanish
SAL025	Acquired	Not sequenced	SAL saliva this study	Exogenous		White British
SAL026	Acquired	Not sequenced	SAL saliva this study	Exogenous		White British
SAL027	Acquired	Not sequenced	SAL saliva this study	Exogenous		White British
SAL028	Acquired	Not sequenced	SAL saliva this study	Exogenous		White British
SAL030	Acquired	Not sequenced	SAL saliva this study	Exogenous		White British
SAL031	Acquired	Not sequenced	SAL saliva this study	Exogenous		Cypriot
SAL032	Acquired	Not sequenced	SAL saliva this study	Exogenous		White British
SAL033	Acquired	Not sequenced	SAL saliva this study	Exogenous		Mixed European
SAL034	Acquired	Not sequenced	SAL saliva this study	Exogenous		White British
SAL035	Acquired	Not sequenced	SAL saliva this study	Exogenous		White British
SAL036	Acquired	Not sequenced	SAL saliva this study	Exogenous		Indian
SAL037	Acquired	Not sequenced	SAL saliva this study	Exogenous		White British
SAL038	Acquired	Not sequenced	SAL saliva this study	Exogenous		Polish
SAL039	Acquired	Not sequenced	SAL saliva this study	Exogenous		White British
SAL040	Acquired	Not sequenced	SAL saliva this study	Exogenous		White British
SAL041	Acquired	Not sequenced	SAL saliva this study	Exogenous		White British
SAL042	Acquired	Not sequenced	SAL saliva this study	Exogenous		White British
SAL043	Acquired	Not sequenced	SAL saliva this study	Exogenous		White British
SAL044	Acquired	Not sequenced	SAL saliva this study	Exogenous		White British
SAL045	Acquired	Not sequenced	SAL saliva this study	Exogenous		White British
SAL046	Acquired	Not sequenced	SAL saliva this study	Exogenous		White British
SAL047	Acquired	Not sequenced	SAL saliva this study	Exogenous		White British
SAL048	Acquired	Not sequenced	SAL saliva this study	Exogenous		British Chilean
SAL049	Acquired	Not sequenced	SAL saliva this study	Exogenous		Chinese
SAL050	Acquired	Not sequenced	SAL saliva this study	Exogenous		White British
SAL051	Acquired	Not sequenced	SAL saliva this study	Exogenous		White British
SAL052	Acquired	Not sequenced	SAL saliva this study	Exogenous		White/Asian British
SAL053	Acquired	Not sequenced	SAL saliva this study	Exogenous		Indian
SAL054	Acquired	Not sequenced	SAL saliva this study	Exogenous		White British
SAL055	Acquired	Not sequenced	SAL saliva this study	Exogenous		Unknown
K1	Acquired	Not sequenced	Marques FZ et al Mol Med:21 p739-748 (2015)	Exogenous		Unknown
K10	Acquired	Not sequenced	Marques FZ et al Mol Med:21 p739-748 (2015)	Exogenous		Unknown
TEL-FA G1P1	Acquired	Not sequenced	Telomeres in families. Garrido-Navas, MC et al Life: 10(11) (2020)	Exogenous		
TEL-FA G1P2	Acquired	Not sequenced	Telomeres in families. Garrido-Navas, MC et al Life: 10(11) (2020)	Exogenous		
TEL-FA G2P1	Acquired	Not sequenced	Telomeres in families. Garrido-Navas, MC et al Life: 10(11) (2020)	Exogenous		
TEL-FA G2P2	Acquired	Not sequenced	Telomeres in families. Garrido-Navas, MC et al Life: 10(11) (2020)	Exogenous		
TEL-FA G2P3	Acquired	Not sequenced	Telomeres in families. Garrido-Navas, MC et al Life: 10(11) (2020)	Exogenous		
TEL-FC G1P1	Acquired	Not sequenced	Telomeres in families. Garrido-Navas, MC et al Life: 10(11) (2020)	Exogenous		
TEL-FC G1P2	Acquired	Not sequenced	Telomeres in families. Garrido-Navas, MC et al Life: 10(11) (2020)	Exogenous		
TEL-FC G2P1	Acquired	Not sequenced	Telomeres in families. Garrido-Navas, MC et al Life: 10(11) (2020)	Exogenous		
TEL-FC G2P2	Acquired	Not sequenced	Telomeres in families. Garrido-Navas, MC et al Life: 10(11) (2020)	Exogenous		
TEL-FD G1P1	Acquired	Not sequenced	Telomeres in families. Garrido-Navas, MC et al Life: 10(11) (2020)	Exogenous		
TEL-FD G1P2	Acquired	Not sequenced	Telomeres in families. Garrido-Navas, MC et al Life: 10(11) (2020)	Exogenous		
TEL-FD G2P1	Acquired	Not sequenced	Telomeres in families. Garrido-Navas, MC et al Life: 10(11) (2020)	Exogenous		
TEL-FF G1P1	Acquired	Not sequenced	Telomeres in families. Garrido-Navas, MC et al Life: 10(11) (2020)	Exogenous		
TEL-FF G1P2	Acquired	Not sequenced	Telomeres in families. Garrido-Navas, MC et al Life: 10(11) (2020)	Exogenous		
TEL-FF G2P1	Acquired	Not sequenced	Telomeres in families. Garrido-Navas, MC et al Life: 10(11) (2020)	Exogenous		
TEL-FF G2P2	Acquired	Not sequenced	Telomeres in families. Garrido-Navas, MC et al Life: 10(11) (2020)	Exogenous		
TEL-FH G1P1	Acquired	Not sequenced	Telomeres in families. Garrido-Navas, MC et al Life: 10(11) (2020)	Exogenous		
TEL-FH G2P1	Acquired	Not sequenced	Telomeres in families. Garrido-Navas, MC et al Life: 10(11) (2020)	Exogenous		
TEL-FH G2P2	Acquired	Not sequenced	Telomeres in families. Garrido-Navas, MC et al Life: 10(11) (2020)	Exogenous		
TEL-FH G2P3	Acquired	Not sequenced	Telomeres in families. Garrido-Navas, MC et al Life: 10(11) (2020)	Exogenous		
TEL-FM G1P2	Acquired	Not sequenced	Telomeres in families. Garrido-Navas, MC et al Life: 10(11) (2020)	Exogenous		
TEL-FM G2P1	Acquired	Not sequenced	Telomeres in families. Garrido-Navas, MC et al Life: 10(11) (2020)	Exogenous		
TEL-FM G2P2	Acquired	Not sequenced	Telomeres in families. Garrido-Navas, MC et al Life: 10(11) (2020)	Exogenous		
TEL-FM G2P3	Acquired	Not sequenced	Telomeres in families. Garrido-Navas, MC et al Life: 10(11) (2020)	Exogenous		
TEL-FK G1P1	Acquired	Not sequenced	Telomeres in families. Garrido-Navas, MC et al Life: 10(11) (2020)	Exogenous		
TEL-FK G1P2	Acquired	Not sequenced	Telomeres in families. Garrido-Navas, MC et al Life: 10(11) (2020)	Exogenous		
TEL-FK G2P1	Acquired	Not sequenced	Telomeres in families. Garrido-Navas, MC et al Life: 10(11) (2020)	Exogenous		
TEL-FK G2P2	Acquired	Not sequenced	Telomeres in families. Garrido-Navas, MC et al Life: 10(11) (2020)	Exogenous		
TEL-FL G1P1	Acquired	Not sequenced	Telomeres in families. Garrido-Navas, MC et al Life: 10(11) (2020)	Exogenous		
TEL-FL G1P2	Acquired	Not sequenced	Telomeres in families. Garrido-Navas, MC et al Life: 10(11) (2020)	Exogenous		
TEL-FL G2P1	Acquired	Not sequenced	Telomeres in families. Garrido-Navas, MC et al Life: 10(11) (2020)	Exogenous		
TEL-FL G2P2	Acquired	Not sequenced	Telomeres in families. Garrido-Navas, MC et al Life: 10(11) (2020)	Exogenous		
TEL-FL G2P3	Acquired	Not sequenced	Telomeres in families. Garrido-Navas, MC et al Life: 10(11) (2020)	Exogenous		
TEL-FL G2P4	Acquired	Not sequenced	Telomeres in families. Garrido-Navas, MC et al Life: 10(11) (2020)	Exogenous		
Rx-F6a G3P1	Acquired	Not sequenced	Telomeres in families. Garrido-Navas, MC et al Life: 10(11) (2020)	Exogenous		
Rx-F6a G4P2	Inherited	Not sequenced	Telomeres in families. Garrido-Navas, MC et al Life: 10(11) (2020)	Unknown		
Rx-F6a G4P3	Inherited	Not sequenced	Telomeres in families. Garrido-Navas, MC et al Life: 10(11) (2020)	Unknown		
Rx-F3a G3P2	Inherited	Not sequenced	Telomeres in families. Garrido-Navas, MC et al Life: 10(11) (2020)	Unknown		
Rx-F3a G4P1	Acquired	Not sequenced	Telomeres in families. Garrido-Navas, MC et al Life: 10(11) (2020)	Exogenous		
Rx-F3a G4P3	Inherited X2	Not sequenced	Telomeres in families. Garrido-Navas, MC et al Life: 10(11) (2020)	Unknown		

Supplementary Table 2. Estimated Time to Most Recent Common Ancestor (TMRCA) for carriers of iciHHV-6A and iciHHV-6B with different chromosomal locations.

Species	Chromosome location	No. genomes	TMRCA ± SD
HHV-6A	17p	14	105 033 ± 19 139
HHV-6A	18q	5	22 976 ± 10 275
HHV-6A	19q	8	68 928 ± 14 070
HHV-6B	9q	11	20 855 ± 12 552
HHV-6B	17p (major group)	7	23 409 ± 11 226
HHV-6B	19q	6	24 579 ± 11 260

Supplementary Table 3. Measuring the percentage of acquired HHV-6B with a telomere, as an indicator of integration

	SAL015	SAL027	SAL039	SAL040	SAL044	Tel-FA G1P2	K1	K10
Total DNA input (ng)	3600	1800	1800	900	900	1800	225	225
Cell equivalent	5.45×10^5	2.73×10^5	2.73×10^5	1.36×10^5	1.36×10^5	2.73×10^5	3.41×10^4	3.41×10^4
Reactions with HHV-6B telomere	5	3	9	2	19	4	0	4
Copies of ciHHV-6 per cell	9.17×10^{-6}	1.1×10^{-5}	3.30×10^{-5}	1.47×10^{-5}	1.39×10^{-4}	1.47×10^{-5}	0	1.17×10^{-4}
Copies of HHV-6B per cell	0.0027	0.002933	0.001667	0.001333	0.012467	0.00087	0.000525	0.0124
Percentage integrated /%	0.34	0.38	1.98	1.1	1.12	1.69	0	0.95

Supplementary Table 4. Variation between samples in the frequency of truncations at DR_L-T2 and percentage lengthened.

Sample name	DNA source	Truncations at DRL-T2 per cell	Percentage lengthened	Lengthened per cell
NWA008	Lymphoblasts	0.0169	14.6	0.0025
CEPH1375.02	Lymphoblasts	0.0091	4.55	0.0004
COR264	Lymphoblasts	0.0078	15.8	0.0012
4B-11p15.5	Lymphoblasts	0.0248	3.33	0.0008
5B-17p13.3	Lymphoblasts	0.0158	0.00	0.00
YOR546	Lymphoblasts	0.0136	18.2	0.0025
OL	Lymphoblasts	0.0172	0.00	0.00
d37	Pluripotent cells	0.0093	80.9	0.0076
CRL-1730	Pluripotent cells	0.019	37.0	0.007
401027	Blood	0.0025	63.7	0.0016
801018	Blood	0.0016	28.6	0.0005
211007	Blood	0.0025	77. 8	0.0019
704016	Blood	0.0009	100	0.0009
704021	Blood	0.0007	33.3	0.0002
801086	Blood	0.0032	68.8	0.0022
506007	Blood	0.0027	80.0	0.0022
607009	Blood	0.0084	67.6	0.0057
410005	Blood	0.0064	96.4	0.0061
d32	Sperm	0.0063	4.41	0.0003
d44	Sperm	0.0066	6.25	0.0004
d56	Sperm	0.0059	8.87	0.0005
Rx-F6a G4P2	Saliva	0.005	66.7	0.0033
Rx-F6a G4P3	Saliva	0.0012	66.7	0.0008

Supplementary Table 5. Measuring the frequency of truncations at DR_R-T1 in various samples

Sample name	DNA source	No. Cells (estimated from total DNA analysed)	No. of STELA reactions	No. of STELA products	No. of reactions with $pvT1_R$	Estimated DR_R-T1 telomeres per cell
NWA008	Lymphoblasts	4848	64	172	1	0.0002
COR264	Lymphoblasts	4848	64	123	7	0.0014
HGDP01065	Lymphoblasts	3864	64	61	11	0.0028
401027	Whole blood	8712	98	393	8	0.0009
211007	Whole blood	4848	64	143	3	0.0006
704021	Whole blood	2424	32	201	3	0.0012
506007	Whole blood	2424	32	200	7	0.0029
d32	Sperm	4848	64	65	6	0.0012
d56	Sperm	2424	32	70	4	0.0017
Rx-F6a G2P2	Saliva	4848	64	132	4	0.0008

Supplementary Table 6 Primers used in this study

Population screening for iciHHV-6A and iciHHV-6B			
MS32	32-9.2R	GAGGGAAGTCATAGACAACAGCTG	
	32-9.7F	CAACCATGTGAGGACAAAGCG	
DR3	DR3F	TCCGTTCCCTCATCGGCATCT	
	DR3R	GAACGTGGCCGTTACAGTTTC	
U11	HHV-6 probe 5F1	TTTTTACATCACGACGCGATC	
	HHV-6-U11-R1	GGGACGCGAATCGGAGGAAGC	
DR5 (HHV-6A)	DR5F	CACATATCCATGAACGGACACAC	
	DR5R	CGTCGACTTCTCGTTCTTTATGC	
DR7 (HHV-6B)	DR7F-HST(C)	AGGCGTGACTCTGGGAAAC	
	DR7R2-HST	CGTATATCGCATCCTTACGTCT	
Amplifying and sequencing DRR-pvT1 and DRL-pvT1			
DRR-T1	U100Fw2	5'-TATCTCCGAACATGATGCTG-3'	
	DR1R	5'-GAAGAAGATGCGGTTGTCTTGTT-3'	
DRL-T1	DR1R	GAAGAAGATGCGGTTGTCTTGTT	
	Telorette 2	TGCTCCGTGCATCTGGCATCTAACCCT	
	Teltail	TGCTCCGTGCATCTGGCATC	
pvT1	DR421R	GAGKGGTTGAAAGAGGGGTAG	
	TJ1F	AACCCTAAGTCTAGCCCTTG	
iciHHV-6B STELA and sequencing			
	DR1R	GAAGAAGATGCGGTTGTCTTGTT	
	Telorette 2	TGCTCCGTGCATCTGGCATCTAACCCT	
	Teltail	TGCTCCGTGCATCTGGCATC	
	DR2R-STELA	TGCAGTCTCCACAGGGCATA	
	Telorette 2BC38	GCGTGCTCGCAGTATCACAGCTAACCCT	
	Teltail2BC38	GCGTGCTCGCAGTATCACAGC	
	UDL6R	TTTCGCTCACGTGGCAGTCT	
	DR8RT2	ATACCCTCGCCCGTTCTTTG	
Subtelomere-iciHHV-6B amplification			
	DR8F(A/B)	CATAGATCGGGACTGCTTGAA	
	DR8FT2	TCGGACCCTTGCTATTCTGG	
	17p311	CCACGGATTGCTTTGTGT	
	2p2	GAGCTGCGTTTTGCTGAGCAC	
ddPCR			
	DR6B-F	GCAGGCCGTCCAAACTGT	
	DR6B-R	ACGGTAGGTGGATCCGTTCTC	
	DR6B probe	FAM-CGGCTATACGAGTCGGCACCGG-BHQ	
	HHV-6B POL F	GGATGAGACCCATCGGTTTGTG	
	HHV-6B POL R	GGCCAGCCAGTCCTTTAGTAGA	
	HHV-6B POL Probe	FAM-TTCCAAGCACAGACTCGCGAACACAAGG-BHQ	
	PAC1F	TCCTCGCGTTTCAAAAATTAC	
	PAC1R-33	CCCTTTTTTTTAACCCCCCCG	

Supplementary Table 6 Primers used in this study (continued)

Overlapping amplicons (HHV-6A)		
HHV-6 DR	DR1F	ACCTTGGCCCGAGCAAGAATG
	DR8R	GGATTACGGAGGTGAATGTTGC
HHV-6A T1	DR8F	GCAGAGACAAAAGTATGCGGAAG
	HHV-6 probe 40R	GCGATTCTCGTATCGGGTTA
HHV-6 40	HHV-6 probe 40 F	AAAAACTCCCCATTGGTTGC
	HHV-6 probe 40 R	GCGATTCTCGTATCGGGTTA
HHV-6 51	HHV-6 probe 51F	GGATACACCCCACTCCACAT
	HHV-6 probe 51R	GAGTGCAATACAGAAGCCGG
HHV-6 42	HHV-6 probe 42 F	CCATTTCTTGCGAATGTTGA
	HHV-6 probe 42 R	GATACGTCAAGACGGGGAAA
HHV-6 5	HHV-6 probe 5F1(U11)	TTTTTACATCACGACGCGATC
	HHV-6 probe 5R	ATGGTCCTCCATGGGTTCTT
HHV-6 18	HHV-6 probe 18 F	ATGGCGCACGCTAAAAAG
	HHV-6 probe 6R2	TGTAACGGAGGAATGGGAAG
HHV-6 43	HHV-6 probe 43 F	GGCAGTTGTCCAAAAATCTGA
	HHV-6 probe 43 R	CCTGACTGTGGTCAACAACG
HHV-6 17	HHV-6 probe 17 F	TCGAACTAAACCCGAGACCT
	HHV-6 probe 17 R	GCCATGTGGTTTGAGAGGAT
HHV-6 7	HHV-6 probe 7F	CGAMAAGCTCATGCTTACCC
	HHV6 probe 7R	AACTTGAAGCTGGCGACATT
HHV-6 13	HHV-6 probe 13 F	TCTCACTTCCGAAACTTCTATGC
	HHV-6 probe 13 R	CAGTTGTTGCTTCCGATTCC
HHV-6 52	HHV-6 probe 52F	TATCCGCTCGAACACCAACT
	HHV-6 probe 52R	CCAGCAAGAAAAGGAGCAGT
HHV-6-15	HHV-6 probe 15 F	CGTGACGTGTGCCAATCT
	HHV-6 probe 15 R	GCTCAGTTGTCGAGGGAGAC'
HHV-6 50	HHV-6 probe 50 F	CATCAAAAAGACAGCCAGGA
	HHV-6 probe 50 R	GTTGGTATGGCCGAAGATCA
HHV-6 32	HHV-6 probe 32 F	ACACGCAACATGGCAAATAA
	HHV-6 probe 32 R	CGTGCCATAGCGAAATGTAA
HHV-6 49	HHV-6 probe 49 F	CAGGAAAGGGACGGTGATAA
	HHV-6 probe 49 R	ATCGAAAGCACCACCTTCAC
HHV-6 30	HHV-6 probe 30F2	GTGAAGGACCGTTGAGGTGT
	HHV-6 probe 30 R	ATGCTTGCCTTTTCTCATGG
HHV-6 29	HHV-6 probe 29 F	TGTCTCTCCTTCTGGCACCT
	HHV-6 probe 29 R	GCAATCTTAGCAGCCGACTC
HHV-6 47	HHV-6 probe 47 F	GCTGTCGAGTCCACCATTTT
	HHV-6 probe 47 R	TAACGTTCGGCGGAATTAAC
HHV-6 3	Probe3 C1	CGCAGATAGCTTGTTGACCA
	Probe3 C2	CACTTCAGTTCCAGGGGTGT
HHV-6 11	HHV-6 probe 11 F	CGGAAACCATAGCTGTCCAT
	HHV-6 probe 11 R	GCTTATGCTTCCCAATTCCA
HHV-6 24	HHV-6 probe 24 F	GCGGTAAACGGCATACATTT
	HHV-6 probe 24 R	TGTACCTGGCAGCATCTGAG
HHV-6 25	HHV-6 probe 25 F	ATTGTTTATGCGTGCAGACG
	HHV-6 probe 25 R	CCGTTGCTTTCTCTTCCATC
HHV-6 4	Probe4 D1	GGGTTTAACGTAGCGAACCA
	Probe4 D2	CCGGAGAATGAAATCCTTGA
HHV-6 41	HHV-6 probe 41 F	TCGGACGTGTAAGATGTTGAA
	HHV-6 probe 41 R	CGGATCACTCCCGAAATCTA
HHV-6 44	HHV-6 probe 44 F	GGTGGATTACGCCACTGTTT
	HHV-6 probe 44 R	AAACTGCACGAAATCCGAAG
HHV-6 9	HHV-6 probe 9F (U83 A/BF)	GCGCAAACAATGTGCGTAGT
	HHV-6 probe 9R	TCTCCTCTTCCGWTGACACC
HHV-6 45	HHV-6 probe 45 F	TATCTTTGGTCGGGGCTCTT
	HHV-6 probe 45 R	TGATTGCAACAGTGATGGTACA
HHV-6 21	HHV-6 probe 21 F	CACATCTGTATGCTAATGATTGCT
	HHV-6 probe 21 R	AGATTGATTGCACCCGAAAC
HHV-6 27	HHV-6 probe 27 F	CAAGGTGGAGGTTTCTTTGG
	HHV-6 probe 27 R	AGGACCGTGTCCCATCATAG
HHV-6 28	HHV-6 probe 48 F	CTGGCCCAAAACAGAAATTG
	HHV-6probe 48 R	GAGAGTTTTCCATGGCCACA
HHV-6 21	HHV-6 probe 26 F	CATGGTGGTTCTCCTGTGTG
	HHV-6 probe 26 R	GAGGGTGGGCACGTATTTTA
HHV-6 46	HHV6A probe 46 F	GGTCAGGTCCTCACGACAGT
	DR1R	GAAGAAGATGCGGTTGTCTTGTT

Supplementary Table 6 Primers used in this study (continued)

Overlapping amplicons (HHV-6B)		
HHV-6 DR-1	DR1F	5'-ACCTTGGCCCGAGCAAGAATGC-3'
	DR3R	5`-GAACGTGGCCGTTACAGTTTC-3`
HHV-6 DR-2	DR3F	5`-TCCGTTCCCTCATCGGCATCT-3'
	DR7R2-HST	5`-CGTATATCGCATCCTTACGTCT-3'
HHV-6 DR-3	DR7F-HST(C)	5`-AGGCGTGACTCTGGGAAAC-3'
	DR8RB	5`-CGCCCGCGACTGCCATAGAG-3'
HHV-6 10	Pac2F	5'-TGGGAGGCGCCGTGTTTTTC-3'
	HHV6 probe 10 R	5'-TTGCATCGATACCGTTTCTG-3'
HHV-6 1	Probe A1	5′-TCACCGGATTCGACATGTAA -3′
	Probe A2	5′-TTAAAGTACGGGGTGCAAGG -3′
HHV-6 14	HHV6 probe 14 F	5'-ACACTCGCATTCCGAAAGTT-3'
	HHV6 probe 14 R	5'-AGTCGCTGAGTCCTTGGGTA-3'
HHV-6 5	HHV6 probe 5F (U11)	5'-TTTTTACATCACGACGCGATC-3'
	HHV6 probe 5R	5'-ATGGTCCTCCATGGGTTCTT-3'
HHV-6 18	HHV6 probe 18 F	5'-ATGGCGCACGCTAAAAAG-3'
	HHV6 probe 6R2	5'-TGTAACGGAGGAATGGGAAG-3'
HHV-6 16	HHV6 probe 16 F	5'-CCAAGCACTTGACCAGTTGA-3'
	HHV6 probe 16 R	5'-TTGTCGGGACTGATGATGAA-3'
HHV-6 17	HHV6 probe 17 F	5'-TCGAACTAAACCCGAGACCT-3'
	HHV6 probe 17 R	5'-GCCATGTGGTTTGAGAGGAT-3'
HHV-6 7	HHV6 probe 7F	5'-CGAGAAGCTCATGCTTACCC-3'
	HHV6 probe 7R	5'-AACTTGAAGCTGGCGACATT-3'
HHV-6 13	HHV6 probe 13 F	5'-TCTCACTTCCGAAACTTCTATGC-3'
	HHV6 probe 13 R	5'-CAGTTGTTGCTTCCGATTCC-3'
HHV-6 2	Probe B1	5'-TCGGTCTGCTCATAGTCACG -3'
	Probe B2	5'-CAGGGCTGTTGTCGGTAAAT -3'
HHV-6 15	HHV6 probe 15 F	5'-CGTGACGTGTGCCAATCT – 3'
	HHV6 probe 15 R	5'-GCTCAGTTGTCGAGGGAGAC-3'
HHV-6 33	HHV6 probe 33 F	5'-TCATCTTGCTCATTCTCCCTAA-3'
	HHV6 probe 33 R	5'-TCACTTGCAGTCGTTTGAGG-3'
HHV-6 32	HHV6 probe 32 F	5'-ACACGCAACATGGCAAATAA-3'
	HHV6 probe 32 R	5'-CGTGCCATAGCGAAATGTAA-3'
HHV-6 31	HHV6 probe 31 F	5'-TCGGAAGCGGAGATTTCTAA-3'
	HHV6 probe 31 R	5'-CCACCTTCGCAACAACAATA-3'
HHV-6 30	HHV6 probe 30 F	5'-TGAATTTTGTCGTGCTCTGC-3'
	HHV6 probe 30 R	5'-ATGCTTGCCTTTTCTCATGG-3'
HHV-6 29	HHV6 probe 29 F	5'-TGTCTCTCCTTCTGGCACCT-3'
	HHV6 probe 29 R	5'-GCAATCTTAGCAGCCGACTC-3'
HHV-6 23	HHV6 probe 23 F	5'-AGCAGCCGAAAGTAGTTCCA-3'
	HHV6 probe 23 R	5'-TCGGCGGAATTAACAAAAAC-3'
HHV-6 3	Probe C1	5'-CGCAGATAGCTTGTTGACCA -3'
	Probe C2	5'-CACTTCAGTTCCAGGGGTGT -3'
HHV-6 11	HHV6 probe 11 F	5'-CGGAAACCATAGCTGTCCAT-3'
	HHV6 probe 11R	5'-GCTTATGCTTCCCAATTCCA-3'
HHV-6 24	HHV6 probe 24 F	5'-GCGGTAAACGGCATACATTT-3'
	HHV6 probe 24 R	5'-TGTACCTGGCAGCATCTGAG-3'
HHV-6 25	HHV6 probe 25 F	5'-ATTGTTTATGCGTGCAGACG-3'
	HHV6 probe 25 R	5'-CCGTTGCTTTCTCTTCCATC-3'
HHV-6 4	Probe D1	5'-GGGTTTAACGTAGCGAACCA -3'
	Probe D2	5'-CCGGAGAATGAAATCCTTGA -3'
HHV-6 12	HHV6 probe 12 F	5'-CATGGTTCCGTCTTCCAAGT-3'
	HHV6 probe 12 R	5'-TGTGTGGAAACACCCTTCAA-3'
HHV-6 19	HHV6 probe 19 F	5'-CGGAGATATGACAAGTAGAGAGAGG-3'
	HHV6 probe 19 R	5'-CAATGAATTCCTCAGCGACT-3'
HHV-6 9	HHV6 probe 9F (U83 A/BF)	5'-GCGCAAACAATGTGCGTAGT-3'
	HHV6 probe 9R	5'-TCTCCTCTTCCGATGACACC-3'
HHV-6 20	HHV6 probe 20 F	5'-GTGTGGTGGAGTTCCGAGTT-3'
	HHV6 probe 20 R	5'-TGATCCATTCGAAGAAAATGC-3'
HHV-6 21	HHV6 probe 21 F	5'-CACATCTGTATGCTAATGATTGCT-3'
	HHV6 probe 21 R	5'-AGATTGATTGCACCCGAAAC-3'
HHV-6 27	HHV6 probe 27 F	5'-CAAGGTGGAGGTTTCTTTGG-3'
	HHV6 probe 27 R	5'-AGGACCGTGTCCCATCATAG-3'
HHV-6 28	HHV6 probe 28 R	5'-TGGATATTTGAATGTACCATCGAG-3'
	HHV6 probe 28 R	5'-TCGTGTTTAGAGTCCCGGTAA-3'
HHV-6 26	HHV6 probe 26 F	5'-CATGGTGGTTCTCCTGTGTG-3'
	HHV6 probe 26 R	5'-GAGGGTGGGCACGTATTTTA -3'
HHV-6 22	HHV6 probe 22 F	5'-AACGGTCAGGTTCTCACGAC-3'
	HHV6 probe 22 R	5'-TATCTGTCTTCCAGAGCAACAG-3'
HHV-6 T1R	U100Fw2	5'-TATCTCCGAACATGATGCTG-3'
	DR1R	5'-GAAGAAGATGCGGTTGTCTTGTT-3'